THE
PHYSICAL REVIEW
A Journal of Experimental and Theoretical Physics Established by E. L. Nichols in 1893
VOL. 54, NO. 4 AUGUST 15, 1938 SECOND SERIES

The Absorption of the Penetrating Component of the Cosmic Radiation*

W. M. NIELSEN, *Duke University, Durham, North Carolina*
AND
K. Z. MORGAN, *Lenoir-Rhyne College, Hickory, North Carolina*
(Received June 10, 1938)

The nature of the penetrating component of the cosmic radiation has been studied by making G. M. counter measurements in a cavern at a depth below rock of approximately 60 m water equivalent. Observations on the vertical counting rate were made inside and outside the cavern with various thicknesses of lead between the counters. In agreement with the results of previous investigators the counting rate with no absorber between the counters is approximately one-twentieth of the counting rate outside. The small absorption of the penetrating ionizing radiation at this depth in 550 g/cm² of lead shows that the penetrating component is to be associated with an ionizing particle. It is therefore not necessary to assume the transmission of cosmic-ray energy to these large depths by nonionizing particles, e.g., neutrinos. Comparison of the absorption of the penetrating component inside and outside the cavern shows that the penetrating ionizing radiation undergoes a hardening on transmission through large thicknesses of material. The percentage of the radiation of the less penetrating type is very nearly the same inside and outside the cavern (25 percent to 30 percent, respectively). This suggests that such soft radiation is in approximate equilibrium with the penetrating component even at the earth's surface. The character of the absorption curve for the soft component under a depth of 60 m water equivalent shows that it must be possible for the penetrating component to generate secondaries of considerable energy.

INTRODUCTION

IT is now quite definitely established that the general cosmic radiation is composed of a soft and a hard component. The experimental data on the soft component, particularly the variation of cosmic-ray intensity with altitude at different geomagnetic latitudes, can be satisfactorily explained if one assumes that it is composed of electrons and photons which behave according to the theory of radiation.[1, 2] It is, however, quite impossible on this view to account for all of the observed intensity at and below sea level so that some of the radiation which reaches low altitudes must be associated with a more penetrating type of radiation. The transmission of cosmic-ray energy through large thicknesses of matter has been extensively studied in a number of depth-ionization investigations. Such measurements have recently been extended by Wilson[3] down to depths of approximately 1500 meters of water equivalent. In order to study some of the properties of the penetrating component we have performed an experiment designed to measure the absorption of the ionizing particles present in the cosmic radiation when filtered by a considerable thickness of material.

* A report on this paper was presented at the Washington Meeting of the American Physical Society, April 1938.
[1] Heitler, Proc. Roy. Soc. **A161**, 261 (1937).
[2] L. W. Nordheim, Phys. Rev. **51**, 1110 (1937); **53**, 694 (1938).
[3] Wilson, Phys. Rev. **53**, 337 (1938). See the literature there cited for earlier intensity *versus* depth measurements.

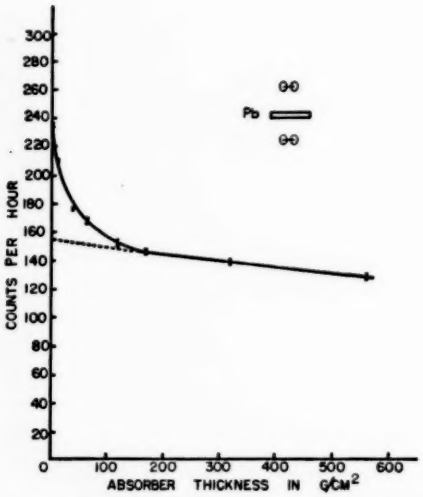

FIG. 1. Counting rate at earth's surface as a function of lead absorber thickness.

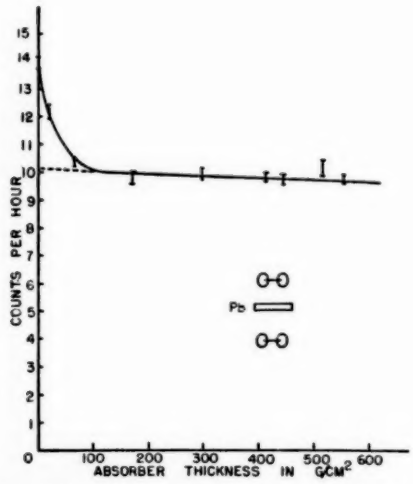

FIG. 2. Counting rate under an additional 60 m water equivalent as a function of lead absorber thickness.

THE EXPERIMENT

The experiment was carried out in Linville Caverns in western North Carolina at an altitude of approximately 2500 feet. The depth of rock above the experimental site was approximately seventy-five feet measured by a surveyor's transit. The rock is of a limestone formation. We have calculated the depth to be sixty meters water equivalent, assuming the specific gravity of the rock to be 3.28. This calculation must necessarily be only a rough approximation because of a possible inhomogeneity in the rock and because of the sloping contour of the mountain overhead. The solid angle defined by the rays which pass through the counters was such that the minimum distance to the mountain side was approximately sixty-four feet; the maximum distance was, of course, considerably more than seventy-five feet. There is apparently a transition effect in the first 20 m water equivalent in going from air to rock[3] or from air to water.[4] By making measurements at a depth of 60 m water equivalent we are fairly certain of avoiding complications due to such transition effects. The counters and counter circuits were essentially the same as used in previous investigations.[5] Insofar as possible the apparatus was mounted in paraffin covered ply-wood boxes in which drying agents were placed to safeguard against difficulties due to excessive dampness The flexible leads to the sealed counter tubes were wound with rubber tape. In this work we have operated four counters in pairs as shown in the inset of Fig. 1. The two groups of counters were placed vertically above each other with their axes parallel. The distance between the center of the upper and the center of the lower pair of counters was 63 cm.

Measurements were made of the counting rate with various thicknesses of lead between the counters outside and inside the cavern. The efficiencies of the counters outside the cavern were measured by the method of Street and Woodward.[6] From such measurements we estimate the over-all efficiency of the apparatus for detection of coincidences to be approximately 80 percent.

RESULTS AND DISCUSSION

The curve of Fig. 1 shows the data observed outside the cavern. The data obtained inside are shown in Fig. 2. The counting rates at the two locations with no lead between the counters are 235 c/hr. and 14 c/hr., respectively. The ratio of the corrected outside counting rate (293 c/hr.) to that inside[7] is in approximate agreement with

[4] Ehmert, Zeits. f. Physik **106**, 751 (1937).
[5] K. Z. Morgan and W. M. Nielsen, Phys. Rev. **52**, 564 (1937).
[6] Street and Woodward, Phys. Rev. **46**, 1024 (1934).
[7] No attempt was made to measure the counting efficiency of the apparatus inside the cavern. The error made by assuming that it recorded all rays which passed through both groups of counters will not appreciably affect the ratio indicated above.

the measurements of Wilson[3] and Ehmert[4] who observe a reduction of about twenty-fold between ground level and a depth of 60 m water equivalent.

It is obvious from the curves of Fig. 1 and Fig. 2 that the ionizing radiation both outside and inside the cavern consists of a soft and a hard component. Observations similar to those shown in Fig. 1 have been made by a number of investigators[8] with essentially similar results. There are, however, several important conclusions which may be drawn from a comparison of the curves and we shall therefore discuss them in some detail.

The absorption coefficient of the penetrating component calculated from the data of Fig. 1 is 0.0004 cm^2/g, a value in reasonable agreement with the results of previous investigators.[8]

The straight line of Fig. 2 has been drawn to correspond to an absorption coefficient of 0.0002 cm^2/g, a value slightly smaller than that given by the data of Wilson at approximately the same depth. Obviously, the absorption coefficient is not here accurately measured. It is to be emphasized, however, that the value obtained applies to the ionizing particles present in the cosmic radiation after filtering through a considerable layer of material. The large penetrating power of such particles as here observed, makes it unnecessary to assume that the cosmic radiation is to any appreciable extent, transmitted down to these large depths by a nonionizing and penetrating type of radiation, e.g. neutrinos.[9] It seems clear that our results indicate that practically all this energy is carried down by ionizing rays and that the role played by neutral particles must be a minor one.

A comparison of the data contained in the two curves shows that the ionizing radiation undergoes a hardening as it penetrates to lower depths. A decrease in the absorption coefficient of the cosmic radiation with increasing depth below sea level has generally been observed in ionization chamber[10] and counter[3, 4] measurements. Such observations in the past have been concerned with the change in slope of the depth-intensity curve obtained by measurements of the cosmic-ray intensity for various depths of absorbing material above the sensitive portion of the apparatus. It is clear that such measurements give no direct information on the penetrating power of the observed ionizing radiation. It is, therefore, of some interest to point out that the results of the present investigation show that the hardening of the radiation is directly to be associated with the penetrating ionizing particles. This conclusion also follows immediately if one accepts the well established depth-ionization curves of others and if, as shown above, the cosmic radiation is transmitted through the large depths of material by penetrating ionizing particles.

We have made an estimate of the amount of soft radiation in the two sets of data by subtracting the contribution due to the penetrating component as shown in Fig. 1 and Fig. 2. We thus find the percentage of soft radiation to be very nearly the same outside and inside the cavern (30 and 25 percent, respectively). This suggests that even at approximate sea level the penetrating component must be very nearly in equilibrium with its secondaries. The parallel variation in the intensity of the soft and the hard components suggest rather strongly that a large percentage of the soft component at both levels is generated by the more penetrating type of radiation. The fact that a soft component is observed at all at large depths implies that it must be generated by a more penetrating type of radiation which as we have shown is of an ionizing character.

An examination of those portions of the curves which correspond to the absorption of the softer component shows that the half-value thickness corresponds to a thickness of 20 g/cm^2. Any difference in this respect between the soft component inside and outside the cavern is not large enough to be disclosed by the experimental data. There can hardly be any doubt but that the soft component is closely associated with showers. We are therefore forced to conclude that showers are generated either directly or indirectly by the ionizing penetrating component. It would also appear that the complexity at any rate of the smaller showers under heavy layers of

[8] Auger, Leprince-Ringuet and Ehrenfest, J. de phys. **7**, 58 (1936) and others.
[9] Heisenberg, Zeits. f. Physik **101**, 533 (1936).
[10] Rossi, *La Radiation Cosmique* (Hermann, Paris 1935).

matter is approximately the same as that of the showers observed at sea level. The general features of this conclusion are in agreement with the results of an earlier investigation[5] on shower production under thick layers of various materials. We observed transition effects which indicated that the showers were electronic in character. We suggested that such showers might have their origin in the generation of shower producing radiation (possibly secondary electrons and photons) by the penetrating component. It also follows from these transition curves that some of such secondary particles must have considerable energy.

We wish to thank Mr. J. Q. Gilkey of Marion, North Carolina for his kindness in making Linville Caverns available for these measurements and to acknowledge the interest of Professor L. W. Nordheim and his helpful suggestions in our work.

AUGUST 15, 1938 PHYSICAL REVIEW VOLUME 54

The Formation of Deuterons by Proton Combination

H. A. BETHE, *Cornell University, Ithaca, N. Y.*

AND

C. L. CRITCHFIELD, *George Washington University, Washington, D. C.*

(Received June 23, 1938)

The probability of the astrophysically important reaction $H+H=D+\epsilon^+$ is calculated. For the probability of positron emission, Fermi's theory is used. The penetration of the protons through their mutual potential barrier, and the transition probability to the deuteron state, can be calculated exactly, using the known interaction between two protons. The energy evolution due to the reaction is about 2 ergs per gram per second under the conditions prevailing at the center of the sun (density 80, hydrogen content 35 percent by weight, temperature $2\cdot10^7$ degrees). This is almost but not quite sufficient to explain the observed average energy evolution of the sun (2 ergs/g sec.) because only a small part of the sun has high temperature and density. The reaction rate depends on the temperature approximately as $T^{3.5}$ for temperatures around $2\cdot10^7$ degrees.

§1. INTRODUCTION

IT seems now generally accepted that the energy production in most stars is due to nuclear reactions involving light elements. Of all the elements, hydrogen is favored by its large abundance, by its large internal energy which makes a considerable energy evolution possible, and by its small charge and mass which enable it to penetrate easily through nuclear potential barriers. Again, of all reactions involving hydrogen, the most primitive is the combination of two protons to form a deuteron, with positron emission:

$$H+H=D+\epsilon^+. \qquad (1)$$

In fact, this reaction must stand in the beginning of any building up of chemical elements; it has already been discussed in this connection by v. Weizsäcker.[1] However, there seems to be a general belief that reaction (1) is too rare to account for any appreciable fraction of the energy production in stars and that it can serve only to *start* the evolution of elements in a star which will then be carried on by other, more probable, processes. It is the purpose of this paper to show that this belief is unfounded but that reaction (1) gives an energy evolution of the correct order of magnitude for the sun.

On the other hand, we do not want to imply that reaction (1) is the only important source of energy. An analysis of all possible nuclear reactions with light elements[2] shows that the capture of protons by carbon and nitrogen will also play an important role. It is more important

[1] v. Weizsäcker, Physik. Zeits. **38**, 176 (1937).
[2] Bethe, to appear shortly in the Physical Review.

than (1) for heavy stars, less important for light ones and about equally important for the sun.

In calculating the energy evolution from reaction (1), it must be considered that (1) is followed by a number of other reactions which are all "fast" in comparison with (1) because they involve the emission of radiation or of heavy particles rather than of β-rays.[3] The deuterons formed in reaction (1) will first capture another proton, with γ-ray emission:

$$D+H=He^3+\gamma. \tag{2}$$

The ratio of the rates of reactions (2) and (1) is about 10^{18} which means that, in equilibrium, there will be about one deuteron for 10^{18} protons. This makes collisions between two deuterons very improbable and thus excludes any appreciable production of neutrons by such collisions.

The fate of the He^3 formed in (2) depends to some extent on the question whether this nucleus or H^3 is more stable. The most recent determination[4] of the energy evolution in the reaction $H^2+H^2=He^3+n^1$ seems to show that He^3 is more stable while older determinations[5] gave the opposite result. The processes which occur are:

If He^3 is more stable:

$$\begin{aligned} He^3+He^4&=Be^7+\gamma,\\ Be^7&=Li^7+\epsilon^+,\\ Li^7+H&=2He^4. \end{aligned} \tag{3}$$

If H^3 is more stable:

$$\begin{aligned} He^3+\epsilon^-&=H^3,\\ H^3+H&=He^4+\gamma. \end{aligned} \tag{4}$$

The net effect is in both cases the same, *viz.* the combination of four protons and two electrons to form an α-particle. (The emission of a positron is equivalent to the consumption of an electron since the positron will ultimately annihilate an electron.) One α-particle is formed for each process (1). The energy produced per process (1) is therefore equal to the difference in weight between four hydrogen atoms and one helium atom, *viz.* (cf. reference 5, 6) $Q=4\cdot 1.008\,13-4.003\,86=0.028\,66$ mass units, i.e.,

$$Q=4.3\cdot 10^{-5}\text{ erg}. \tag{5}$$

While the energy evolution in (3) and (4) is exactly the same, the processes lead to the formation of different intermediate products which could be of influence on the building up of heavier elements. However, it can be shown[2] that the building up of elements heavier than He^4 is negligible under any circumstances so that the question of stability of He^3 or H^3 is actually not important.

In order to calculate the probability of the proton combination, the following factors have to be considered:

(1) The probability of collision of two protons which involves the penetrability of their mutual potential barrier. This can be calculated very accurately since the force between two protons is very well known from scattering experiments.[7]

(2) The probability of emission of a positron during the collision. This involves a theory of the β-decay. All available experimental evidence points to the conclusion that the original Fermi theory gives good agreement with the experimental dependence of lifetime on energy.

(3) The energy distribution of the protons in the star which is given by the Boltzmann law.

§2. The Probability of Positron Emission

According to Fermi's theory, the probability of β-emission (per second) is

$$\beta=gf(W)\,|G|^2. \tag{6}$$

Here G is the matrix element of the nuclear transition,

$$G=\int \psi_i\psi_f d\tau, \tag{7}$$

ψ_i and ψ_f the initial and final state of the nucleus, except for the substitution of one neutron by a proton. f is a function of the energy W of the emitted β-particle,

$$f(W)=(W^2-1)^{\frac{1}{2}}\left(\frac{1}{30}W^4-\frac{3}{20}W^2-\frac{2}{15}\right)+\frac{1}{4}W\log\left[W+(W^2-1)^{\frac{1}{2}}\right], \tag{8}$$

[3] Cf. Bethe, Rev. Mod. Phys. **9**, 188, § 76C (1937).
[4] Bonner, Phys. Rev. **53**, 711 (1938).
[5] See Livingston and Bethe, Rev. Mod. Phys. **9**, 373 (1937).
[6] Bainbridge, Phys. Rev. **53**, 922A (1938).
[7] Tuve, Heydenburg and Hafstad, Phys. Rev. **50**, 806 (1936).

where W is expressed in units of mc^2 and includes the rest mass. A lower limit for the Fermi constant g can be deduced by assuming that $G=1$ for transformations such as $N^{13}\rightarrow C^{13}+\epsilon^+$. This reaction has a half-life of 11.0 minutes and an upper limit of the β-spectrum (observed) of about 1.25 Mev, therefore $\beta=\log 2/660=1.05\cdot 10^{-3}$ sec.$^{-1}$, $W=3.5$, $f(W)=11.86$ and

$$g=0.9\cdot 10^{-4} \text{ sec.}^{-1}. \tag{9}$$

The (maximum) energy of the positron emitted in the combination of two protons follows from the very accurately known masses of proton and deuteron,[5] *viz.*:

Two protons $=2\cdot(1.008\ 13-0.000\ 55)=2.015\ 16$
Deuteron $=\quad 2.014\ 73-0.000\ 55=2.014\ 18$

Positron energy, including mc^2 0.000 98
(mass units), equivalent to $1830\cdot 0.000\ 98\ mc^2$
$=1.80\ mc^2$.

For $W=1.8$, we have $f(W)=0.132$ and therefore, with (6) and (9),

$$\beta=1.2\cdot 10^{-5}|G|^2 \text{ sec.}^{-1}. \tag{10}$$

A similar value is obtained by extrapolating the empirical Sargent curves to lower energy. β would be larger, if the matrix element G for the transformation $N^{13}\rightarrow C^{13}$ is less than one. On the other hand, the Konopinski-Uhlenbeck theory would give about 10 times less for the decay constant. However, that theory seems to give too strong a dependence of decay constant on energy throughout, and will therefore not be used.

In calculating the matrix element G for the proton combination (1), it must be considered that the wave function of the deuteron is symmetric with respect to interchange of space and spin coordinates of proton and neutron while the wave function of two protons is antisymmetric.[8] In particular, when the two protons are in an S state (which is most favorable for their coming close together), their spins will be antiparallel (singlet) whereas the ground state of the deuteron is a triplet S state. The transition is therefore allowed only if the Gamow-Teller form[9] of the β-theory is used. This formulation permits a change of direction of the spin of the proton which transforms into a neutron, and therefore a change of the total spin by one unit. Strong evidence for this theory is found[10] in the short life of He^6; the β-transformation $He^6\rightarrow Li^6$ leads very probably from a ^1S to a ^3S state and is closely analogous to our process $2H\rightarrow D$. We shall therefore accept the Gamow-Teller theory in this paper. Moreover, we shall assume that the matrix element G in (10) can be calculated simply by integrating over the spatial coordinates of the two particles, i.e., that the summation over spins which is also implied in G gives unity. This assumption does not seem serious in view of the uncertainty in the numerical factor in (10).

If the original Fermi theory were taken instead of the Gamow-Teller theory, the transition $H+H=D+\epsilon^+$ could occur only by virtue of the "small" components of the Fermi interaction, *viz.* $\alpha_{\text{heavy particle}}\cdot\alpha_{\text{electron-neutrino}}$. Since the Dirac operator α_{heavy} (velocity) is "odd," its application on the ^3S wave function of the deuteron ground state will give a function of ^3P character. This can combine with the ^3P part of the wave function of the incident protons. Due to the smallness of the latter and of the α-operator itself, the transition probability will be greatly reduced, *viz.*, approximately by a factor

$$(W/I)^2(E/Mc^2)\approx 10^{-5},$$

where $W=1.8\ mc^2$ is the energy evolution in the process, $I=4.4\ mc^2$ the binding energy of the deuteron, $E\approx 50$ kev the kinetic energy of the protons and $Mc^2=931$ Mev. In this case, then, the energy evolution in the sun due to proton combination would be negligibly small.

§3. The Collision Cross Section

According to the general principles of quantum theory, the cross section σ for the combination of two protons of relative velocity v is given by (6), (7) if we insert for ψ_i the wave function of two protons normalized to unit incident current. Thus we have

$$\sigma=gf(W)v^{-1}\left|\int\psi_p\psi_d d\tau\right|^2, \tag{11}$$

where ψ_d is the wave function of the ground state of the deuteron and ψ_p is normalized per unit

[8] We are indebted to Professor Oppenheimer for drawing our attention to this point.

[9] Gamow and Teller, Phys. Rev. **49**, 895 (1936).

[10] Goldhaber, Phys. Rev. (to be published).

density at infinity. The integration goes over the space of the relative coordinates of the two protons (or proton and neutron, in the deuteron).

If we assume a square potential well of radius r_0 and depth V_0, the normalized wave function of the deuteron is[11]

$$\psi_d = \begin{cases} (B/r)\exp(-(x-x_0)) & \text{for } r>r_0 \\ (B/r)\sin \mu x/\sin \mu x_0 & \text{for } r<r_0 \end{cases} \quad (12)$$

with the abbreviations

$$x=r/b, \quad x_0=r_0/b, \quad (12a)$$

$$b=\hbar(M\epsilon)^{-\frac{1}{2}}=4.37\cdot 10^{-13}\text{ cm}, \quad (12b)$$

$$\mu=(V_0-\epsilon/\epsilon)^{\frac{1}{2}}, \quad (12c)$$

$$B=(2\pi b)^{-\frac{1}{2}}(1+x_0)^{-\frac{1}{2}}(1+\mu^{-2})^{-\frac{1}{2}}. \quad (12d)$$

M is the proton mass, ϵ the binding energy of the deuteron, i.e., 2.17 Mev. Depth and width of the well are related by the condition

$$\mu \cot \mu x_0 = -1. \quad (12e)$$

The wave function of two protons, normalized to unit density, has the form e^{ikz} at large distances. (For considerations of symmetry, see §4.) It can be expanded in spherical harmonics and, at the small velocities prevailing in stars ($\sim$10 kilovolts), only the zero order term will be important. It has, at large distances, the form

$$\psi_p=\sin(\rho-\varphi)/\rho, \quad (13)$$

where

$$\rho=kr, \quad k=Mv/2\hbar \quad (13a)$$

and φ is a phase (depending logarithmically on ρ). At small distances, i.e., inside the nuclear potential well, we have

$$\psi_p=\frac{w}{r}=\frac{A}{r}\sin\frac{(MD)^{\frac{1}{2}}}{\hbar}r, \quad (14)$$

where D is the depth of the potential well between two protons, assumed "square" and of radius r_0, A is a normalization factor. Outside of the well, ψ_p is a solution of the Schrödinger equation in the Coulomb field which may be written[12]

$$\psi_p=e^{iK}\cos K(F+G\tan K)/kr. \quad (15)$$

Here F is the regular and G the irregular solution of the Coulomb equation which behave asymptotically as $\sin(\rho-\varphi_0)$ and $\cos(\rho-\varphi_0)$, respectively. As can be seen easily, (15) goes over asymptotically into (13). K is the phase shift due to the nuclear field, fixed by the condition of continuity of (14), (15) at $r=r_0$; we have[12]

$$\tan K = F^2\delta/[1-FG\delta] \quad (16)$$

with

$$\delta=\left(\frac{d\log F}{d\rho}-\frac{d\log w}{d\rho}\right)_{r_0}. \quad (16a)$$

For the small proton energies concerned, $F(r_0)$ is very small (see below), both because of the Coulomb barrier and the small value of k. Therefore K will be very small ($K=0.0017$ for $v=e^2/\hbar$, i.e. for a relative kinetic energy of 12.5 kev which gives the largest contribution to the cross section at a temperature of $5\cdot 10^7$ degrees) and $e^{iK}\cos K$ (cf. (15)) can be replaced by unity. Then the factor A in the internal wave function (14) is

$$A=\frac{F(r_0)+G(r_0)\tan K}{k\sin(MD)^{\frac{1}{2}}r_0/\hbar}. \quad (17)$$

According to Yost, Wheeler and Breit,[12] the Coulomb wave functions may be written (for orbital momentum $L=0$)

$$F=C\rho\Phi, \quad G=C^{-1}\Theta, \quad (18)$$

where

$$C=(2\pi\eta)^{\frac{1}{2}}e^{-\pi\eta}, \quad \eta=e^2/\hbar v \quad (19)$$

contains the effect of the Coulomb barrier, and Φ and Θ are slowly varying functions of r which have the value 1 for $r=0$. Inserting into (16), (15) we get

$$\tan K = C^2 k r_0 \lambda, \quad (20)$$

$$\lambda=\Phi^2\zeta/(1-\Phi\Theta\zeta), \quad (20a)$$

$$\rho=\left(\frac{d\log F/w}{d\log\rho}\right)_{r_0} = \left(1+r\frac{d\log\Phi}{dr}-r\frac{d\log w}{dr}\right)_{r_0}, \quad (20b)$$

$$\psi_p=C[\Phi(r)+\lambda(r_0/r)\Theta(r)] \quad (r>r_0), \quad (21)$$

$$\psi_p=C\frac{r_0}{r}[\Phi(r_0)+\lambda\Theta(r_0)] \times\frac{\sin \nu r/b}{\sin \nu r_0/b} \quad (r<r_0). \quad (22)$$

[11] Bethe and Bacher, Rev. Mod. Phys. **8**, 110 (1936).
[12] Yost, Wheeler and Breit, Phys. Rev. **49**, 174 (1936); J. Terr. Mag. **40**, 443 (1935).

In the last expression, we have introduced the abbreviation

$$\nu=(MD)^{\frac{1}{2}}\hbar^{-1}b=(D/\epsilon)^{\frac{1}{2}}, \tag{22a}$$

which will be useful for the integration. λ represents the effect of the resonance due to the nuclear potential well.

For slow protons, the wave functions at small r are almost independent of the proton energy and have the form[12]

$$\Phi(y)=y^{-\frac{1}{2}}I_1(2y^{\frac{1}{2}})$$
$$=1+\frac{y}{1!2!}+\frac{y^2}{2!3!}+\frac{y^3}{3!4!}+\cdots, \tag{23}$$

$$\Theta(y)=-2y^{\frac{1}{2}}K_1(2y^{\frac{1}{2}})=1+y(\log y+2\gamma-1)\Phi$$
$$-\sum_{s=1}^{\infty}\frac{y^{s+1}}{s!s+1!}\sum_{t=1}^{s}\left(\frac{1}{t}+\frac{1}{t+1}\right) \tag{23a}$$

with

$$y=2r/a,\quad a=2\hbar^2/Me^2=5.75\cdot10^{-12}\text{ cm}, \tag{23b}$$
$$\gamma=0.577\cdots\quad\text{(Euler's constant)}.$$

The deviations from (23), (23a) for $\eta=1$ are of the order of a percent.

Collecting our formulae, we may now write for the cross section (11)

$$\sigma=\frac{gf(W)}{v}C^2\frac{(4\pi b^2)^2}{2\pi b}\Lambda^2, \tag{24}$$

where

$$(1+x_0)^{\frac{1}{2}}(1+\mu^{-2})^{\frac{1}{2}}\Lambda=\Lambda_1+\Lambda_2+\Lambda_3, \tag{25}$$

$$\Lambda_1=\frac{x_0[\Phi(r_0)+\lambda\Theta(r_0)]}{\sin\mu x_0\sin\nu x_0}\int_0^{x_0}\sin\mu x\sin\nu x dx, \tag{25a}$$

$$\Lambda_2=\int_{x_0}^{\infty}xdx\exp\left(-(x-x_0)\right)\Phi(2bx/a), \tag{25b}$$

$$\Lambda_3=\lambda x_0\int_{x_0}^{\infty}dx\exp\left(-(x-x_0)\right)\Theta(2bx/a). \tag{25c}$$

The integrations are elementary and give

$$\Lambda_1=\frac{\frac{1}{2}x_0^2[\Phi(r_0)+\lambda\Theta(r_0)]}{\sin\mu x_0\sin\nu x_0}$$
$$\times\left[\frac{\sin(\mu-\nu)x_0}{(\mu-\nu)x_0}-\frac{\sin(\mu+\nu)x_0}{(\mu+\nu)x_0}\right], \tag{26a}$$

$$\Lambda_2=1+x_0+(2b/a)(1+x_0+\tfrac{1}{2}x_0^2)$$
$$+\tfrac{1}{2}(2b/a)^2(1+x_0+\tfrac{1}{2}x_0^2+\tfrac{1}{6}x_0^3)+\cdots, \tag{26b}$$

$$\Lambda_3=\lambda x_0\{1+(2b/a)[\log(2b/a)+2\gamma-1]\Lambda_2$$
$$-[(2b/a)^2\tfrac{3}{2}(1+x_0+\tfrac{1}{2}x_0^2)$$
$$+\tfrac{1}{2}(2b/a)^3(7/3)(1+x_0+\tfrac{1}{2}x_0^2+\tfrac{1}{6}x_0^3)$$
$$+\cdots]+\sum_{s=1}^{\infty}(2b/a)^s f_s(x_0)/(s-1)! \tag{26c}$$

with

$$f_s(x_0)=s!^{-1}\int_{x_0}^{\infty}\exp\left(-(x-x_0)\right)x^s\log x dx, \tag{26d}$$

$$f_1=1+(1+x_0)\log x_0-E_i(-x_0)\exp(x_0), \tag{26e}$$

$$f_2=\tfrac{3}{2}+\tfrac{1}{2}x_0+(1+x_0+\tfrac{1}{2}x_0^2)\log x_0$$
$$-E_i(-x_0)\exp(x_0), \tag{26f}$$

$$f_3=(11/6)+(5/6)x_0+\tfrac{1}{6}x_0^2$$
$$+(1+x_0+\tfrac{1}{2}x_0^2+\tfrac{1}{6}x_0^3)\log x_0$$
$$-E_i(-x_0)\exp(x_0). \tag{26g}$$

Table I gives the numerical results for two values of the radius r_0 of the potential well, *viz.* e^2/mc^2 and $e^2/2\ mc^2$. The depth D of the proton-proton well was taken from Breit, Condon and Present.[13] All other quantities were calculated from the formulae in the text. It is seen that the contribution of the inside of the potential well, Λ_1, is rather small even for the larger r_0, which shows that the result will not depend sensitively on the shape of the potential well.

TABLE I. *Numerical results for two values of the radius.*

	$r_0=e^2/mc^2$	$r_0=e^2/2\ mc^2$
x_0	0.645	0.322
V_0 (Mev)	20.9	66.5
D (Mev)	10.3	47.0
μ	2.94	5.45
ν	2.18	4.65
$(rd\log w/dr)$	0.236	0.110
$\Phi(r_0)$	1.050	1.025
$\Theta(r_0)$	0.769	0.854
$(rd\log\Phi/dr)$	0.050	0.025
ζ	0.814	0.915
λ	2.63	4.80
Λ_1	0.689	0.277
Λ_2	1.949	1.547
Λ_3	1.205	1.030
$(1+x_0)(1+\mu^{-2})$	1.835	1.367
Λ	2.84	2.44
Λ^2	8.08	5.93

[13] Breit, Condon and Present, Phys. Rev. **50**, 825 (1936).

Furthermore, the contribution Λ_3 which is due to resonance is smaller than Λ_2 which would be present even if there were only the Coulomb field between the two protons. The final result for Λ^2 increases somewhat with increasing radius of the well. For $\eta=1$, a numerical calculation gave $\Lambda^2=8.8$ instead of 8.1.

§4. Symmetry, Statistics, etc.

If N is the number of protons per cm^3, the probability of finding one proton with velocity $\mathbf{v}_1$ and one with $\mathbf{v}_2$, is

$$N^2\varphi(\mathbf{v}_1)\varphi(\mathbf{v}_2)d\mathbf{v}_1d\mathbf{v}_2, \tag{27}$$

where φ is the Boltzmann distribution function. In calculating the total probability of our process, we must integrate over each pair of volume elements $d\mathbf{v}_1d\mathbf{v}_2$ only once; if we want to integrate over $\mathbf{v}_1$ and $\mathbf{v}_2$ independently, (27) must be divided by 2 (this corresponds to the fact that the total number of proton pairs is $\frac{1}{2}N^2$). We can transform to relative velocity $\mathbf{v}=\mathbf{v}_1-\mathbf{v}_2$ and center-of-gravity velocity $\mathbf{V}=\frac{1}{2}(\mathbf{v}_1+\mathbf{v}_2)$ and integrate over the latter, then we obtain (including the factor $\frac{1}{2}$ mentioned)

$$\tfrac{1}{2}N^2\varphi(\mathbf{v})d\mathbf{v} \tag{27a}$$

$$\varphi(\mathbf{v})d\mathbf{v}=(M/4\pi kT)^{\frac{3}{2}} \times\exp\,(-Mv^2/4kT)4\pi v^2dv. \tag{28}$$

Of the proton pairs with given velocities $\mathbf{v}_1\mathbf{v}_2$, one in four will have opposite spins, three in four parallel spins. The latter have an antisymmetrical spatial wave function and therefore do not contribute to the cross section of our nuclear process. The former have a symmetrical wave function which is, normalized to unit density:

$$[(\exp\,(i\mathbf{k}_1\cdot\mathbf{r}_1+i\mathbf{k}_2\cdot\mathbf{r}_2)) +(\exp\,(i\mathbf{k}_2\cdot\mathbf{r}_1+i\mathbf{k}_1\cdot\mathbf{r}_2))]/\sqrt{2}. \tag{29}$$

Separating off the motion of the center of gravity and expanding into spherical harmonics, we obtain

$$(\exp\,(ikz)+\exp\,(-ikz))/\sqrt{2} =\sqrt{2}\,\sin\,kr/kr+\cdots, \tag{29a}$$

which differs from (13) by a factor of $\sqrt{2}$. This gives a factor 2 in the cross section and, with the factor $\frac{1}{4}$ for the *a priori* probability of opposite spin, there remains a factor $\frac{1}{2}$.

Table II. *Energy evolution due to proton combination, for* $\rho c_H^2=10$ *g/cm*^{3}.

t(million degrees)	5	10	15	20	30	40	50	100
τ	19.8	15.70	13.72	12.56	10.89	9.90	9.18	7.28
ϵ(ergs/g sec.)	0.0040	0.15	0.76	2.2	9.1	20	36	150

The total number of processes per cm^3 per sec. becomes thus

$$p'=\tfrac{1}{4}N^2\int\varphi(\mathbf{v})d\mathbf{v}v\sigma. \tag{30}$$

By the insertion of (24), (28), (19), this becomes

$$p'=\pi^{\frac{1}{2}}gf(W)N^2b^3\Lambda^2\left(\frac{M}{kT}\right)^{\frac{1}{2}}\int_0^\infty v^2dv \times\frac{2\pi e^2}{hv}\exp\left(-\frac{2\pi e^2}{hv}-\frac{Mv^2}{4kT}\right). \tag{31}$$

The integrand has a strong maximum very close to

$$v=(4\pi e^2kT/hM)^{\frac{1}{2}}. \tag{31a}$$

Approximating it, in the usual way, by a Gaussian around the maximum, we find

$$p'=16\pi\cdot3^{-5/2}\cdot gf(W)N^2b^3\Lambda^2\tau^2e^{-\tau} \tag{32}$$

with

$$\tau=3(\pi^2Me^4/4h^2kT)^{\frac{1}{3}}. \tag{33}$$

If t is the temperature in millions of degrees, we have

$$\tau=33.8t^{-\frac{1}{3}}. \tag{33a}$$

§5. Result

We insert into (32) the values of the constants b (cf. (12b)), $gf(W)$ from (10), Λ^2 from Table I (for $r_0=e^2/mc^2$), and assume that the concentration of hydrogen (by weight) is c_H and the density (in g/cm^3) is ρ. Then the number of processes per *gram* per second is

$$p=p'/\rho=16\pi\cdot3^{-5/2}\cdot1.2\cdot10^{-5}\cdot(6.02\cdot10^{23})^2 \cdot(4.37\cdot10^{-13})^3\cdot8.10\cdot\rho c_H^2\tau^2e^{-\tau} \tag{34}$$
$$=0.95\cdot10^7\rho c_H^2\tau^2e^{-\tau}.$$

Each combination of two protons leads (§1) ultimately to the formation of an α-particle out of four protons and two electrons, with an energy liberation of $4.3\cdot10^{-5}$ erg. Therefore the

energy production is

$$\epsilon = 410 \rho c_H^2 \tau^2 e^{-\tau} \text{ ergs/gram sec.} \quad (35)$$

The density at the center of the sun[14] is about 80, the hydrogen content $c_H \approx 0.35$, therefore $\rho c_H^2 \sim 10$. Table II gives the energy evolution due to the proton-proton reaction at various temperatures. With a hydrogen content of 35 percent, the central temperature of the sun is about $20 \cdot 10^6$ degrees. At this temperature, the energy production is about 2.2 ergs/g sec. This is of the same order as the observed average energy production of the sun (2.0 ergs/g sec.). Thus we come to the conclusion that the *proton-proton combination gives an energy evolution of the right order of magnitude for the sun.*

For a quantitative comparison, it must be remembered that both the temperature and the density of the sun decrease fairly rapidly from the center outwards, and that the rate of reaction decreases with both of these quantities. The average energy production per gram will thus be considerably smaller than that at the center, perhaps by a factor of 10. Since our calculations are rather accurate, it seems that there must be another process contributing somewhat more to the energy evolution in the sun. This is probably the capture of protons by carbon (reference 2).

For many problems, it is necessary to know the temperature dependence of the energy production ϵ. It is convenient to express this dependence as a power law, $\epsilon \sim T^n$. Then (cf. (35))

$$n = d \log \epsilon / d \log T = \tfrac{1}{3}(\tau - 2). \quad (36)$$

At 20 million degrees, this gives in our case $n = 3.5$. This is large enough to make the point source model of stars a rather good approximation. On the other hand, it is too slow a dependence on temperature to explain, with temperatures of the order $2\text{–}4 \cdot 10^7$ degrees, the very high rates of energy production found in very heavy stars. However, we believe that our process is the principal source of energy in stars lighter than the sun.

[14] Stromgren, Ergebn. d. exakt. Naturwiss. **16**, (1937).

AUGUST 15, 1938 PHYSICAL REVIEW VOLUME 54

On the Production of Heavy Electrons*

L. W. NORDHEIM AND G. NORDHEIM
Duke University, Durham, North Carolina

(Received June 3, 1938)

The barytron theory of nuclear forces shows a close correspondence to the theory of the electromagnetic field. Estimates based on this analogy are given for the probabilities of the processes leading to actual production of barytrons. A comparison with the experimental evidence regarding the occurrence of barytrons in the cosmic radiation shows that the theoretical cross sections are too small to explain the properties of the hard component. The difficulty is increased by the short lifetime of the barytrons which is estimated to be of the order $\sim 10^{-8}$ sec. from radiative β-decay. Therefore no simple picture of barytron production in terms similar to radiation theory can be given. This failure, however, indicates only the inapplicability of perturbation calculations, but does not constitute an actual disproof of the link between nuclear forces and cosmic radiation.

INTRODUCTION

AT present there are two different lines of evidence for the existence of a new particle, the barytron,[1] of electronic charge (positive and negative) and of a mass μ about 200 times the electronic mass m.

From cosmic-ray investigations there can be little doubt that a large percentage of the hard component, which itself constitutes the greater part of all radiation from sea level downwards, can be neither electrons nor protons[2] but must

* A preliminary report on this paper has been given by L. W. Nordheim and E. Teller at the Washington Meeting of the American Physical Society, April 1938.

[1] This name was proposed at the Washington Meeting of the American Physical Society, April 1938.

[2] Anderson and Neddermeyer, Phys. Rev. **51**, 884 (1937); Street and Stevenson, Phys. Rev. **51**, 1005 (1937).

consist of rays of intermediate mass. An actual determination of the mass[3] from ionization-range-curvature measurements has only been possible for a few rays but they all show, within the rather wide limits of error, masses about 200 m.

The other line is purely theoretical and arises from the attempts to build up a field theory of nuclear forces similar to the connection of the Coulomb law and the electromagnetic field. As is well known such a theory was proposed by Heisenberg and others[4] on the basis of Fermi's theory of β-decay. According to this theory a heavy particle (proton or neutron) can emit or absorb an electron-neutrino pair much as a charged particle can emit or absorb light quanta. Such a scheme leads to an interaction between heavy particles due to a "playing ball" effect, which implies the emission of the "field particles" (electrons and neutrinos) by one heavy particle and subsequent reabsorption by another. With the β-field as determined from radioactive decay, however, grave difficulties arose.[5] The interaction between heavy particles is far too small for distances of the known range of nuclear forces ($\sim 10^{-13}$ cm) but diverges at small separations at least as r^{-5} because of the simultaneous action of two transmitting particles. This behavior can be avoided only by rather artificial modifications which cannot be formulated in a consistent and relativistically invariant way.[6]

It was noted by Yukawa[7] as early as 1935, before the experimental evidence on a new particle, that a part of these difficulties could be avoided by assuming the interaction field to be associated with single particles of finite rest mass (i.e. barytrons).

It has been suggested by Yukawa[8] and several other authors[9] that the new cosmic-ray particles are identical with those introduced in the field theory of nuclear forces. In order to see, whether such an interpretation is possible on the basis of the "nuclear force field" theory now under discussion, it is necessary to investigate conditions under which the barytrons can actually be created.

The only method available for this task at the present time is a correspondence treatment on lines similar to those used in ordinary radiation theory. As a logical preliminary step for the discussion of the connection of cosmic-ray phenomena and nuclear forces we have tried therefore:

Firstly, to work out as far as possible the consequences of such a correspondence treatment.

Secondly, to deduce from observational data the cross sections for barytron production necessary to account for their actual occurrence in the atmosphere.

The result so far has been a negative one, i.e., the estimated cross sections come out too small by a factor larger than 10 even in the most favorable case (barytron production by photons).

We show this in Part I by rather general and qualitative arguments which should apply to any field theory which can be treated in the same way as ordinary radiation theory and in Part II for a special form of the nuclear field (the one initially proposed by Yukawa) for which the calculations can be carried out explicitly.

This failure of the correspondence treatment does not imply necessarily that such a connection between nuclear forces and cosmic-ray phenomena is ruled out altogether. It may mean only that it is not legitimate to extrapolate the nuclear field theory in its present state as developed for the low energy phenomena of nuclear forces and β-decay to the higher energy range of cosmic radiation. In the formalism of the theory such a failure will manifest itself in the occurrence of divergences in the application of perturbation theory. It is known that such divergences already occur in ordinary quantum electrodynamics, though the omission of the divergent terms leads in that case to reasonable results in agreement with experiment. From our investigation it seems then necessary to conclude that this expedient does not work for the nuclear field theory and that it is not possible, therefore,

[3] Compare the discussion by Corson and Brode, Phys. Rev. **53**, 773 (1938); Williams and Pickup, Nature **141**, 836 (1938).
[4] Compare Nordsieck, Phys. Rev. **46**, 234 (1934); Tamm and Iwanenko, Nature **133**, 981 (1934).
[5] Compare f.i. the report by Bethe and Bacher, Rev. Mod. Phys. **8**, 82 (1936).
[6] For such an attempt compare Camp, Phys. Rev. **51**, 1046 (1937) and Nordheim, Nordheim, Oppenheimer and Serber, Phys. Rev. **51**, 1037 (1937).
[7] Yukawa, and others, Proc. Phys. Math. Soc. Japan **17**, 58 (1935); **19**, 1034 (1937); **20**, 1 (1938).
[8] Yukawa, Proc. Phys. Math. Soc. Japan **19**, 712 (1937).
[9] Oppenheimer and Serber, Phys. Rev. **51**, 1113 (1937); Bhabha, Nature **141**, 117 (1938).

to give a simple correspondence picture for the production of barytrons. It is not impossible, however, that the barytron production can be described on lines indicated by Heisenberg[10] in his discussion of field theories containing a fundamental length.

Part I. Possible Processes and Orders of Magnitude

Section 1. General properties of barytrons

An interaction between heavy particles due to the exchange of one single particle with finite rest mass gives rise to a potential, the space dependence of which is given by

$$I(r)=(G^2/r)\exp(-r/\lambda_0);\quad \lambda_0=\hbar c/\mu, \qquad (1)$$

where G is a constant of the dimension of a charge and λ_0 the "Compton wave-length" of the barytron.[11] This interaction corresponds to a screened Coulomb field. The proportionality to r^{-1} is the same as in the Coulomb case because only one particle has to be transmitted; the screening is due to the finite rest mass in contrast to light quanta. To understand this factor one might say that it represents essentially the probability distribution of finding a barytron at distance r from a proton or neutron when there is not energy enough actually to create it.

Equation (1) gives the order of magnitude[12] and range for nuclear forces for $\mu\sim M/10$ and

$$A=G^2/\hbar c\sim\mu/M\sim 1/10, \qquad (2)$$

where A can be considered as the analog to the fine structure constant $\alpha=1/137=e^2/\hbar c$ in ordinary radiation theory. The fact that $A\ll 1$ gives some hope that a correspondence treatment of the nuclear field has some meaning. It signifies that higher order processes (i.e. those involving a greater number of barytrons) should be of lesser importance than those of lowest order. We shall therefore study only these. In case the value (2) should turn out not to be small enough to ensure this convergence it would be, of course, not possible to derive any conclusions by the standard methods of perturbation theory.

In order to have a simultaneous explanation of radiative β-decay it is necessary to assume that the barytrons have electronic charge (positive and negative), obey Einstein-Bose statistics, and that they can disintegrate spontaneously into an electron and a neutrino. The lifetime can be estimated in the following way: The probability of finding a barytron in the neighborhood of a neutron-proton pair in a nucleus is of the order 1/10 (ratio of binding energy per particle and rest energy of the barytrons). The lifetime τ_N of a nucleus subject to β-decay should be therefore $\sim 1/10$ of the lifetime of a free barytron τ_B if just the energy is available to create one. Now in Fermi's theory τ_N is proportional at least to ϵ_0^{-5}, where ϵ_0 is the available energy (maximum energy of electrons). Therefore $\tau_B/\tau_N(\epsilon_0)\sim(\mu/M)(\epsilon_0/\mu)^5$. The lifetime of light elements of $\epsilon_0\sim 5m$ is of the order 100 sec. and therefore the lifetime of a barytron should be $\sim 10^{-8}$ sec. This estimate will be verified for the model discussed in Part II but it apparently should not depend sensitively on special assumptions regarding the mechanism.

The limited lifetime would lead to the conclusion that the barytrons have to be produced as secondaries in the atmosphere itself. As τ_B is so extremely small (a barytron of energy 10^{10} ev $=100\mu$ would only have a free path $l\leqq c\cdot\tau_B\cdot 100$ cm ~ 300 m) the barytrons must be created very near to the place where they are observed or their connection with the β-decay has to be given up altogether.

On basis of these conceptions the most probable mechanisms for the actual production of barytrons are discussed in the next two sections.

Section 2. Production of barytrons by protons or neutrons

This mechanism is quite analogous to the emission of light quanta by charged particles. A proton carrying with it a "nuclear force field" can actually emit barytrons when passing with sufficient energy through another nuclear force field, e.g. of a nucleus at rest. If the theory converges in the sense discussed in Section 1 the

[10] Heisenberg, Zeits. f. Physik **101**, 533 (1936).

[11] We denote the rest energies (i.e., mass $\times c^2$) of electrons, barytrons and protons by m, μ, M, respectively.

[12] For a short range potential, zero binding energy for the two particles problem (deuteron) results when approximately

$$\int_0^\infty I(r)dr\leqq\hbar^2/M; \qquad (1a)$$

(comp. Bethe and Bacher, reference 5, p. 109). Inserting (1) into (1a) the relation (2) is obtained. The actual value for A might be slightly larger than μ/M.

emission of a single barytron should be the most probable process and representative of the whole effect.

Because of the resemblance of $I(r)$ to a Coulomb field a very rough estimate of the order of magnitude of this effect can be obtained by a simple "translation" of the ordinary formula of radiative emission. The dictionary is:

Radiation	Nuclear force field theory
$\alpha=e^2/\hbar c=1/137$;	$A=G^2/\hbar c=\mu/M$ $=\alpha 137\mu/M\sim 1/10$;
$r_0=e^2/m$;	$R_0={}^2G/M=r_0(137\mu/M)\cdot\mu/M$ $\sim 0.075(\mu/M)\cdot r_0$ $\sim 7.5\times 10^{-3}r_0$;
	$\rho_0=e^2/\mu=r_0 m/\mu\sim 5\cdot 10^{-3}r_0\sim R_0$.

The cross sections of ordinary radiative processes for high energies are of the order of magnitude $Z^2\alpha r_0^2$, where Z is the atomic number. From this we obtain for example for the ratio of the probability ϕ_B for the production of a barytron by a proton over the one $\phi_{h\nu}$ for the production of a light quantum by an electron of the same energy as the proton, the order of magnitude

$$\frac{\phi_B}{\phi_{h\nu}}\sim\frac{X}{Z^2}\frac{AR_0^2}{\alpha r_0^2}\sim 0.75\left(\frac{\mu}{M}\right)^3\frac{X}{Z^2}<10^{-3}. \quad (3)$$

The factor X is introduced to take care of the composite structure of the nucleus and should be approximately equal to its mass[13] number. The ratio of these probabilities therefore is of the order of 10^{-3}.

To show the significance of this result we remark that an electron has about an even chance to create a quantum of comparable energy in one unit length of the radiation theory of showers,[14] which is for air $\sim 1/30$ of the whole atmosphere. Therefore a proton will generate approximately only $30\times 10^{-3}\sim 1/30$ barytrons when traversing the whole atmosphere. As the number of protons in the cosmic radiation is certainly much smaller than the number of barytrons, the above emission process cannot explain the occurrence of the latter near sea level so long as the analogy formula has any meaning.

Section 3. Production of barytrons by light quanta or electrons[15]

A production of barytrons by light quanta or electrons can only be effected by a simultaneous action of the electromagnetic and nuclear-force field. The simplest mechanism of this kind is the direct photoeffect, i.e. a photon is absorbed by a proton and a barytron is reemitted. The process is due to the combined effects of the interactions photon-barytron and barytron-proton (compare Section 6). It follows then from dimensional arguments that the cross section must be of the order $\rho_0\times R_0=e^2/\mu\times G^2/M\times F(E/M)$, where F is a homogeneous function of the primary energy E and the rest energies of the particles concerned. If this function is assumed to be of the order unity for high energies[16] the ratio of the cross sections for producing a barytron by a photon over the cross section for the production of a normal electron-positron pair would be of the order of magnitude

$$\frac{\phi_B{}^{h\nu}}{\phi_{e1}{}^{h\nu}}\leqq\frac{X}{Z^2}\frac{\rho_0 R_0}{\alpha r_0^2}\sim\frac{X}{Z^2}\left(\frac{137m}{M}\right)^2<10^{-2}. \quad (4)$$

This is larger than (3) by roughly a factor 10 and as we can expect the presence of many more quanta than protons in the high atmosphere it might offer a more promising picture.

On the assumption that the hard component of the cosmic radiation is produced as a secondary radiation by photons, one can now estimate from observational results how large the ratio (4) has to be in order that enough hard rays are produced. If, in the production process, the whole energy of a quantum is given to the barytron, the total number of barytrons of energy E produced in the atmosphere will be

$$N(E)=\int\phi_B{}^{h\nu}(E)n(E,x)Y(x)dx, \quad (5)$$

[13] As the range of the nuclear forces is of the same order as the average distance between its constituents one should expect an independent superposition of their action with regard to our emission effect.

[14] Bhabha and Heitler, Proc. Roy. Soc. **A159**, 432 (1937); Carlson and Oppenheimer, Phys. Rev. **51**, 220 (1937).

[15] The hypothesis that the hard component is produced by the soft component in the atmosphere itself has been first put forward by Bowen, Millikan and Neher, Phys. Rev. **53**, 217 (1938).

[16] As we shall see in the later discussion this assumption is subject to grave doubts since, with the present form of the theory, the function F generally decreases with increasing energy.

where $\phi_B{}^{h\nu}(E)$ is the cross section as a function of energy, $n(E, x)$ the number of quanta of energy E as a function of depth x below the top of the atmosphere, and Y the number of atoms per unit volume. If we measure the cross section in units of the cross section of normal pair production and the depth in the unit length l_0 of multiplication theory[14] ($l_0 \sim 0.35$ m water equivalent for air) $dl = \phi_{el}{}^{h\nu} Y dx$, and (5) reduces to

$$N(E) = \int \phi_B(E) n(E, l) dl. \tag{6}$$

The distribution $n(E, x)$ of quanta in the atmosphere can be obtained in sufficient approximation from the analysis of one of the authors.[17] According to the multiplication theory the number of quanta will be slightly larger (by a factor of ~ 1.5) than the number of electrons of the same energy and shows approximately the same energy distribution, which is

$$n(E)dE = f(x)E^{-s}dE, \quad \text{for } E > E_0, \tag{7}$$

where $f(x)$ gives the dependence on depth. The exponent s lies between 2 and 3, and E_0 is the energy down to which the multiplication of rays extends, i.e. $\sim 1.5 \times 10^8$ ev for air. The form of the distribution is nearly independent of altitude and therefore $f(x)$ is approximately proportional to the total soft intensity in the atmosphere which, in turn, gives the greater part of the intensity in the atmosphere itself. The number of slow electrons below E_0 should, furthermore, be of the same order as those above E_0 (i.e. those obeying the distribution (7)). Therefore one can say that the number of quanta of energy above E_0 at a certain depth will be roughly equal to the total number of soft particles, i.e. to nearly the total measured intensity, and that their energies will roughly follow the same distribution (7). Integrating the intensity distribution (Fig. 3 of reference 17) at the equator[18] over depth one obtains in the units used there 600 particle meters or, as 1 m water equivalent ~ 3 unit lengths, about 2000 photon lengths for photons above an energy of 1.5×10^8 ev. The number $Q(E)$ of photon lengths for quanta of an energy larger than E will be therefore

$$Q(E) = 2000(E_0/E)^{s-1}; \quad E > E_0 = 1.5 \times 10^8 \text{ ev}. \tag{7a}$$

The number of hard particles at sea level[19] is around 7 (in the units used above) and certainly more than half of these, i.e. around 4, have energies larger than 10^9 ev.

We make now the most favorable assumption that no barytrons get lost in the atmosphere itself by spontaneous disintegration. (This would mean, of course, that the theory of β-decay, outlined in Section 1, could not be correct.) Then most of the barytrons will come from the upper part of the atmosphere where the intensity of quanta is largest, and will have already lost an energy of 1 to 2×10^9 ev by ionization. Therefore, only quanta above about 2 to 3×10^9 ev should be counted. With $s \sim 2.5$ we obtain from (7a) $Q \sim 40$ for $E = 2 \times 10^9$ ev.

This means that such a quantum must have a chance of about 1 in 10 to create a barytron of comparative energy, before it is absorbed through the normal production of an electron pair. This estimate should hold for any mechanism. In case the production cross section depends on energy, the ratio 1/10 would mean an average over all energies, and if the production occurs in multiple processes, the cross section would be smaller in proportion. But it has to be noted, that the actual energy distribution of the hard rays as measured by Blackett[20] demands that

[17] Nordheim, Phys. Rev. **51**, 1110 (1937); **53**, 694 (1938).

[18] Only few of the photons produced by the field sensitive part of the soft primaries would be energetic enough to produce barytrons which could travel down to sea level. This would be consistent with the smallness of the geomagnetic effect at sea level (15 to 20 percent), and it would seem therefore quite possible to account for the features of this effect on the photon hypothesis.

[19] Compare Table III, reference 17. These figures were estimated from experimental data and not deduced from the tentative analysis given there.

[20] Blackett, Proc. Roy. Soc. **A159**, 1 (1937). It is interesting to remark that the energy distribution for the hard rays would be in agreement with the one observed and compatible with the absorption curve of the hard rays underground if the cross section for barytron production is independent of the quantum energy like the cross section of electron pair production. In this case the energy distribution would be the same as the energy distribution of the producing quanta, i.e., of the form (7) which is at least in qualitative agreement with observation as shown in reference 17. According to this hypothesis of the secondary nature of the hard component it is not necessary to assume that the hard rays produce hard secondaries in great amounts. The main cause for absorption of the hard rays will then be again energy loss through ionization and the distribution law (7) will give also in this case an absorption law $E \sim x^{s-1}$ (x = depth) as observed.

also barytrons of very high energies are produced.[21]

The correspondence formula (4) gives for the ratio of barytron production to electron pair production by photons for air a value of about 2×10^{-3} ($m/M=1850$; $Z^2=50$, $X\sim20$), which is thus too small by a factor ~50. It seems, therefore, not to be possible to give a simple account of the barytron production on lines similar to radiation theory.

The discrepancy would still be larger, if the lifetime of the barytron is actually as short as estimated in sections 1 and 4. The connection between the barytrons and radioactive β-decay is, however, not cogent, and it might be changed by a reformulation of the β-theory.

Part II. A Model Theory for Barytron Production

Section 4. Interaction Hamiltonian and lifetime of barytrons

The considerations of the preceding sections were of a purely qualitative nature and based on simple analogies to the theory of radiation. It remains to be seen whether the characteristic properties of the barytron field (i.e. that it describes the motion of charged particles of finite rest mass having no negative energy states) introduce any features which might invalidate this analogy. For this reason we give in the following sections an actual model theory for the effects in question. For this it is necessary to have an interaction which can be applied to high energy phenomena. This demands that the perturbation developments converge at least in the same way as those in quantum electrodynamics. The only nuclear force field so far proposed which satisfies this requirement is the scalar one,[22] originally introduced by Yukawa. Though this field admittedly does not give satisfactory results for the spin dependence of nuclear forces, it seems to be worth while to study the mechanism of barytron production with a definite model. The result is that the orders of magnitude come near to the estimates of Part I though there are some differences in details.

For the scalar field of Yukawa the interaction with the heavy particles is described by the Hamiltonian

$$\mathfrak{H}=2\sqrt{\pi}\,\hbar c\cdot G\int\{\varphi^*(\psi_N^*\beta\psi_P)+\varphi(\psi_P^*\beta\psi_N)\}dV, \quad (8)$$

where ψ_N, ψ_P are the wave functions of a heavy particle in the neutron or proton state. They are assumed to obey Dirac's wave equation so that $(\psi_N^*\beta\psi_P)$, etc., are the simplest scalars. β is the Dirac operator and φ is the scalar wave function of the barytron, which is assumed to obey the Klein-Gordon equation, and is subject to second quantization according to the procedure of Pauli and Weisskopf[23] for Einstein-Bose particles. G is an interaction constant with the dimension of a charge; the other factors are chosen so that the simple form (1) of the potential, without any additional constant, is obtained.

For the quantization of the barytron field following the procedure of Pauli-Weisskopf, a Fourier decomposition can be used.

$$\varphi=\sum q_B\exp((i/\hbar c)\mathbf{B}\cdot\mathbf{r});$$
$$q_B=-\frac{i}{(2E_B)^{\frac{1}{2}}}(-a_B+b_B^*); \quad (9)$$
$$q_B^*=-\frac{i}{(2E_B)^{\frac{1}{2}}}(a_B^*-b_B).$$

[21] Similar considerations would apply to the purely electromagnetic production of positive and negative pairs of barytrons by quanta. The cross section for this process is, as well known, for high energies, nearly independent of energy the ratio to normal electron pair production being of the order $(m/\mu)^2$. As two barytrons are created in a single act this ratio had to be of the order 1/20 or $\mu\lesssim5$ m. For the probable value of $\mu\sim100$ to 200 m this kind of production can only contribute less than 1 percent of the total. The action of electrons compared to photons will in both cases (mixed electromagnetic-nuclear field and purely electromagnetic production) be smaller by a factor $\sim1/137$.

[22] An alternative form of the barytron field of vectorial nature and resembling therefore more closely the electromagnetic field, has recently been suggested independently by Yukawa (reference 7), Fröhlich, Heitler, and Kemmer, Proc. Roy. Soc. **A166**, 154 (1938); and Bethe, Phys. Rev. Abstract (1938). The possibilities for the interaction Hamiltonian of the barytron field with heavy particles have been studied in detail by Kemmer, Proc. Roy. Soc. **A166**, 127 (1938). The interaction (8) used here is the same as Kemmer's with his interaction constant $g_a\neq0$ and all others zero. It seems that a formal perturbation treatment of the emission processes with his generalized interaction would give rise to terms which contain positive powers of the initial energy and which, therefore, would become very large at high energies. On the other hand, the divergences in this theory are far more serious and such formal developments would have no physical meaning. It might be, however, that this lack of convergence gives an indication of qualitatively new phenomena (multiple processes of higher order in the sense of Heisenberg) which might finally bring the solution of the barytron problem, though at present no method exists for treating these questions.

[23] Pauli and Weisskopf, Helv. Phys. Acta **7**, 709 (1934).

Here E_B and $\mathbf{B}$ are the energy and the momentum vector (in energy units i.e. $\mathbf{B}$ = momentum $\times c$) and the quantities a_B etc. stand for the operators

a_B^* = creation of a barytron of positive charge,
b_B^* = creation of a barytron of negative charge,
a_B = annihilation of a barytron of positive charge,
b_B = annihilation of a barytron of negative charge.

From (8) and (9) we obtain the following matrix elements for the change of a proton into a neutron with momentum $\mathbf{N}/c$ and emission of a positively charged barytron

$$\mathcal{H}_{P;\,N+B^+} = \frac{-iG\hbar c(2\pi)^{\frac{1}{2}}}{(E_B)^{\frac{1}{2}}}(u_N^*\beta u_P), \qquad \mathbf{P}=\mathbf{N}+\mathbf{B}^+; \quad E_B^2=\mathcal{B}^2+\mu^2, \tag{10}$$

where u_P and u_N are the four component Dirac amplitudes of the corresponding states (all wave functions are assumed to be normalized per unit volume). The matrix element for the reverse process of absorption of a barytron with negative charge by a neutron is the conjugate complex to (10), and for the process $\mathbf{N}\rightarrow\mathbf{P}+\mathbf{B}^-$, i.e. the emission of a negatively charged barytron by a neutron, the subscripts P and N in (10) have to be exchanged.

From the matrix elements (10) the interaction potential between a proton and a neutron is obtained by the normal second order perturbation formula. For states of motion for which the kinetic energies of the heavy particles are small compared to μ the β-brackets in (8) can be replaced by unity, and the energies of the intermediate states are simply the energies of the intermediate barytrons. Positive and negative barytrons give the same contribution, and one obtains therefore for the interaction potential

$$V(r)=2\pi\hbar^2c^2G^2P\cdot 2\iiint\frac{\exp\left(-(i/\hbar c)\mathbf{B}\cdot\mathbf{r}\right)d\mathbf{B}}{(2\pi\hbar c)^3(B^2+\mu^2)} = -\frac{G^2}{r}\exp\left(-r\mu/\hbar c\right)\cdot P, \tag{11}$$

where r is the distance between neutron and proton, and the factor $(2\pi\hbar c)^{-3}$ represents the density of barytron states in momentum space. P is an operator which exchanges the proton-neutron character of the heavy particles. Its effect on a function antisymmetrical in the character variables (as must be assumed for an ^3S state which is symmetrical in all other variables) is a change of sign, while the sign is preserved for a symmetrical character function (^1S state). Equation (11) gives therefore a Heisenberg force of space dependence (1), but repulsive for the ^3S state of the deuteron.[7, 24]

In order to describe the radioactive β-decay an additional interaction between barytrons and electrons and neutrinos has to be introduced. The simplest possible assumption is, in analogy to (8), that

$$\mathcal{H}_\beta = g\hbar c 2\sqrt{\pi}\{\varphi(\psi_n^*\beta\psi_{el}) + \text{conjugate complex}\}. \tag{12}$$

which couples the emission of an electron ψ_{el} and the absorption of a neutrino ψ_n (that is emission of an antineutrino) with the production of a positive or disappearance of a negative barytron and so on. Here g is a new interaction constant also of the dimension of a charge. A second-order perturbation theory over the stages $N\rightarrow P+B^-$; $B\rightarrow$ electron + antineutrino gives then the formula for the probability of β-decay as

$$dW=\frac{2}{\pi}\left(\frac{gG}{\hbar c}\right)^2\left(\frac{m}{\mu}\right)^4\frac{(\epsilon_0-\epsilon)^2(\epsilon^2-m^2)^{\frac{1}{2}}\epsilon d\epsilon}{m^5}\cdot\frac{m}{\hbar}, \tag{13}$$

where ϵ is the energy of an emitted electron and ϵ_0 its maximal possible energy (determined by the total available energy).

This formula is identical with the one derived from a Fermi interaction of the usual form

$$\mathcal{H}_F = G_F\cdot m(\hbar c/m)^3\{(\psi_n^*\beta\psi_{el})(\psi_P^*\beta\psi_N) + \text{conj. compl.}\}, \tag{14}$$

where G_F is a dimensionless constant and

$$G_F^2=\left(\frac{2\pi gG}{\hbar c}\frac{m^2}{\mu^2}\right)^2.$$

As G_F is of the order[25] 5×10^{-12}, we obtain by use of (2)

$$\frac{g^2}{\hbar c}=\frac{1}{4\pi^2}\frac{\hbar c}{G^2}\left(\frac{\mu}{m}\right)^4G_F^2\sim10^{-74}.$$

[24] Lamb and Schiff, Phys. Rev. **53**, 651 (1938).

[25] Calculated from the data given by Nordheim and Yost, Phys. Rev. **51**, 992 (1937). For light positron emitters for which the heavy particle matrix element is ~1 one has $(2\pi)^{-3}G_F^2\cdot(m/\hbar)=\tau_0^{-1}=\tau_f^{-1}\sim10^{-4}$.

The decay probability of a free barytron (i.e. its reciprocal lifetime) at rest becomes on the other hand

$$W=\frac{1}{\tau}=\frac{g^2}{\hbar c}\cdot\frac{\mu}{\hbar}=\sim 1.2\left(\frac{\mu}{m}\right)^4; \qquad (15)$$

i.e. the lifetime is of the order 10^{-8} seconds in agreement with the estimate of Section I.

As another simple effect for barytrons we mention the scattering by a neutron or proton,[26] i.e. the analogy of the Compton effect for light quanta. The total cross section integrated over all scattering angles for this effect is, with the interaction (8), given by

$$\sigma=\pi R_0^2\left\{\frac{(1+2/\gamma)^2}{1+2\gamma}+\frac{2(1+\gamma)}{(1+2\gamma)^2}\right\};\quad \gamma=\frac{E_0}{M}, \qquad (16)$$

where E_0 is the initial energy of the barytron. For $E_0>M$ the cross section decreases as M/E_0 as in the ordinary Compton effect. For $E_0<M$ (analogy to Thomson scattering) one obtains a factor $(M/E_0)^2$ to the geometrical cross section πR_0^2. This factor is due to the special form (8) of our interaction. In ordinary radiation theory one has instead of the β-brackets in (8) the Dirac α-operators which are of the order v/c where v is the velocity of the charged particles. Expressed in the formalism of perturbation theory the ordinary Compton scattering is due to virtual transitions into negative energy states while with the β-interaction this is not necessarily so.

As most of the results in this section have already been obtained by Yukawa we have omitted the detailed derivations.

Section 5. The radiative emission of barytrons by heavy particles

According to the conservation of charge, barytrons can be emitted in collisions of heavy particles according to the schemes given in (17).

$$\begin{aligned}
&\text{I.}\quad P_0+N_0\rightarrow P_1+P_2+B^-\\
&\text{II.}\quad N_0+P_0\rightarrow N_1+N_2+B^+\\
&\text{III.}\quad P_1+P_2\rightarrow P+N+B^+\\
&\text{IV.}\quad N_1+N_2\rightarrow N+P+B^-.
\end{aligned} \qquad (17)$$

The cross sections for these processes will be equal so that we need only to consider the reaction (I). With the matrix elements (10), connecting the change of character of a heavy particle with the emission or absorption of a barytron, the reaction has to go over two successive intermediate states and there exist the six possibilities given in (18).

$$\begin{array}{lll}
a & b & c\\
P_0\rightarrow N'+B^{+\prime} & P_0\rightarrow N'+B^{+\prime} & P_0\rightarrow N'+B^{+\prime}\\
N_0+B^{+\prime}\rightarrow P_2 & N_0+B^{+\prime}\rightarrow P_1 & N'\rightarrow P_1+B^-\\
N'\rightarrow P_1+B^- & N'\rightarrow P_2+B^- & N_0+B^{+\prime}\rightarrow P_2\\
d & e & f\\
P_0\rightarrow N'+B^{+\prime} & N_0\rightarrow P_2+B^{-\prime} & N_0\rightarrow P_1+B^{-\prime}\\
N'\rightarrow P_2+B^- & P_0+B^{-\prime}\rightarrow N'' & P_0+B^{-\prime}\rightarrow N''\\
N_0+B^{+\prime}\rightarrow P_1 & N''\rightarrow P_1+B^- & N''\rightarrow P_2+B^-
\end{array} \qquad (18)$$

So long as the heavy particles can be considered as free the formulae (17) and (18) are directly the equations for the conservation of the respective momenta. The dashes in (18) denote intermediate states. We consider the process from the system of reference in which the neutron is initially at rest, i.e. $\mathbf{N}_0=0$. According to perturbation theory the differential cross section will then be

$$d\phi=\frac{2\pi}{\hbar}\frac{E_{P_0}}{P_0c}|H_{s_0s}|^2\delta(E_s-E_{s_0})d\rho_B d\rho_{P_1} \qquad (19)$$

$$\text{with}\quad H_{s_0s}=\sum_{s's''}\frac{H_{s_0s'}H_{s's''}H_{s''s}}{(E_{s_0}-E_{s'})(E_{s'}-E_{s''})}, \qquad (19a)$$

where the indices s_0, s', s'', s denote the initial, two successive intermediate, and the final state of the total system and $d\rho_B$ and $d\rho_{P_1}$ the density functions for the corresponding particles

$$d\rho_B=\frac{\mathbf{B}E_B dE_B d\Omega_B}{(2\pi\hbar c)^3};\quad d\rho_{P_1}=\frac{\mathbf{P}_1 E_{P_1} d\Omega_{P_1}}{(2\pi\hbar c)^3} \qquad (20)$$

with $d\Omega_B$ and $d\Omega_{P_1}$ the elements of the solid angles for the barytron and one of the final protons, respectively. The factor $\delta(E_s-E_{s_0})$ denotes the conservation of energy. Only those values of the momenta will contribute to the integral cross section for which the resonance denominators in the sum (19a) are small. We in-

[26] A positive barytron can only be scattered by a neutron and a negative one only by a proton.

vestigate separately the case A of high energy of the oncoming proton, i.e. $E_{P_0} > M$ and case B of small energy i.e. $E_{P_0} < M$.

A. Relativistic case: $E_{P_0} > M$.—The smallest resonance denominators are obtained for small values of the momenta $\mathbf{B}^{+\prime}$ and $\mathbf{B}^{-\prime}$ for the intermediate barytron, i.e. for small momenta transfers between the two heavy particles. If we neglect the symmetrization in the final protons, i.e. in P_1 and P_2 and designate with P_2 the particle in which the original neutron N_0 goes over, then only the series a and e in (18) contain the corresponding small resonance denominator and need alone to be taken into account.[27] For these terms we have then

$$\begin{aligned} &\mathbf{B}^{+\prime} = \mathbf{P}_0 - \mathbf{P}_1 - \mathbf{B}^- = -\mathbf{B}^{-\prime}; \quad E'_{B^+} = E'_{B^-} \\ &\mathbf{N}' = \mathbf{N}'' = \mathbf{P}_1 + \mathbf{B}^- \sim \mathbf{P}_0. \end{aligned} \tag{21}$$

Since only very small momentum transfers contribute (see the formulae (30) and (31)), E_{P_2} will still be only $\sim M$. Therefore we can neglect differences $E_{P_2} - E_{N_0}$ against E_B' even in the denominators and we have as an expression for the conservation of energy

$$E_{P_0} = E_{P_1} + E_{B^-}. \tag{22}$$

Denoting the energies of the heavy particles from now on by E_0, E_1, E', E'' and those of the barytrons by $E_B = \epsilon$ and $E_B' = \epsilon'$ we obtain from (10), (18), (19a), (21) and (22)

$$\mathcal{K}_{sos} = \frac{i(2\pi)^{\frac{1}{2}} G^3 \hbar^3 c^3}{\epsilon^{\frac{1}{2}} \cdot \epsilon'^2} \left\{ \frac{(u_{N'}{}^* \beta u_{P_0})(u_{P_1}{}^* \beta u_{N'})}{\epsilon' + E' - E_0} - \frac{(u_{N''}{}^* \beta u_{P_0})(u_{P_1}{}^* \beta u_{N''})}{E'' - E_0 - \epsilon'} \right\}. \tag{23}$$

[27] This procedure is allowed as long as E_{P_1} and E_{P_2} are of different order of magnitude, i.e., as long as $E_B - < E_{P_0}$. We have checked the correctness of these and other similar neglections later on by more detailed calculations, which are elementary but tedious and have, therefore, been omitted here.

Summing over positive and negative energy states of the intermediate neutron and the spins of the initial and final states and transforming the resonance denominators

$$\begin{aligned} E'^2 - (E_0 - \epsilon')^2 &= 2(E_0\epsilon' - \mathbf{P}_0 \cdot \mathbf{B} - \tfrac{1}{2}\mu^2) \\ &\leqq 2(E_0\epsilon' - \mathbf{P}_0 \cdot \mathbf{B}'), \\ E''^2 - (E_0 + \epsilon')^2 &= 2(E_0\epsilon' + \mathbf{P}_0 \cdot \mathbf{B}' + \tfrac{1}{2}\mu^2) \\ &\leqq 2(E_0\epsilon' + \mathbf{P}_0 \cdot \mathbf{B}'), \end{aligned} \tag{24}$$

we obtain for the differential cross section (terms containing $\mathbf{B}'$ in the nominator are neglected)

$$d\phi = \frac{1}{\pi^2} A R_0^2 \frac{P_1}{P_0} \times \frac{M^4 E_0^2 (M^2 + E_0 E_1 - \mathbf{P}_0 \cdot \mathbf{P}_1) \mathbf{B} d\epsilon d\Omega_B d\Omega_{P_1}}{\epsilon'^2 \{E_0^2 E'^2 - (\mathbf{P}_0 \cdot \mathbf{B}')^2\}^2}. \tag{25}$$

This expression contains the dependence on the direction of the final particles through the scalar product $(\mathbf{P}_0 \cdot \mathbf{P}_1)$ in the nominator and through the intermediate momentum $\mathbf{B}'$ and energy ϵ' in the denominator.

For the integration we introduce the following variables: the vector

$$\mathbf{Q} = \mathbf{P}_1 + \mathbf{B} \tag{26}$$

through its absolute value Q (which determines the opening angle θ between $\mathbf{P}_1$ and $\mathbf{B}$ with $QdQ = P_1 B \sin\theta d\theta$) and the polar angles ϑ and φ (the latter is cyclic) with respect to the axis $\mathbf{P}_0$, and finally the azimuth ψ of the plane $(P_1 B)$ around $\mathbf{Q}$ (ψ is contained only in $\mathbf{P}_0 \cdot \mathbf{P}_1$). The integration over the azimuths φ and ψ leads to

$$\begin{aligned} &\int\int (M^2 + E_0 E_1 - \mathbf{P}_0 \cdot \mathbf{P}_1) d\varphi d\psi \\ &= 4\pi^2 \{M^2 + E_0 E_1 - (P_0/2Q)(P_1^2 + Q^2 - B^2) \cos\vartheta\} \end{aligned}$$

and we obtain for (25)

$$d\phi = 2A R_0^2 P_0^{-1} d\epsilon \times T,$$

$$T = \int\int \frac{E_0^2 M^4 \{2Q(M^2 + E_0 E_1) - P_0(P_1^2 + Q^2 - B^2) \cos\vartheta\} \sin\vartheta d\vartheta dQ}{\epsilon'^2 \{E_0^2 \epsilon'^2 - P_0^2 (P_0 - Q\cos\vartheta)^2\}^2}. \tag{27}$$

With

$$\epsilon'^2 = \mu^2 + B^2 = \mu^2 + P_0^2 + Q^2 - 2P_0 Q \cos\vartheta \tag{28}$$

and the new variables

$$z = 1 - \cos\vartheta \quad \text{and} \quad y = P_0 - Q \tag{29}$$

we obtain (only the lowest powers in z and y which give the chief contribution to the cross section are retained)

$$T\sim\int_{\Delta}^{y_0}dy\int_0^2 dz\frac{4P_0E_0^2M^6}{(\mu^2+y^2+2P_0^2z)\{E_0^2\mu^2+M^2y^2+2zE_0^2P_0^2\}^2},$$
$$\sim\frac{2M^6}{P_0}\int_{\Delta}^{y_0}\frac{dy}{y^2}\left\{\frac{1}{E_0^2\mu^2+M^2y^2}+\frac{1}{P_0^2y^2}\lg\frac{\mu^2+y^2}{\mu^2+M^2y^2/E_0^2}\right\}. \tag{30}$$

The limits for y are

$$\Delta=P_0-(P_1+B)\leqq\epsilon\left\{\frac{M^2}{2E_0E_1}+\frac{\epsilon-B}{\epsilon}\right\},$$
$$y_0=P_0-|P_1-B|\leqq\text{smaller of } 2\epsilon \text{ or } 2E_1, \tag{31}$$

(relativistic approximations and (22) are used). Only the lower limit Δ is important which signifies the minimum possible momentum transferred to the initial neutron. Carrying out the integration over y we obtain in sufficient approximation as final result

$$d\phi=16AR_0^2\left(\frac{M}{\mu}\right)^2\left(\frac{M}{E_0}\right)^2\times\frac{1}{1+(\mu E_0/\epsilon M)^2}\frac{E_0-\epsilon}{E_0}\frac{d\epsilon}{\epsilon}. \tag{32}$$

This cross section has a maximum as a function of the emitted energy for $\epsilon\sim(\mu/M)E_0$.

It is interesting to compare (32) with the result one would obtain in the limit of vanishing rest mass of the barytron (which would give a pure Coulomb law for the proton-neutron interaction). Putting $\mu\to 0$ in (30) and integrating one obtains

$$d\phi_{\mu\to 0}\sim\frac{32}{3}AR_0^2\frac{E_0}{M}\frac{(E_0-\epsilon)^3}{\epsilon^3}\frac{d\epsilon}{M}. \tag{33}$$

We see that this would give a much larger effect than the analogous formula of radiation theory and especially a strong divergence for small ϵ. This is apparently due to the used β-interaction instead of the α-operators (see the end of section 4) which increases the cross section enormously. The finite rest mass, however, introduces a very effective limitation for the decrease of the resonance denominators.

By use of the correspondence picture of Weizsaecker-Williams for the description of radiative effects we can explain the factors in (32) as follows: The increase by the factor $(M/\mu)^2$ comes from the choice of the β-interaction. (For this reason it would perhaps be more logical to introduce G^2/μ as the critical "barytron radius" in place of G^2/M as in Section 2.) The decrease by the other energy dependent factors is due to the screening expressed by the exponential factor in (1).

Integrating (32) over ϵ we obtain for the total cross section for the production of a barytron of any energy

$$\phi\sim16AR_0^2\left(\frac{M}{\mu}\right)^2\left(\frac{M}{E_0}\right)^2\left[\lg\frac{M}{\mu}-1\right] \tag{34}$$

and for the average energy loss of a proton (N = number of atoms per unit volume and X = the effective number of scattering particles in the atom, which is of the order[28] $3Z$,

$$-dE/dx\sim XN8AR_0^2(M/\mu)^2M^2/E_0. \tag{35}$$

For energies from 10^9 to 10^{10} ev (34) is of the same order of magnitude as would follow from the analogy consideration of Section 3.

B. Nonrelativistic case: $E_{P_0}<M$.—It is necessary to investigate this case separately because of the large effect of the β-interaction at small energies. In this case ($E_0<M$) the energies of all heavy particles concerned will be smaller than M and therefore all the β-brackets in the matrix elements can be replaced by unity. Furthermore all energy differences of the heavy particles in the denominators can be neglected compared to the barytron energies ϵ and ϵ', but all six series of the intermediate states (18) have to be taken into account. The evaluation of the cross section is otherwise similar to the relativistic case and leads to the result

$$d\phi\sim8AR_0^2\left(\frac{M}{\mu}\right)^2\frac{T_0^{\frac{1}{2}}(T_0-\epsilon)^{\frac{1}{2}}}{(2T_0-\epsilon)^2}\frac{Bd\epsilon}{\epsilon^2} \tag{36}$$

[28] According to the scheme (17) a proton can emit a barytron in a single way when encountering another proton but in two ways in an encounter with a neutron.

and integrated

$$\phi \sim 2AR_0^2(M/\mu)^2 \lg T_0/\mu, \tag{37}$$

where $T_0 = P_0^2/2M$ is the kinetic energy of the oncoming particle. We see that the cross section (37) is a smooth continuation of the relativistic case (34) with only a slightly different numerical factor.

To obtain an estimate of the importance of the emission effect investigated in this section we calculate the probability W that a proton creates a barytron when passing through matter before it is stopped entirely by normal ionization. Since the specific energy loss (35) is small compared to the specific energy loss γ by ionization, the energy as a function of depth x is

$$E(x) = E_0 - \gamma x,$$

where E_0 is the initial energy. We have then with the help of (34)

$$W = XN\int \phi(E(x))dx = XN\int_M^{E_0} \phi(E)\frac{dE}{\gamma}$$

$$\sim 16XNAR_0^2\left(\frac{M}{\mu}\right)^2\frac{M}{\gamma}, \tag{38}$$

if E_0 is sufficiently large. Inserting the numerical values for air we obtain

$$W \sim (XM/\mu)\times 10^{-2} \sim 2\times 10^{-2}$$

which as has been discussed in Section 3 is insufficient to explain the occurrence of barytrons in the cosmic radiation.

Section 6. Barytron production by photons

The simplest reactions of this type are

$$\begin{aligned} &\text{I.} \quad k+P \rightarrow N+B^+, \\ &\text{II.} \quad k+N \rightarrow P+B^-, \end{aligned} \tag{39}$$

where $k = h\nu$ and $\mathbf{k}$ are energy and momentum (in energy units) of the light quantum. Since both reactions will have the same cross section we consider only (I). The process goes in two different ways over one intermediate state each. The first possibility consists in the conversion of the light quantum into a positive-negative barytron pair and subsequent reabsorption of the negative barytron by the proton. The second consists in the emission of the positive barytron by the proton and subsequent absorption of the light quantum by the barytron. The momentum relations are

$$\begin{aligned} &\text{I.} \quad \mathbf{k} \rightarrow \mathbf{B}^+ + \mathbf{B}^- \qquad \text{II.} \quad \mathbf{P} \rightarrow \mathbf{B}^+ + \mathbf{N} \\ &\qquad \mathbf{P} + \mathbf{B}^- \rightarrow \mathbf{N} \qquad\quad \mathbf{B}' + \mathbf{k} \rightarrow \mathbf{B}^+ \\ &\qquad\qquad \mathbf{B}' = -\mathbf{B}^- \end{aligned} \tag{40}$$

The relations between the energy of the emitted barytron and its direction relative to the direction of the initial light quantum (angle ϑ) are very similar to those of the original Compton effect, i.e. in sufficient approximation (if we assume the initial proton to be at rest, i.e. $\mathbf{P}=0$)

$$\begin{aligned} &\epsilon^+ = \frac{k}{1+(k/M)(1-\cos\vartheta)}; \quad k \gg \mu, \\ &\epsilon^+ \sim k; \qquad\qquad\qquad\qquad k < M. \end{aligned} \tag{41}$$

The matrix elements for pair production and absorption are according to Pauli and Weisskopf[29]

$$\begin{aligned} \mathcal{H}_{\text{pair}} &= -e\hbar c\left(\frac{\pi}{2k}\right)^{\frac{1}{2}} \frac{\mathbf{e}_k\cdot(\mathbf{B}^+ - \mathbf{B}^-)}{(\epsilon^+\epsilon^-)^{\frac{1}{2}}}; \\ \mathcal{H}_{\text{abs}} &= e\hbar c\left(\frac{\pi}{2k}\right)^{\frac{1}{2}} \frac{\mathbf{e}_k\cdot(\mathbf{B}^+ + \mathbf{B}')}{(\epsilon^+\epsilon')^{\frac{1}{2}}}. \end{aligned} \tag{42}$$

where ϵ^+ and $\epsilon^- = \epsilon'$ denote the energies of the barytrons and $\mathbf{e}_k$ the unit vector of polarization of the quantum ($\mathbf{e}_k$ is orthogonal to $\mathbf{k}$). The matrix element for the second step is again (10). We have then

$$\mathbf{e}_k\cdot(\mathbf{B}^+ - \mathbf{B}^-) = \mathbf{e}_k\cdot(\mathbf{B}^+ + \mathbf{B}') = 2\mathbf{e}_k\cdot\mathbf{B}^+$$

and the cross section becomes

$$\begin{aligned} d\phi &= \frac{2\pi}{\hbar c}\rho_B\delta(E_s - E_{s_0})\left|\sum\frac{H_{s_0s'}H_{s's}}{E_{s'} - E_{s_0}}\right|^2 \\ &= G^2e^2\delta(E_s - E_{s_0})(\mathbf{e}_k\cdot\mathbf{B}^+)\left|\frac{2\epsilon^-(u_N^*\beta u_P)}{(\epsilon^+ - k)^2 - \epsilon^{-2}}\right|^2\frac{B^+d\Omega}{k\epsilon^{-2}}. \end{aligned} \tag{43}$$

[29] Pauli and Weisskopf, reference 23 formulae (49) and (53). It is interesting to note that in (42) the difference $\mathbf{B}^+ - \mathbf{B}^-$ enters (in reference 23 the definition of one of the momenta is reversed). This clearly has to be so as the resultant electric current of the two barytrons is proportional to this difference.

We treat again separately the cases of high and low energy.

A. Relativistic case: $k \gg \mu$.—We sum over the spin states of the heavy particle and use the following relations coming from the conservation of energy and momentum (compare (39) and (40))

$$\delta(E_s - E_{s0})d\Omega = 2\pi \left|\frac{d\epsilon^+}{dE}\right|_\vartheta \sin\vartheta d\vartheta = 2\pi \frac{E_N B}{Mk}\frac{M d\epsilon^+}{\epsilon^{+2}}, \quad (44)$$

$$\epsilon^{-2} = N^2 + \mu^2 = \mu^2 + (k-\epsilon^+)^2 + 2M(k-\epsilon^+). \quad (45)$$

Then we obtain for the differential cross section with $E_N = M + k - \epsilon^+$

$$d\phi = 2\pi G^2 e^2 \frac{M+E_N}{Mk^2} \cdot \frac{2M^2(k-\epsilon^+)B^4 d\epsilon^+}{k\epsilon^{+3}[\mu^2 + 2M(k-\epsilon^+)]^2}. \quad (46)$$

The total cross section will be then (putting $\epsilon^+ = \epsilon$)

$$\phi = 4\pi R_0\rho_0 \frac{M^2\mu}{k^3}\int_{\epsilon_{nm}}^{k} \frac{[2M+(k-\epsilon)](k-\epsilon)\epsilon d\epsilon}{[\mu^2+2M(k-\epsilon)]^2}. \quad (47)$$

The main contribution to this integral comes from the region $k-\mu < \epsilon < k$ which means that practically always the whole energy is given to the barytron. Carrying out the integration over ϵ we have with sufficient approximation

$$\phi = \pi R_0\rho_0 F(k),$$
$$F(k) = \frac{\mu M}{k^2}\left\{2\lg\left(1+\frac{2Mk}{\mu^2}\right) - \frac{9}{4} + \frac{k}{2M}\right\}. \quad (48)$$

This expression contains the factor $R_0\rho_0$ as discussed in Section 3 but the dimensionless factor $F(k) = F(h\nu)$ decreases strongly for high energies similar to the ordinary Compton effect, which again means that the effect cannot account for the number of observed barytrons.

B. Nonrelativistic case: $k \sim \mu$.—Here the β-brackets in (10) are unity,

$$\epsilon^+ \sim k, \quad \frac{d\epsilon^+}{dE} = 1,$$

and the integral cross section becomes after some calculation

$$\phi = 2\pi R_0\rho_0 \frac{M\mu B}{k^3}\left[\frac{k}{B}\lg\frac{k+B}{k-B} - 2\right];$$
$$B^2 = k^2 - \mu^2. \quad (49)$$

This is of the same order as one would expect from the extrapolation of (48) to low energies. For $k \sim \mu$, (49) contains a factor M/μ in addition to the dimensional expression $R_0\rho_0$. This cross section would actually approach the magnitude required by observation (comp. Section 3) if it were independent of energy.

The authors wish to express their thanks to Professor E. Teller for stimulating discussions on the subject.

Note added in proof: A more exact evaluation of the fundamental constant G of the theory has recently been given by Sachs and Goeppert-Mayer (Phys. Rev. **53**, 991 (1938)). They obtain a value ~ 0.3 for $G^2/\hbar c$ instead of 0.1 as assumed in this paper. The cross sections of the production processes are thereby increased very effectively (especially for the process discussed in Section 3) so that they approach already those required by observation. Furthermore, the convergence of the perturbation calculations becomes doubtful, even for the scalar barytron field. This means that the energy dependence of the cross sections cannot be determined any more. Even if the possibility for a better estimate of the production probabilities seems thus to be still more remote, the prospect for establishing the discussed connection between nuclear forces and the hard component of the cosmic radiation is certainly much better now.

Neutron Scattering Cross Sections of Para- and Orthohydrogen, and of N_2, O_2, and H_2O*

F. G. BRICKWEDDE,** JOHN R. DUNNING,† HAROLD J. HOGE,** AND JOHN H. MANLEY,††

(Received June 17, 1938)

Measurements were made of the transmission of liquid para- and normal hydrogen for the slow neutrons obtained from a Rn-Be source by scattering in paraffin. In some of the experiments the paraffin was at room temperatures and in others it was cooled with liquid air. Teller, and Schwinger and Teller, have shown how the spin dependence of the interaction between neutrons and protons can be investigated by such measurements. As the neutrons captured by the protons were less than 1 percent of the scattered neutrons, the scattering by the thin layers of liquid hydrogen used was determined from the transmission measurements. The scattering cross section of liquid hydrogen for slow neutrons was found to depend upon the velocity of the neutrons and on the *ortho-para* composition of the hydrogen. The following values were obtained for the neutron scattering cross sections, σ, of liquid ortho- and parahydrogen: for $\sim$300°K neutrons (paraffin at room temperatures), σ (*ortho*) $=56\times10^{-24}$ cm² per molecule, σ (*para*) $=29\times10^{-24}$; for $\sim$120°K neutrons (paraffin cooled with liquid air), σ (*ortho*) $=79\times10^{-24}$ and σ (*para*) $=18\times10^{-24}$. We were able to prove conclusively: (1) that the interaction between neutrons and protons is dependent upon the relative alignment of their spins, and (2) that the energy of the singlet state of the deuteron, in which the spins of the proton and neutron are antiparallel, is greater than the energy of these particles when far apart, that is, the singlet state of the deuteron is virtual. The scattering+capture cross sections of liquid oxygen and liquid nitrogen were measured for $\sim$300°K neutrons, and of water for $\sim$300° and $\sim$120°K neutrons. The cross sections for the 300°K neutrons were: $\sigma(O)=4\times10^{-24}$ cm² per atom, $\sigma(N)=13\times10^{-24}$ cm² per atom and $\sigma(H_2O)=91.2\times10^{-24}$ cm² per molecule. For the $\sim$120°K neutrons $\sigma(H_2O)=116\times10^{-24}$ cm² per molecule. The scattering cross sections of the protons in water, $(1/2)[\sigma(H_2O)-\sigma(O)]$, were 43.6×10^{-24} cm² per proton for $\sim$300°K neutrons and 56×10^{-24} cm² per proton for $\sim$120°K neutrons.

INTRODUCTION

THE abnormally large scattering cross section of hydrogen for slow neutrons led to the assumption that the interaction between neutron and proton depends on the spins of these particles. This hypothesis, attributed to Wigner by Feenberg and Knipp,[1] had been generally accepted although it lacked direct experimental verification.[2] Teller[3] pointed out that the existence or nonexistence of a spin dependent neutron-proton interaction could be determined from a study of the scattering of slow neutrons by para- and orthohydrogen. He showed that if the interaction proved to be spin dependent it should be possible to tell from such experiments whether the singlet level of the deuteron is stable or virtual. In the detailed analyses subsequently carried out by Schwinger and Teller[4] it was shown that the effects were large enough to be readily detected experimentally, and that it might also be possible to obtain information concerning the range of the neutron-proton forces. Schwinger[5] has since pointed out that such experiments would also serve to confirm the choice of $\frac{1}{2}$ rather than $\frac{3}{2}$ for the spin of the neutron, a choice hitherto made entirely because of its simplicity.

In discussing the para- and orthohydrogen scattering cross sections for slow neutrons, briefly referred to as the *para* and *ortho* cross sections, three possibilities are to be considered:

(1) No dependence of forces on spin
(2) Spin dependent forces with
  (a) a real (stable) singlet level of the deuteron
  (b) a virtual singlet level of the deuteron.

In case (1) the only difference to be expected in the *para* and *ortho* scattering cross sections arises from the different spacing of their rotational energy levels. At room temperature only the first few levels are occupied, and for neutrons of energy comparable to the excitation energies

* Publication assisted by the Ernest Kempton Adams Fund for Physical Research of Columbia University.

** National Bureau of Standards, Washington, D. C.
† Columbia University, New York, N. Y.
†† Columbia University, New York, N. Y. Now at the University of Illinois.

[1] E. Feenberg and J. K. Knipp, Phys. Rev. **48**, 906 (1935).

[2] See reference 4 for a discussion of the evidence to be obtained from Amaldi and Fermi's measurements of the cross section for radiative capture.

[3] E. Teller, Phys. Rev. **49**, 420 (1936).

[4] J. Schwinger and E. Teller, Phys. Rev. **52**, 286 (1937).

[5] Julian Schwinger, Phys. Rev. **52**, 1250 (1937).

of these levels parahydrogen should have the larger cross section, since the closer spacing of its levels makes inelastic scattering more probable. The difference should be small however and should be negligible for neutrons either above or below this energy range. In the absence of spin forces all scattering must be of the *para→para* or *ortho→ortho* type, that is the rotational quantum number of the scattering molecule must change by $0, \pm 2, \pm 4, \cdots$.

In cases (2a) and (2b) the presence of spin forces makes possible in addition *para→ortho* and *ortho→para* scattering ($\Delta J = \pm 1, \pm 3, \cdots$). If, as is the case in liquid hydrogen, the scattering molecules are in their lowest rotational levels ($J=0$ for *para*, $J=1$ for *ortho*) spin forces should cause the *para* and *ortho* cross sections to differ markedly for neutrons of energy insufficient to excite the $0\rightarrow 1$ transition. For neutrons of this energy no inelastic scattering is possible in parahydrogen, while in orthohydrogen the scattering process involving the $1\rightarrow 0$ transition remains.

For slow neutrons whose wave-length is comparable to the distance between the protons in a hydrogen molecule interference effects are important, and it is chiefly in these that cases (2a) and (2b) differ. The phase of a neutron wave scattered by a proton depends on the sign of the binding energy involved, and changes by approximately π when the binding energy changes sign. Hence in case (2a) the scattered waves corresponding to singlet and triplet interaction would have like phases, while in case (2b) they would have opposite phases. Case (2b) brings a possibility of obtaining destructive interference in parahydrogen with its antiparallel proton spins, for here interactions of the singlet and triplet type should occur simultaneously. The scattered waves should interfere destructively, with the result that for low energy neutrons the scattering cross section of parahydrogen should be much smaller than that of orthohydrogen, where this type of interference cannot occur. However, simple calculations based on the idea that the spin of a neutron impinging on a parahydrogen molecule is parallel to one proton spin and antiparallel to the other are not legitimate, although the trends they indicate are in the right direction. Schwinger and Teller have considered the problem more carefully and have given the necessary detailed calculations based on the use of appropriate wave functions.

Experiments to test their predictions, undertaken jointly by Columbia University and the National Bureau of Standards, have been carried out in the Bureau's Low Temperature Laboratory. Preliminary reports[6, 7] have already been published.

Considerations of intensity and geometrical arrangement render it more feasible to perform transmission than scattering experiments. Since the neutron-proton capture cross section[8, 9] is of the order of 0.3×10^{-24} cm^2, less than 1 percent of the average scattering cross section, the difference between the scattering+capture cross section given by transmission experiments and the true scattering cross section is inappreciable. Good geometrical conditions are exceedingly important in transmission experiments. Experiments under other conditions, employing non-parallel neutron beams, and with both source and detector close to the scattering sample have been shown to be especially unreliable with scattering samples containing hydrogen. The uncertain angular distribution of the neutrons, together with large corrections for multiple scattering, slowing down processes, back scattering, etc., make such experiments very difficult to interpret. The design of the present apparatus was such as to make the errors introduced by geometrical factors negligible.

Since the apparatus was well adapted for use with other liquefied gases, the transmissions of liquid O_2 and N_2 were also measured. As a useful check on the accuracy of the work, several measurements were also made with water in the apparatus.

Apparatus and Procedure

The apparatus divides naturally into two parts: one the equipment for preparing and analyzing liquid hydrogen and maintaining it in the path of the neutron beam, and the other the source, detector, and amplifier system. The

[6] J. R. Dunning, J. H. Manley, H. J. Hoge, F. G. Brickwedde, Phys. Rev. **52**, 1076 (1937).
[7] J. R. Dunning, H. J. Hoge, J. H. Manley, and F. G. Brickwedde, Phys. Rev. **53**, 205 (1938).
[8] E. Amaldi and E. Fermi, Phys. Rev. **50**, 899 (1936).
[9] G. A. Fink, Phys. Rev. **50**, 738 (1936).

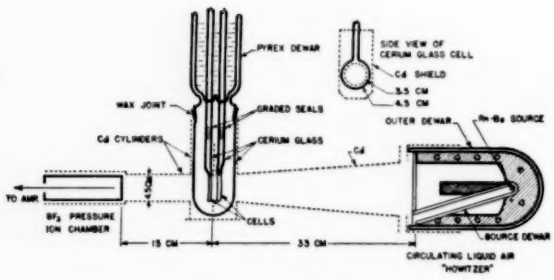

FIG. 1. Arrangement of source and detector relative to scattering sample. Scattering material was condensed in one or both of the two cells in the lower vacuum chamber of the special Dewar flask.

arrangement of this second part of the apparatus is shown in Fig. 1. The sample was contained in either or both of two cerium glass cells which formed part of a specially designed Dewar flask. The Rn-Be source of approximately 500 millicuries was contained in a "howitzer" in which the neutrons were slowed down. This howitzer[10] consisted of a mass of paraffin in the shape of a deep, very thick walled cup contained in a Dewar flask. Copper tubing for the circulation of liquid air was imbedded in the paraffin, and thermocouples were provided at two different points for temperature measurement. Immediately in front of the source was a solid copper cylinder to shield the detector from gamma-rays. The source was placed in a small source Dewar (2 cm diameter) containing a thermocouple and a heater. These were used when the howitzer was cooled with liquid air, to avoid any change in efficiency of the source due to localized condensation of the Rn. When using liquid air it was also necessary to heat the outer copper baffle at the mouth of the howitzer, to prevent the collection of moisture or frost. The effectiveness of the howitzer in cooling the neutrons will be discussed later in the paper.

The neutron beam was well diaphragmed and shielded by cadmium as shown in Fig. 1. The opening in the cadmium diaphragm placed between the two cells was 3.5 cm in diameter, 1 cm less than the diameter of the cells. The detector was an ionization chamber 3 cm in diameter and 13 cm in length, filled to a pressure of 3 atmospheres with BF_3 gas. The average solid angle subtended by the chamber at the cells was less than 0.02 steradian. The chamber was connected to a linear amplifier whose output was recorded by a scale-of-two thyratron counter.

All glass in the path of the neutron beam was a special cerium glass, whose exceptionally low boron content results in very small neutron absorption. Total glass in the path of the beam was about 6 mm, the cell walls being slightly less than a millimeter thick and the Dewar walls slightly more. Total absorption by empty cells, Dewar walls, and silvered surfaces was about 6 percent for room temperature ($\sim$300°K) neutrons. Cell volumes were determined by weighing mercury and diameters by direct measurement. These data gave the mean internal cell thicknesses, which appeared very uniform over the entire area of a cell. In any case only a difference in the mean thickness of the exposed (60 percent) and shielded (40 percent) area of a cell would cause appreciable error. Transmission measurements with water in the cells were used to check the cell thicknesses. Satisfactory agreement was found in all cases except one. In this case (0.234 cm cell) the transmission data were used to determine the thickness of the cell, resulting in a small reduction of the value originally found.

Figure 2 is a diagram of the apparatus used in the preparation and analysis of the liquid hydrogen samples. Glass tubes leading to the cells passed through liquid hydrogen in the upper part of the Dewar. Hydrogen of the desired composition was condensed in these tubes and ran down into the cells. This arrangement permitted the amount of hydrogen in the cells to be kept constant during the course of the measurements, for any hydrogen lost by evaporation was simply recondensed and returned to the cells. Since the level of the liquid in the cells could not be observed, the volume of gas condensed was measured. This was done either by taking the hydrogen from a cylinder or tank of known volume and measuring the fall in pressure, or by using a Toepler pump of known capacity. A considerable margin of safety was allowed, sufficient to bring the level of the liquid well up into the connecting tubes.

Hydrogen to be condensed in the cells was taken from a supply tank of especially prepared electrolytic hydrogen, the purity of which was

[10] P. N. Powers, H. Carroll, J. R. Dunning, Phys. Rev. **51**, 1112 (1937).

believed to be in excess of 99.98 mole percent. This hydrogen was passed over hot copper (600°C) and through a liquid-air trap to remove oxygen, which is an active *ortho-para* conversion catalyst in liquid hydrogen.[11] Passage over hot copper also insured attainment of the high temperature equilibrium concentration of 75 percent *ortho* 25 percent *para* (normal hydrogen). When normal hydrogen was desired in a cell, this gas was condensed directly into it. When parahydrogen was desired, the normal hydrogen was first condensed in a tube containing a conversion catalyst in granular form. The catalyzing chamber was kept at 20.4°K by surrounding it with liquid hydrogen. At this temperature the equilibrium concentration is 99.8 percent parahydrogen.[12]

Hydrogen from the catalyzing chamber was either condensed directly in the cells or stored until needed in a tank which could be filled at liquid-air temperature and emptied at room temperature.

A promoted iron catalyst[13] of the kind used in the synthesis of ammonia was placed at our disposal by Dr. P. H. Emmett. The catalyst, received in the form of an oxide, was prepared for use by reducing in hydrogen at 500°C, outgassing while hot and cooling to 20.4°K before admitting hydrogen again. Liquid hydrogen condensed on the catalyst was allowed to remain in contact with it 15 minutes or longer before use.

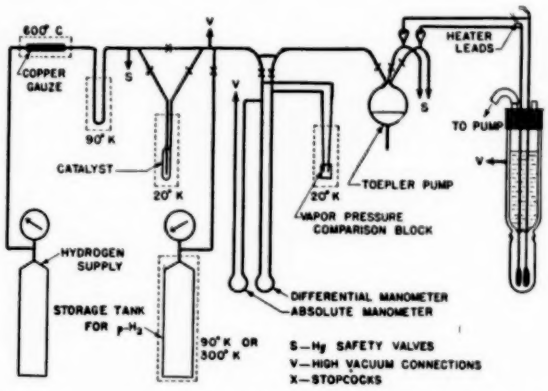

FIG. 2. Apparatus used in the preparation and analysis of the liquid hydrogen samples.

[11] R. B. Scott, F. G. Brickwedde, H. C. Urey, and M. H. Wahl, J. Chem. Phys. **2**, 454 (1934).

[12] R. W. Harkness and W. E. Deming, J. Am. Chem. Soc. **54**, 2850 (1932).

[13] P. H. Emmett and R. W. Harkness, J. Am. Chem. Soc. **57**, 1624 (1935).

The *ortho-para* composition of the contents of any cell was determined immediately after transmission measurements on it had been completed. Brickwedde and Scott[14] have measured the vapor pressures of normal hydrogen, parahydrogen, and mixtures of several intermediate concentrations, using a differential oil manometer to measure the pressure differences. With the aid of their results the composition of an unknown sample of hydrogen may be determined by comparing its vapor pressure with that of normal hydrogen. In the neighborhood of their boiling points the vapor pressures of para- and normal hydrogen differ by about 26 mm Hg; that of *para* is higher. This is approximately 1 mm fall in vapor pressure for each 3 percent increase in *ortho* content. In making an analysis about one-fourth of the contents of a cell was removed; then a sample from the cell and a sample of freshly prepared normal hydrogen were condensed in separate compartments in the vapor pressure comparison block. Their vapor pressure difference was then read on the differential mercury manometer, the total pressure on the normal hydrogen being given by the absolute manometer. The copper comparison block was connected to the glass system by 3 mm copper-nickel tubes.

When parahydrogen (99.8 percent) is condensed in a cell there is no change in composition with time since the material is in equilibrium. With normal hydrogen this is not true, for even with no catalyst present the *ortho* content decreases at the rate of about 1 percent per hour.[11] When analysis of a sample from a cell filled with normal hydrogen showed a composition of, for example, 72 percent orthohydrogen, it was assumed that the composition had changed linearly with time from 75 percent at the time of condensation until the time of analysis. The compositions given in Table I correspond to the mean time of transmission measurement. Strictly the change with time is not quite linear since it depends on collisions between two orthohydrogen molecules. Because the frequency of this type of collision is proportional to the square of the orthohydrogen concentration the corrections were negligible for all "*para*" samples.

It was necessary to reduce the pressure above the liquid hydrogen bath until its temperature

[14] To be published.

fell almost to the triple point before liquid hydrogen would collect in the cells. With the bath at this temperature and the gas pressure in the cell slightly above one atmosphere rapid condensation would begin after 15 or 20 minutes. Liquid was kept in the cells under a pressure of 200–600 mm Hg, the mean temperature of the samples being taken as 18.4°K. To remove liquid a small heating coil of No. 38 constantan wire (50 ohms) was placed in the bottom of each cell, below the edge of the cadmium diaphragm.

Measurements

Each transmission value was computed from the results of from 3 to 6 ten minute counts. Roughly one-third of the counts were taken with a cadmium sheet 0.08 cm thick placed just in front of the howitzer, so that the effect of the high energy cadmium-penetrating neutrons could be determined. After a set of counts a cell was either filled or emptied and another set taken. The normal order was: (1) both cells empty, (2) first (thicker) cell full, (3) both cells full, (4) second cell full (first empty), (5) both cells empty. With both cells empty the approximate number of neutrons counted in 10 minutes was 2500, of which all but approximately 18 percent were cut off by interposing the cadmium sheet. After a series of cell fillings with normal hydrogen a similar series was taken with parahydrogen,

TABLE I. *Transmissions and cross sections (scattering+capture) of para- and normal hydrogen for neutrons of four different energy distributions. T is the neutron temperature; C is the composition in percent of orthohydrogen of the scattering medium; x is the thickness; I/I_0, the transmission; σ, the cross section per molecule.*

T	C % $o-H_2$	x	I/I_0	$-\ln I/I_0 = n\sigma x$	σ(obs.)	σ(obs.) $-\sigma$(calc.)§	Cross Sections of Pure Components (by Extrapolation)
		cm			10^{-24} cm^2	10^{-24} cm^2	10^{-24} cm^2
~300°K	74.2	0.234	0.780	0.249	48.6	−0.2	$\sigma_{ortho}=55.8$
	72.5	0.32	0.705	0.351	50.1	+1.7	
	73.9	0.35	0.695	0.363	47.4	−1.4	
	74.0	0.58	0.538	0.620	48.7	−0.1	
	73.3	0.93	0.371	0.991	48.6	0.0	
	1.7	0.234	0.871	0.139	27.1	−2.3	$\sigma_{para}=29.0$
	1.4	0.32	0.809	0.212	30.1	+0.7	
	3.0	0.58	0.671	0.40	31.4	+1.6	
	2.5‡	0.814	0.593	0.521	29.3	(−0.4)	
~120°K	74.5	0.234	0.720	0.329	64.2	+1.1	$\sigma_{ortho}=78.7$
	73.8‡	0.32	0.656	0.422	60.1	(−2.6)	
	72.6	0.58	0.449	0.80	63.0	+1.1	
	74.0	0.814	0.34	1.079	60.6	−2.2	
	1.4	0.234	0.911	0.092	18.0	−0.4	$\sigma_{para}=17.6$
	4.1	0.32	0.879	0.128	18.3	−1.8	
	6.5	0.58	0.740	0.301	23.6	+2.0	
	5.0	0.814	0.690	0.371	20.8	+0.2	
	5.9, 74.3 } 25.6	0.58, 0.234 } 0.814	0.50*	0.693	38.9	+5.7	
	73.7‡, 16.2 } 57.2	0.58, 0.234 } 0.814	0.39*	0.941	52.7	+0.2	
~120°K filtered through 0.58 cm $n-H_2$	74.2, 73.4	0.58, 0.234	0.769†	0.263	51.1	—	$\sigma_{ortho}=63.0$
	73.7, 16.2	0.58, 0.234	0.878†	0.130	25.4	—	$\sigma_{para}=18.1$
~120°K filtered through 0.58 cm $p-H_2$	5.9, 74.3	0.58, 0.234	0.671†	0.399	77.6	—	$\sigma_{ortho}=100.1$
	6.5, 1.4	0.58, 0.234	0.932†	0.070	13.8	—	$\sigma_{para}=12.6$

* Transmission of both cells considered as a unit, one containing $p-H_2$, the other $n-H_2$.
† Transmission of second cell for filtered beam from first cell.
‡ Estimated.
§ Deviations from linear equations of Fig. 3.

TABLE II. *Transmissions of liquid O_2 and N_2 and cross sections (scattering+capture) per atom for ~300°K neutrons. The thickness is designated by x. I/I_0 is the transmission and σ is the cross section.*

MATERIAL	x	I/I_0	$-\ln I/I_0 = n\sigma x$	σ	AVERAGES
	cm			10^{-24} cm²	10^{-24} cm²
Liquid O_2	0.35	——	——	——	$\sigma(0)=4.05$
	0.58	0.905	0.995	3.98	
	0.93	0.847	0.166	4.12	
Liquid N_2	0.35	0.870	0.140	11.5	$\sigma(N)=12.7$
	0.58	0.761	0.273	13.5	
	0.93	0.657	0.420	13.0	

TABLE III. *Transmission of water and the cross sections (scattering+capture) of (1) water per molecule and of (2) the protons of water per proton, for neutrons of ~300°K. and ~ 120° K. T is the neutron temperature; x is the thickness; I/I_0 is the transmission; $\sigma_p=\frac{1}{2}(\sigma(H_2O)-\sigma(0))$. Average for "room temperature" neutrons $\sigma_p=42.2\times10^{-24}$ cm². The 0.93 cm thickness was not used in obtaining this value.*

T	x	I/I_0	$-\ln I/I_0 = n\sigma x$	$\sigma(H_2O)$	σ_p
	cm			10^{-24} cm²	10^{-24} cm²
~300°K	0.23_4	0.495	0.703	....	....
~270°K	0.32	0.370	0.994	92.0	44.0
~300°K	0.35	0.349	1.05	89.1	42.5
"	0.58	0.190	1.66	85.0	40.5
"	0.58	0.170	1.77	90.5	43.2
"	0.93	0.079	2.54	81.2	38.6
~120°K	0.23_4	0.400	0.915	116.0	56.0

all with the howitzer at room temperature. Then the howitzer was cooled with liquid air to approximately 100°K and the process repeated. In this condition the transmission was also measured with parahydrogen in the first cell, normal hydrogen in the second, and vice versa. Data on the cadmium penetrating background have not been included in the tables. This background has in all cases been subtracted to give the transmission values reported. Data for hydrogen are given in Table I. In calculating the cross sections, n the number of molecules per cm³ was taken from the results of Scott and Brickwedde.[15] It is interesting to note that because of the large thermal expansion of liquid hydrogen this number is approximately 3 percent greater at 18.4°K than at 20.4°K, the boiling point of normal hydrogen.

The procedure with liquid O_2, N_2, and H_2O was similar to that with hydrogen except that no measurements on O_2 and N_2 were made while the howitzer was cooled with liquid air. Data for liquid O_2 and N_2 are given in Table II; for water in Table III.

DISCUSSION OF RESULTS

The dependence of cross section on composition and on neutron energy is shown in Fig. 3, where cross section per hydrogen molecule has been plotted against percent orthohydrogen in the scattering layer. Each of the four straight lines refers to neutrons of a different energy distribution. The equations of the lines were determined simply to make the sum of the deviations zero for the *para* group of points and likewise zero for the points taken with normal hydrogen. The intercepts of these lines on the 0 and 100 percent axes give the cross sections of pure para- and pure orthohydrogen for neutrons of each energy distribution. The values of these intercepts are given in the last column of Table I. The use of linear extrapolation requires some justification. For very thin layers a linear relation between cross section and composition is to be expected, since this requires only that the cross section of an individual molecule be independent of whether its neighbors are para- or ortho-molecules. For thick layers a nonlinear relation is to be expected because of multiple scattering. The geometry of the present apparatus was such as to minimize any complications due to multiple scattering, since a neutron was effectively removed from the beam by its first collision, its subsequent history being of no importance. The transmission curves for water (Fig. 4) which has approximately the same proton density as liquid hydrogen showed a reasonably smooth exponential decrease which is experimental evidence that multiple scattering was not significant.

The energy distribution of the neutrons is the most uncertain factor in the interpretation of the results. This depends on the effectiveness of the howitzer in cooling down the neutrons from their high energy and establishing something of the nature of a Maxwellian distribution. A howitzer similar to the one used in these experiments had previously been tested with a velocity selector.[16–18] With the howitzer at room tempera-

[15] R. B. Scott and F. G. Brickwedde, J. Chem. Phys. **5**, 736 (1937).

[16] J. R. Dunning, G. B. Pegram, G. A. Fink, D. P. Mitchell, E. Segrè, Phys. Rev. **48**, 704 (1935).

[17] G. A. Fink, J. R. Dunning, G. B. Pegram, D. P. Mitchell, Phys. Rev. **49**, 103 (1936).

[18] G. A. Fink, Phys. Rev. **50**, 738 (1936).

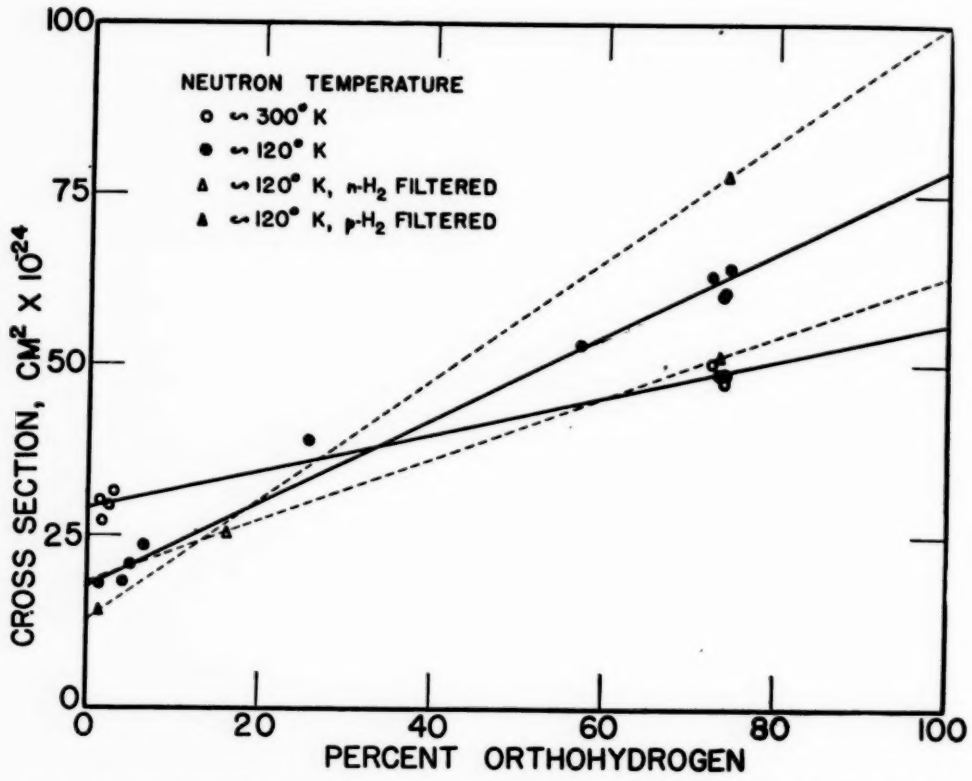

FIG. 3. Dependence of neutron cross section (scattering + capture) per molecule on *ortho-para* composition of the liquid hydrogen scattering sample. Each straight line refers to neutrons of a different energy distribution. The indicated temperatures are only approximate.

ture the emergent neutrons absorbable in cadmium were found to possess a distribution whose maximum corresponded approximately to thermal equilibrium with the paraffin. However, it was shown that more high energy neutrons were present than in a true Maxwellian distribution. The effect of all high energy neutrons above the cadmium absorption limit (about 0.4 ev[19, 20]) is eliminated by the cadmium difference method, but there still remains a long high energy "tail" extending up to about 0.4 ev.

The obtaining of a beam of neutrons with a Maxwellian distribution of velocities characteristic of liquid-air temperatures is of greater difficulty than for room temperatures.[16–18, 21, 22] The cooling efficiency of the howitzer used in these experiments was investigated by Mr. P. N. Powers of Columbia University, who measured the absorption of the emerging neutrons in boron. Using the cadmium difference method, he found that the absorption cross section of the neutrons in boron was 1.6 times greater when the howitzer was cooled with liquid air than when it was at room temperature.

Experiments have indicated that absorption in boron follows the $1/v$ law[23, 24] hence, if T_1 and T_2 are the "effective" temperatures of the neutron beams obtained when the howitzer is at room temperature and when it is cooled with liquid air, respectively, we have

$$(T_1/T_2)^{\frac{1}{2}}=1.6. \qquad (1)$$

The two imbedded thermocouples indicated that the average temperature of the paraffin was approximately 105°K while liquid air was being circulated. In the ideal case in which the neutron

[19] O. R. Frisch and G. Placzek, Nature **137**, 357 (1936).
[20] J. G. Hoffman and M. S. Livingston, Phys. Rev. **52**, 1228 (1937).
[21] O. R. Frisch, H. von Halban, Jr., Jørgen Koch, Nature **139**, 922 (1937).
[22] P. B. Moon and J. R. Tillman, Proc. Roy. Soc. **A153**, 476 (1936).
[23] F. Rasetti, E. Segrè, G. Fink, J. R. Dunning, G. B. Pegram, Phys. Rev. **49**, 104 (1936).
[24] F. Rasetti, D. P. Mitchell, G. A. Fink, G. B. Pegram, Phys. Rev. **49**, 777 (1936).

beams would be in thermal equilibrium with the paraffin at either temperature and the BF_3 receiver counted all neutrons passing through it, this ratio would be $(300°/105°)^{\frac{1}{2}}=1.69$. Eq. (1) cannot be used to calculate T_1 or T_2 unless some assumption is made concerning the relative effectiveness of paraffin at 300°K and at 105°K in reducing the effective temperatures of the neutrons. The effective temperatures must be higher than the temperature of the paraffin. However, it does not seem probable that they are very much higher since with Eq. (1) this would lead to a much larger difference in neutron temperatures than the change in the temperature of the paraffin. Since T_1 cannot be less than 300°, T_2 cannot be less than 117° which corresponds to a mean energy of 0.015 ev. This difference in temperature will make a considerable difference in the fraction of the neutrons having energies greater than 0.023 ev, which is the minimum energy required to excite the O→1 transition, giving rise to inelastic scattering in $p-H_2$. We are therefore referring to the neutrons as ~300°K and ~120°K neutrons to emphasize the fact that the effective temperature of the cold neutrons is above the temperature of the howitzer.

Since the absorption of neutrons in boron depends upon their velocity, the fraction of the neutrons entering the BF_3 receiver that are counted depends upon the velocity distribution of the neutrons. The receiver used in this investigation would absorb and count about 40 percent of an ~300°K neutron energy distribution. In accordance with the $1/v$ law a larger percentage of the slower neutrons than of the faster ones should be counted. Since in each transmission measurement counts are taken both with and without the scattering sample in the beam, the detector will introduce an error only if the energy distribution of the neutrons is altered by passage through the scattering sample. Since the scattering is to some extent selective this will necessarily be the case. The calculation of this correction is difficult even when the velocity distribution of the neutrons is known. In our experiments the velocity distribution was not exactly known and no correction of this kind has been applied to the measurements. The correction, however, is believed to be small.

This uncertainty in energy distribution is unfortunately characteristic of experiments involving slow neutrons, and is almost always the chief limiting factor in the interpretation of results. It seems probable that the possibility of using parahydrogen as a neutron filter brought out by the present experiments may help to clear up this situation. The use of two separate cells for liquid hydrogen (suggested by Professor Teller) made it possible to study the effect of filtration. By placing parahydrogen in the first cell, a filtered beam was obtained which could then be investigated by placing scattering material in the second cell. As a matter of interest measurements were also made using a normal hydrogen filter, so that in all four different neutron energy groups were investigated. These are designated as ~300°K, ~120°K, ~120°K *para*-filtered, and ~120°K normal-filtered.

It is evident from Fig. 3 that the scattering cross section is sensitive both to hydrogen composition and to neutron temperature. The dependence of cross section on composition increases with decreasing neutron energy. The slope of the ~300°K neutron curve is least, that of the ~120°K neutron curve is greater, while the slope of the *para*-filtered neutron curve is still greater. To see that this last result fits into the picture it should be remembered that according to Schwinger and Teller's theory parahydrogen should be practically transparent for neutrons of less than 0.023 ev. Hence the effect

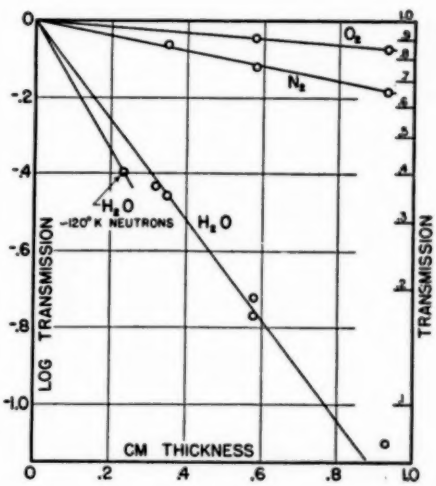

FIG. 4. Transmission of neutrons by water, liquid O_2 and liquid N_2. Neutron temperature ~300°K except as noted.

of *para*-filtration should be to remove high energy neutrons from the ~120°K beam and effectively cool it still further. The curve for normal-hydrogen-filtered neutrons is less interesting and more difficult to interpret. The 25 percent of parahydrogen in the filtering layer would tend to remove high energy neutrons from the beam, while the 75 percent of orthohydrogen would work somewhat in the opposite direction. Less weight is to be given to the dotted curves than to those for ~300°K and ~120°K neutrons, both because of the fewer experimental points involved, and because of the larger number of measurements required to determine a single point.

Figure 3 shows that the *para* cross section is consistently smaller than the *ortho* cross section. This one fact is sufficient to eliminate the possibility of an interaction independent of spin (case 1 discussed in the introduction) for if there were no spin dependence the differences should be in the opposite direction. The problem becomes therefore one of distinguishing between the two cases involving spin dependent forces, (2a) a real singlet deuteron level, and (2b) a virtual singlet deuteron level. Schwinger and Teller[4] have shown that the dependence of the *para* cross section on neutron energy will be very different in the two cases. If the singlet level is real the *para* cross section should be slightly greater (about 30 percent) for "liquid air" (0.012 ev) neutrons than for "room temperature" (0.037 ev) neutrons, while if the singlet level is virtual the cross sections for "liquid air" neutrons should be ~100 times smaller. Moreover if the singlet state should be real the orthohydrogen cross section would be only about 40 percent greater than the parahydrogen cross section for liquid air neutrons, whereas for a virtual state the difference may be very large. Fig. 3 shows (1) that there is a marked decrease in the *para* cross section with decreasing neutron energy and (2) that the ratio of the *ortho* to *para* cross sections for the ~120°K neutron distribution was 4 : 1. Our results therefore prove conclusively that the singlet state of the deuteron is virtual. This confirms the work of Halpern, Estermann, Simpson and Stern.[25] Taking a more general view of the matter it may be said that the virtual level hypothesis is the only one which leads to large differences in the *para* and *ortho* cross sections, and that none of the other possibilities can account for differences as large as those observed.

As Schwinger[5] pointed out, these results also require that the neutron spin be $\frac{1}{2}$ rather than $\frac{3}{2}$.

The presence of the tail of high energy neutrons unfortunately makes it impossible to gain any information concerning the range of the neutron-proton forces from our experiments. The fact that the observed cross section of parahydrogen for ~120°K neutrons is not as small as the theory predicts is to be attributed to these high energy neutrons, whose inelastic scattering completely masks the small elastic *para* scattering (0→0) which depends sensitively on the range of the neutron-proton forces.

It should be borne in mind that Schwinger and Teller's calculations give cross sections not as a function of temperature, but as a function of the energy of a monochromatic neutron beam. Also their calculations are strictly applicable only to hydrogen in the gaseous state, whereas our measurements apply to the liquid. These facts, together with the excess of high energy neutrons in the distributions with which we worked, are sufficient to account for the differences between our results and the predictions of Schwinger and Teller. Specifically, they are sufficient to account for the fact that the *ortho* cross section increases somewhat more rapidly with decreasing neutron "temperature" than was predicted, while the *para* cross section does not decrease as rapidly.

The possibility referred to earlier of using parahydrogen as a filter to obtain slow neutrons does not at first sight appear extremely promising. The ratio 29.0/17.6 found for the cross sections of parahydrogen for ~300°K and ~120°K neutrons is far from the 100 to 1 ratio[26] predicted by Schwinger and Teller for 0.037 and 0.012 ev neutrons. However, the mean energy ($3KT/2$) corresponding to 120°K is not 0.012 but 0.015 ev, and it must be remembered that 300°K and 120°K are to be interpreted not as actual temperatures but as lower limits. It seems reasonable

[25] J. Halpern, I. Estermann, O. C. Simpson and O. Stern, Phys. Rev. **52**, 142 (1937).

[26] As the authors point out this figure cannot be considered as a precise estimate, since it depends on the assumed range of the force of interaction.

therefore that a considerable number of the ~120°K neutrons should have energies greater than 0.023 ev, which is the point at which 0→1 scattering begins to take place and the *para* cross section begins to increase rapidly. It seems probable therefore that the ratio of *para* cross sections for 0.037 and 0.012 ev neutrons is actually much larger than 29.0/17.6. A layer of parahydrogen of suitable thickness should therefore transmit neutrons in the low energy range of a Maxwell distribution, and cut off rather sharply at an energy of 0.023 ev. Such a low energy beam should be quite useful in experimental work.

In the actual transmission measurements and calculations of cross sections, the chief errors involved are in cell thickness, composition of the hydrogen, and statistical fluctuations of the counts. Of these the largest is probably in the determination of cell thicknesses. Although this will affect the absolute values of the cross sections it will have very little influence on the relative values for different *ortho-para* compositions. Boiling may reduce the effective thickness of material in a cell. An estimate of the rate of heat transfer to the cells by radiation indicated that the amount of gas produced by evaporation in one second would not fill more than 2 percent of the cell volumes. We have observed in other experiments that the bubbles in liquid hydrogen are small and rise rapidly. Errors due to the presence of bubbles should be of the order of 1 percent. Uncertainty in the measurement of the composition is 1 percent. The number of counts was sufficient to make the probable error due to statistical fluctuations less than 2 percent. The combined error due to all the above factors certainly cannot be greater than 10 percent.

The results of the measurements on liquid N_2, O_2, and H_2O are in substantial agreement with previous values.[8, 9, 27] Log transmission has been plotted against scattering thickness in Fig. 4. In obtaining proton cross sections from the water measurements the value 4.0×10^{-24} cm² for the cross section of oxygen was taken from Table II. The same value was used for both the ~300°K and ~120°K neutrons since no information on the temperature dependence was available. The ratio of the proton cross sections in water thus obtained is $\sigma_{120}/\sigma_{300}=1.29$. Errors in these measurements are substantially the same as in the hydrogen measurements.

The authors wish to express their appreciation of the cooperation of Director Lyman J. Briggs of the National Bureau of Standards and Dean George B. Pegram of Columbia University which made these experiments possible. They are also indebted to Professor Edward Teller of the George Washington University and to Mr. Julian Schwinger of Columbia University for valuable discussion and advice.

[27] M. Goldhaber and G. H. Briggs, Proc. Roy. Soc. **A162**, 127 (1937).

AUGUST 15, 1938 PHYSICAL REVIEW VOLUME 5

The Isotopic Constitution of Strontium, Barium, Bismuth, Thallium and Mercury

ALFRED O. NIER*
Research Laboratory of Physics, Harvard University, Cambridge, Massachusetts

(Received June 18, 1938)

A mass-spectrographic study of the isotopic constitution of Sr, Ba, Bi, and Tl has been made. Although the sensitivity and resolving power of the apparatus were sufficient to detect extremely rare isotopes, no new ones were found. Relative abundances of the isotopes of Sr, Ba, and Tl were determined. It was possible to show that if Hg^{203} exists it must be with an abundance less than one-tenth of that at one time assigned to it by Aston.

ALTHOUGH a knowledge of the existence or nonexistence of rare stable isotopes is of great value in the study of nuclear physics, relatively few elements have been investigated with apparatus capable of detecting isotopes present in only small amounts. The present paper is a report on the continuation of a sys-

* National Research Fellow.

tematic program, the aim of which is to establish the existence or nonexistence of possible rare isotopes, as well as to determine the relative abundances of the accepted stable ones. Because of the extremely high sensitivity and resolving power of the apparatus it is possible to extend the search for rare isotopes beyond previously attainable limits.

Apparatus

A description of the mass spectrometer employed has already been given.[1] It may be described briefly as an apparatus in which positive ions are formed by the collision of a controlled beam of low energy electrons with the gas or vapor of the elements to be studied. The positive ions are drawn from the ionizing region by suitable electric fields and the m/e analysis is accomplished by means of a 180° magnetic analyzer. Inasmuch as the analyzed ion current is measured by means of an electrometer tube it is relatively easy to obtain accurate determinations of relative abundances. Because of the fact that the metal parts of the mass spectrometer tube are constructed entirely of Nichrome, copper, and tungsten, and are surrounded by a Pyrex envelope without grease or wax joints, the tube may be thoroughly baked, and hence, little difficulty is encountered with impurities. In the study of relatively nonvolatile substances such as Sr, Ba, Bi, and Tl, the element is placed in a small Nichrome furnace inside of the spectrometer tube. The furnace may be heated to a temperature as high as 1200°C and the stream of vapor emitted passes into the electron beam where ions then are formed. For the investigation of volatile substances the furnace is, of course, unnecessary, and the gas or vapor can be admitted to the tube through a capillary leak or by some other means.

In the present work the slits shown in Fig. 1 of reference 1 had the following widths: $S_1 = 0.007''$, $S_2 = 0.006''$, and S_3, the exit slit of the 180° analyzer (not shown in the figure) $= 0.006''$ for Hg, Tl, and Bi; $0.018''$ for Sr and Ba.

Results

Strontium

A clean sample of strontium metal obtained from Eimer and Amend, labeled 99.9 percent pure, was placed in the small furnace, shown in Fig. 1 of reference 1. After thorough baking of the tube to remove impurities, work was begun. It was found that a furnace temperature of the order of 700°C gave sufficiently large positive ion currents without too great a rate of consumption of strontium. A typical mass spectrum is shown in Fig. 1. The isotopes observed were the same as those reported by other investigators.[2–5] In Table I are given the relative abundances found in the present work as well as those given by Sampson and Bleakney.[4] The results are seen to be in good agreement. The writer believes his relative abundances as measured for Sr^{87} and Sr^{86} relative to Sr^{88} to be correct within one percent, while that given for Sr^{84} may be in error by two percent. A possible source of error not taken into account in these measurements is the effect of the free evaporation of Sr atoms from the small furnace. In the case of *ideal* distillation this would mean that the Sr^{84}/Sr^{88} ratio as measured would be $(88/84)^{\frac{1}{2}} = 1.023$ times greater than the true ratio. However, as the Sr atoms are evaporated from a solid surface

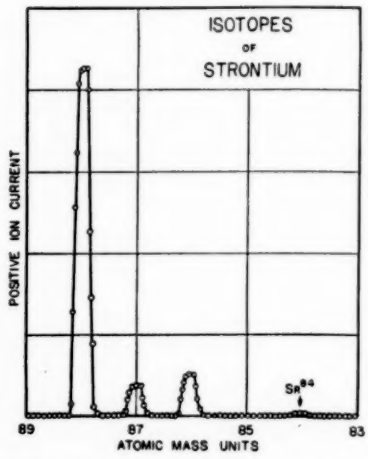

Fig. 1. Mass spectrum showing isotopes of strontium. The experimental points are obtained by plotting positive ion current passing through the exit slit of the analyzer as a function of the energy of the ions while the magnetic field is held constant. As there is a definite relation between the energy and the mass of the ions collected, namely, energy × mass = a constant, the voltage scale can be readily changed to a mass scale, as was done in the figure. The width of the peaks is, of course, due to the finite width of the slits used and the imperfections in focusing.

[1] Nier, Phys. Rev. **53**, 282 (1938).

[2] Blewett and Sampson, Phys. Rev. **49**, 778 (1936).
[3] Dempster, Phys. Rev. **50**, 186 (1936).
[4] Sampson and Bleakney, Phys. Rev. **50**, 456 (1936).
[5] Mattauch, Akad. Wiss. Wien Ber. **145**, 461 (1936).

and not from a liquid (where mixing of particles on the surface with those inside can take place) it does not seem likely that one would have appreciable discrimination.

If one assumes the packing fraction of strontium to be that found by Mattauch[6] for Sr^{86}, namely, -9.0 ± 0.5, and if one uses a conversion factor 1.000275 in going from the physical to the chemical scale, an atomic weight 85.61 is computed for strontium from the writer's as well as from Sampson and Bleakney's relative abundances. On the other hand, if one assumes the packing fraction of Sr to be the same as that found by Aston[7] for Kr^{86}, namely -7.40, the atomic weight 85.62 is computed. From the packing fraction -6.3, deduced from Dempster's[8] packing fraction curve, one obtains the atomic weight 85.63. The chemically determined value is accepted as 85.63.

The real reason for studying strontium was for the purpose of searching for possible rare isotopes. By analogy to most of the heavier even elements one might expect to find strontium to consist of a sequence of isotopes having successive mass numbers flanked by a light isotope two units removed from the lightest isotope in the sequence and a heavier isotope two units above the heaviest isotope in the sequence. Thus, on this basis, one should expect to find a stable isotope, Sr^{90}. However, a careful investigation of this position as well as the other vacant positions around the known stable isotopes failed to show even the faintest trace of any new isotope. It was possible to set the following upper limits for abundances in these positions relative to Sr^{88}: Sr^{92}, Sr^{91}, and Sr^{90}, 1/300,000; Sr^{89}, 1/100,000; Sr^{85}, 1/50,000; Sr^{83}, 1/100,000; Sr^{82}, Sr^{81}, and Sr^{80}, 1/200,000.

Barium

Barium metal obtained from Eimer and Amend, labeled 99 percent pure, was employed as a source of barium. The procedure was the same as that used for strontium. Fig. 2 shows a typical mass spectrum obtained. An idea of the sensitivity of the apparatus is gained when one considers that the points for the rare isotopes, Ba^{132} and Ba^{130}, are plotted to a scale 100 times that for the other isotopes. The isotopes found are the same as those reported by Dempster[9] and Sampson and Bleakney.[4] Table II gives the relative abundances found in the present work, together with the abundances as given by Sampson and Bleakney. The writer believes his abundances relative to Ba^{138} all to be correct within two percent except the ones for Ba^{132} and Ba^{130}, which may be in error by four percent. As in strontium the evaporation of the atoms takes places from the surface of a solid, and hence, one should expect little, if any, separation to take place in the evaporation process.

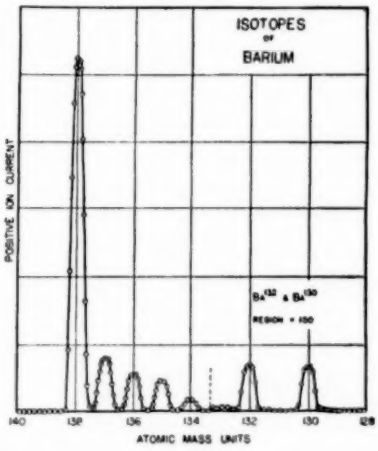

FIG. 2. Mass spectrum showing the isotopes of barium. Current scale in region of Ba^{132} and Ba^{130} is multiplied by a factor of one hundred.

If one assumes the packing fraction of barium to be the same as that given recently by Aston[7] for Xe^{132}, -4.4, and if one uses a conversion factor 1.000275 in going from the physical to the chemical scale, an atomic weight 137.33 is obtained from the writer's data. With a packing fraction -4.0, as deduced from Dempster's[8] curve, the value 137.33 is also found. The chemically determined value is given as 137.36.

As in the case of strontium, the main purpose in investigating barium was to search for possible

TABLE I. *Relative abundances of isotopes of strontium.*

	88	87	86	84	MEAN MASS NUMBER
Abundance	100	8.50	11.94	0.68	87.710
S. & B. values	100	9.10	11.64	0.61	87.713

[6] Mattauch, Naturwiss. **25**, 170 (1937).
[7] Aston, Nature **140**, 149 (1937).
[8] Dempster, Phys. Rev. **53**, 869 (1938).
[9] Dempster, Phys. Rev. **49**, 947 (1936).

TABLE II. *Relative abundances of isotopes of barium.*

	138	137	136	135	134	132	130	MEAN MASS NO.
Abundance	100	15.8	10.9	9.2	3.37	0.136	0.141	137.42
S. & B. values	100	14.9	11.7	7.8	2.35	0.022	0.22	137.47

rare isotopes. However, none was found, and it was possible to set the following upper limits for abundances of hypothetical isotopes relative to Ba^{138}: Ba^{142}, 1/200,000; Ba^{141} and Ba^{140}, 1/100,000; Ba^{139}, 1/35,000; Ba^{133}, Ba^{131}, Ba^{129}, and Ba^{128}, 1/100,000.

Bismuth

Aston[10] found bismuth to consist of a single isotope of mass 209. This fact was verified by Bainbridge and Jordan[11] who showed that no other isotope existed with an abundance greater than two percent. From the present study one can set the following upper limits of abundance for the existence of hypothetical isotopes relative to Bi^{209}: Bi^{213}, Bi^{212}, and Bi^{211}, 1/100,000; Bi^{210} and Bi^{208}, 1/50,000; Bi^{207}, Bi^{206}, and Bi^{205}, 1/100,000. Bismuth is thus seen to be single to a very high degree, indeed.

Thallium

Thallium, an element having an odd atomic number, was found by Schüler and Keyston[12] to consist of two isotopes having the masses 203 and 205. The abundance ratio 203/205 was given as 0.435. The existence of these two isotopes was verified by Aston.[13] As it appears to be a general rule that odd elements do not have more than two stable isotopes it did not seem likely that any additional ones would be found. However, very few elements have been investigated with apparatus capable of detecting truly rare isotopes, and hence a study of thallium is of interest if for no other reason than to better establish the validity of the rule.

Chemically pure thallium metal, obtained from Eimer and Amend, was used as a source of thallium. The 203/205 ratio was found to be 0.410 ± 2 percent, a number in excellent agreement with the ratio 0.417 found by Aston. As the evaporation of the metal takes place from the liquid phase the abundance ratio as measured may be high by a factor, $(205/203)^{\frac{1}{2}} = 1.005$, due to the effect of ideal distillation. Account was taken of this factor in arriving at the number 0.410.

The abundance ratio found corresponds to a mean mass number 204.42 ± 0.01. With a packing fraction of $+2.0$ derived from Dempster's[14] data and a conversion factor 1.000275 in going from the physical to the chemical scale, an atomic weight 204.40 is computed from the writer's data. This is to be compared with a chemically determined value 204.39.

No new isotopes were found, and it was possible to set the following upper limits of abundance for the existence of possible rare ones relative to Tl^{205}: Tl^{209}, Tl^{208}, Tl^{207}, and Tl^{206}, 1/50,000; Tl^{204} and Tl^{202}, 1/30,000; Tl^{201}, Tl^{200}, and Tl^{199}, 1/50,000.

Mercury

Hg^{203} was at one time reported by Aston[15] to exist as a stable isotope with an abundance approximately 1/5000 that of Hg^{202}. Recently the writer[16] undertook a search for this isotope, but because of limited resolving power was able to conclude only that if it existed at all it must be with an abundance less than that assigned to it by Aston. In the present work on Bi and Tl the resolving power of the apparatus was somewhat higher than was the case in the earlier work, mainly because of the narrower slits used. With a pressure of around 10^{-5} mm of Hg in the tube, the sensitivity was sufficient to show definitely that if Hg^{203} existed it must be with an abundance less than 1/50,000 that of Hg^{202}.

[10] Aston, Phil. Mag. **49**, 1197 (1925).
[11] Bainbridge and Jordan, Phys. Rev. **50**, 282 (1936).
[12] Schüler and Keyston, Zeits. f. Physik **70**, 1–2, 1 (1931).
[13] Aston, Proc. Roy. Soc. **A134**, 571 (1932).
[14] Dempster, Phys. Rev. **53**, 64 (1938).
[15] Aston, Nature **130**, 847 (1932).
[16] Nier, Phys. Rev. **52**, 933 (1937).

Domain Theory of Ferromagnetics Under Stress*

Part III. The Reversible Susceptibility

WILLIAM FULLER BROWN, JR.
Columbia University, New York, N. Y.

(Received June 20, 1938)

It is shown that the statistical theory of Parts I and II can be extended so as to give formulas for the magnetization curve and other properties of an ideal reversible specimen, over the range of field values in which magnetization proceeds by a displacement of the boundaries between domains. The application to actual specimens is made by assuming that the reversible properties of an actual specimen are identical with the properties, at the same magnetization, of an ideal specimen having the same initial susceptibility. This leads to a formula for the reversible susceptibility of nickel and iron that was originally suggested by Gans and verified by him experimentally, but for which it is believed no satisfactory derivation has hitherto been offered. In the case of one nickel specimen and of cobalt, where the data do not follow the Gans curve, formulas agreeing better with experiment are obtained by taking account of the anisotropy of the domains. Reasons are given for believing that the replacement of variable by fixed domain volumes, an arbitrary step taken in order to simplify the problem, is probably not essential to the result.

THE behavior of ferromagnetic crystals at fields of order of magnitude 10^2 oersteds has been satisfactorily explained[1] by supposing that an increase of field causes a "rotation" of the magnetization vector toward the field direction. This vector has a constant magnitude, the saturation value J_s; and except in special cases, it has also a uniform direction throughout each crystal—the direction for which the free energy, consisting of a term due to the field and a term due to the crystalline anisotropy forces, is a minimum. The special cases just referred to are those in which there are several such directions, as is the case when the field direction is [110] or [111] in an iron crystal. In these cases the crystal is saturated not as a whole, but only throughout "domains," equal volumes being magnetized in each of the equivalent directions. The properties of large grained polycrystalline specimens in this same range of field values can be calculated by averaging those of crystals.[2]

At fields of order of magnitude 1 oersted, the process is different and a successful quantitative theory is still lacking. Certain fundamental ideas, however, have proved useful and are probably essentially correct. It is supposed that even in the demagnetized state the specimen is saturated throughout domains; equal volumes are magnetized in each of the possible directions, which are now the directions of minimum free energy determined by the anisotropy forces alone—the "directions of easy magnetization." When a field is applied and gradually increased, the electron spins responsible for the magnetization undergo transitions in the boundary region between domains; the effect is a motion of the boundary, so that the more favorably oriented domains grow at the expense of their less favorably oriented neighbors. This displacement of the boundaries is in part reversible, proceeding an infinitesimal distance dx when the field is changed by an infinitesimal amount dH; and in part irreversible, for when a small change of field enables the boundary to pass a local energy barrier, the motion may continue a considerable distance, with dissipation of energy through the setting up of local eddy currents and in other ways.

The most direct evidence of the correctness of this picture is obtained from measurements of the Barkhausen effect[3] and from the study of magnetic powder and colloid patterns.[4] The regions whose reversal of magnetization is

* Publication assisted by the Ernest Kempton Adams Fund for Physical Research of Columbia University.

[1] An outline of the theory and references to the original papers are given in E. C. Stoner, *Magnetism and Matter* (1934), pp. 392 ff., and F. Bitter, *Introduction to Ferromagnetism* (1937), pp. 194 ff.

[2] R. Gans, Ann. d. Physik **15**, 28 (1932).

[3] For references see Stoner, reference 1, p. 436.

[4] F. Bitter, reference 1, pp. 59 ff.; W. C. Elmore, Phys. Rev. **51**, 982 (1937); **53**, 757 (1938).

observed in the Barkhausen effect, although not necessarily identical with the domains, at least set a lower limit to their order of magnitude. It is consistent with the order of magnitude of the dimensions observed in surface powder patterns, but the latter method of study shows that the actual shapes and arrangements of the differently magnetized regions may be very complicated.

Various types of force are operative in this process. The exchange forces are important only in the boundaries between the domains, where their partial annihilation has the effect of a positive surface energy proportional to the total area of the interdomain surfaces, and therefore plays a role in determining the size of the domains. This size in fact seems to be determined primarily by a balance between these forces and magnetic forces dependent upon the size and shape of the specimen, so that the domain size varies approximately as the square root of the shortest dimension of the specimen.[5] The anisotropy forces are important chiefly at higher fields, but according to one theory[6] they are also instrumental in determining the thickness of the interdomain space and hence indirectly the size of the domains. The theory of the behavior of an ideal crystal in an applied field has been attacked by several authors,[5–7] but even in the simplest cases the problem is difficult because nonlinear partial differential equations occur at the outset.

In an actual crystal, though the order of magnitude of the domain size is probably determined by the factors already mentioned, the exact behavior in a field is dependent very largely on forces that vary irregularly from one point to another. Chief among these are internal stresses due to impurities or to imperfect annealing. When these have been reduced to a minimum, there remain unavoidable stresses resulting from the unequal magnetostriction of differently oriented domains. Becker[8] has shown how the internal stresses limit the initial susceptibility in a somewhat idealized model, and Kersten[9] has shown that the magnitude of the highest attainable initial susceptibility in iron-nickel alloys of various compositions is adequately accounted for by setting the internal stress equal to the lower limit determined by magnetostriction. In addition to this effect of mild stresses in controlling the reversible boundary displacement, there is the irreversible effect of local high stresses, which set up energy barriers that lead to Barkhausen reversals and hence to hysteresis.[10]

The importance of irregular forces suggests the possibility of handling the problem by a statistical method, in which the exact nature of the process need not be considered in detail. This method of attack was originated by Heisenberg. The quantities that have so far been calculated by it are the magnetostriction as a function of magnetization; the normal component of magnetization as a function of the component parallel to the field; and the elastic constants as functions of magnetization, given the magnetization curve. In parts I and II under the present title,[11] previous work in this field was summarized, more general formulas were developed, and some errors in earlier calculations were pointed out and corrected. No new principles were introduced, except the device of using thermodynamic relations to eliminate certain unknown quantities; by this means it was possible to avoid an incorrect approximation made in some of the earlier work.

It is possible to extend the theory so as actually to calculate the magnetization curve of an ideal reversible specimen, and from this all the reversible properties of an actual specimen, given a single reversible property—the initial susceptibility. This extension is the subject of the present paper; but in order to make the presentation convincing and to insure against misinterpretation of the results, it will be necessary to review the entire theory briefly, from a somewhat different point of view.

A few general remarks will make the aim clearer. The Becker-Kersten rotation theory, applicable only when the internal stresses σ_i are large and fairly uniform over a domain, gives for

[5] J. Frenkel and J. Dorfman, Nature **126**, 274 (1930).
[6] L. Landau and E. Lifshitz, Physik. Zeits. Sowjetunion **8**, 153 (1935).
[7] F. Bitter, reference 1, pp. 185–192.
[8] R. Becker, Physik. Zeits. **33**, 905 (1932).
[9] M. Kersten, Zeits. f. Physik **12**, 665 (1931).
[10] E. Kondorsky, Physik. Zeits. Sowjetunion **11**, 597 (1937).
[11] W. F. Brown, Phys. Rev. **52**, 325 (1937); **53**, 482 (1938): hereafter cited as I and II, respectively.

the initial susceptibility $\chi_0=(2/9)J_s^2/\lambda_\infty\sigma_i$; λ_∞ is the saturation magnetostriction. Becker's simplified theory of boundary displacement against small, inhomogeneous stresses of amplitude σ_i gives $\chi_0=(1/\pi)J_s^2/\lambda_\infty\sigma_i$. Although the mechanisms assumed are entirely unlike, the results are practically identical. Again, it is possible to develop a theory similar to that of Becker and Kersten, except that internal stresses are replaced by internal fields; the result of either theory may be written in the form $\chi_0 \leqq J_s^2/\epsilon$, where ϵ is an energy density associated with the "random" forces; and in each case the area to the left of the magnetization curve, $\int HdJ$, is approximately equal to the ϵ of the χ_0 formula. In other words, the most important characteristics of the theoretical magnetization curve—its initial slope, and the area between it and the J axis—are determined by energy magnitudes rather than by the exact nature of the internal forces or the exact mechanism through which they make their effect felt. It should therefore be possible to develop at least an approximate theory in which no specific assumptions are made in regard to the nature of the forces or the mechanism. The advantage of such a theory is that it avoids the danger of misinterpreting an agreement between theory and experiment as evidence for the particular forces or mechanism assumed in the theory.

General Theory

The theory will take no account of irreversible phenomena, and therefore the properties predicted by it will be those of an ideal reversible specimen. It is necessary to relate these in some way to the properties of an actual specimen. Now there are certain properties of a ferromagnetic specimen which, to a first approximation, are determined by the magnetization alone and are independent of the previous history and hence of the field strength associated with that magnetization in the particular state under observation. The quantities of which this is true are those measured in a small, approximately reversible change from any initial state: for instance, the elastic constants[12] and the reversible susceptibility[13] (ratio $\Delta J/\Delta H$ when $\Delta H/H$ is small and negative). This suggests that such quantities should have the same value for the actual specimen and for a reversible specimen at the same magnetization. We assume, therefore, that so far as a specimen's properties are functions of the magnetization alone, they are the same functions of magnetization as are the properties of an ideal reversible specimen having the same initial susceptibility.

The correct model for a single crystal is now a group of many domains with fixed orientations of their magnetization vectors, but with variable volumes; the positions of the boundaries are determined by equilibrium between internal and external forces, that is by the minimum of the total free energy due to external fields and stresses and to internal "random" forces. On the supposition that the mechanism by which these internal forces act is unimportant, we proceed to substitute for this model a more manageable one, consisting of a group of N domains of fixed and equal volumes, but with variable orientations of their magnetization vectors: the magnetization of each domain is to be along one of the "easy magnetization" directions, but may change from one of these directions to another when the field or stress is changed. The exact microscopic state of the model under given external conditions is to be that for which the total free energy is a minimum. A macroscopic state of the model, of course, will be described by merely giving the fractional number $n_\sigma=N_\sigma/N$ of domains magnetized in each of the possible directions σ, without regard to which domains these are.

The actual microscopic state, for given field components H_i and stress components X_{ij}, is that corresponding to the minimum value of[14]

$$V=V'+V'', \tag{1}$$

where V' is the ordered free energy per cm^3 due to the applied field and stresses, and V'' is the energy due to the random internal forces. V' is given by

$$\begin{aligned} V' &= -\sum H_iJ_i-\sum X_{ii}e_{ii}'-\sum X_{jk}e_{jk}' \\ &= \sum_\sigma n_\sigma(-\sum H_iJ_{i\sigma}-\sum X_{ii}e_{ii\sigma}' \\ &\qquad -\sum X_{jk}e_{jk\sigma}')=\sum_\sigma n_\sigma V_\sigma. \end{aligned} \tag{2}$$

[12] E. Giebe and E. Blechschmidt, Ann. d. Physik **11**, 905 (1931); O. von Auwers, Ann. d. Physik **17**, 83 (1933); W. T. Cooke, Phys. Rev. **50**, 1158 (1936).

[13] R. Gans, Physik. Zeits. **12**, 1053 (1911); Ann. d. Physik **61**, 379 (1920).

[14] I, Eq. (7). The constant term V_0 has been dropped.

In a large number of samples of the same material, microstates of equal V' will occur equally often if the internal forces are random,[15] but microstates of lower V' will occur oftener. On the other hand there are many more microstates of zero ordered energy than of highly negative. Somewhere between 0 and $-\infty$, there is a "normal" value of V' that will occur most of the time; and among samples with about this value of V', certain values of the partition numbers N_σ will be normal. Just what value of V' is normal for given H_i's and X_{ij}'s depends on the average magnitude of the random forces: the larger these are, the larger will be the external field or stress required to produce a specified magnetization or strain.

Assuming that V' has some value, we may proceed to determine the normal values of the N_σ's, and hence the macroscopic properties of the specimen, by methods similar to those used in statistical mechanics. The result is

$$n_\sigma = \exp(-L_0 V_\sigma)/\sum_\sigma \exp(-L_0 V_\sigma), \qquad (3)$$

where L_0 is determined by

$$\sum_\sigma V_\sigma \exp(-L_0 V_\sigma)/\sum_\sigma \exp(-L_0 V_\sigma) = V'. \qquad (4)$$

This is in essence the method that was introduced by Heisenberg and used by Bozorth and by Gans and v. Harlem. These writers, however, did not actually assume a given value of V', but rather a given value of the component of magnetization in the field direction, J_p. In the problems treated by them the two quantities differ only by a factor H, and moreover it is really J_p and not V' that is known and must be used to eliminate the Lagrangian multiplier L_0; the two procedures therefore lead to the same result. In the work of Akulov and Kondorsky stresses as well as fields are supposed to be present, and a given value of V' must be assumed. There is now a difficulty, however; for V' is not really known, and so L_0 remains an undetermined quantity, whose dependence on the field and stress are unknown. Akulov and Kondorsky endeavored to overcome this difficulty by supposing the magnetization curve at zero stress to be given, and seeking only a formula for the N_σ's good to the first order in the stresses. But in doing this they failed to take account of the effect of stresses upon the magnetization curve, and thus obtained an incorrect result. It was shown in I that this error could be corrected, and the result they sought obtained, by using the thermodynamic relations $\partial J_i/\partial X_{jk} = \partial e_{jk}/\partial H_i$. The equations thus obtained are rather complicated, it is still necessary to know the magnetization curve, and the physical significance of the troublesome Lagrangian multiplier never becomes apparent. The theory at this stage is clearly incomplete.

A similar problem is encountered in statistical mechanics, in calculating the normal partition numbers for a given energy of an isolated system. The energy is really unknown, and so its Lagrangian multiplier L remains indeterminate until it has been given some thermodynamic interpretation. This may be done in a number of ways, for instance by considering *two* systems capable of exchanging energy. The same equations as before are obtained for each system, but with the same L for both; L therefore represents a quantity which is the same for two systems when they are in thermodynamic equilibrium—namely, the temperature. (A more thorough investigation of course shows that L is proportional to the reciprocal of temperature on the usual absolute scale.)

This and other methods, suitably modified, may be applied here. The phrase "suitably modified" is important, for it must be emphasized that this is *not* a problem in statistical mechanics. Our model is not a group of domains continually jumping from one state to another as a result of exchanges of energy. It is a group of domains in a definite, permanent state of lowest total free energy, under the joint action of ordered and random forces—all constant. The direct effect of temperature agitation on the domains as a whole is completely negligible because of their size; its indirect effect in bringing about the equilibrium of the boundaries is fully taken into account in the temperature-dependent "constants" (such as J_s and λ_∞) appearing in the free energy function. Another way of saying this is that the domain order-disorder term in the free energy is negligible compared with the other terms. This term is $-kT \log W$, where W is the number of ways of

[15] More accurately, this is our definition of "random" as applied to these forces.

arranging the domains in the given macroscopic state. For unit volume it is of order of magnitude kTN, where N is the number of domains per cm³. For a wire 1 mm in diameter, $N \leq 10^9$ according to Barkhausen effect measurements, so that this term in the free energy density is of order of magnitude 10^{-5} erg/cm³. The energy associated with the internal forces opposing magnetization is measured by the area $\int HdJ$ to the left of the steep part of the magnetization curve, or roughly by J_s^2/χ_0; even in well-annealed specimens, its order of magnitude is between 10^2 and 10^4 ergs/cm³. Thus thermal agitation of the domains as a whole is negligible by a factor of about 10^{-8}.

Consider, then, two adjacent volumes v_1, v_2 of the same material, subject to different values of the fields or stresses. If we now seek the normal N_σ's for a given total ordered free energy $E'=v_1V_1'+v_2V_2'=E_1'+E_2'$, we obtain equations of the form (3) for each part, but the same Lagrangian multiplier L_0 occurs in both sets of equations. L_0 is determined by the total E', but also it is equally well determined by the E' for either part. If action at a distance by the random forces is negligible, a variation of the fields or stresses in one part does not affect the state of affairs in the other, and so does not affect L_0, which must therefore be a constant of the material (at the given temperature). Its value depends on the random forces. For cubic crystals or isotropic material, it follows from Eq. (41) of I and the corresponding equation for [100] domains, and from Eqs. (15), (23), and (36) of II, that

$$\chi_0=\tfrac{1}{3}L_0J_s^2; \tag{5}$$

hence $1/L_0$ is an energy density of the same order of magnitude as $\int HdJ$ (if the number of directions of easy magnetization is finite), and measures the energy associated with the internal forces. If we assume that these are internal stresses of mean value σ_i, and set $1/L_0=\lambda_\infty\sigma_i$, we get $\chi_0=\frac{1}{3}J_s^2/\lambda_\infty\sigma_i$, a formula differing from Kersten's only in having a numerical factor $\frac{1}{3}$ instead of $2/9$.

Although the discussion has been limited to single crystals for simplicity, the extension to polycrystalline material is easily made by the method of I. Thus we get for the magnetization curve of the ideal reversible specimen of iron or nickel Eq. (12), (20), or (34) of II, according to the type of domain (isotropic, [100], or [111]); in the definition of η preceding each of these equations, L_0 is now to be interpreted as a constant, related to the initial susceptibility by Eq. (5) above. For materials with other types of domain, Eq. (3) or (4) of II must be used.

The Reversible Susceptibility

The magnetization curve thus obtained in terms of χ_0 or L_0, for an ideal reversible specimen, is different from any J–H curve of the actual specimen. But the differential susceptibility dJ/dH calculated from it corresponds to a measurable susceptibility for actual specimens, namely the "reversible susceptibility" mentioned before. The value of the reversible susceptibility χ_r at any magnetization should therefore be equal to the differential susceptibility of the ideal specimen at the same magnetization, if L_0 is chosen so as to give the observed initial susceptibility. (The corresponding value of H, however, bears no simple relation to the H of the actual specimen.)

Thus for material with isotropic domains, χ_r is determined as a function of J by the parametric equations

$$J/J_s=L(\eta), \quad \chi_r/\chi_0=3L'(\eta), \tag{6}$$

where

$$L(\eta)=\coth\eta-1/\eta. \tag{7}$$

These equations were first proposed by Gans in 1911, and were supported by experimental data agreeing very well with the calculated curve.[13] Gans gave no derivation of his formula; he was probably led to it by an attempt to apply the Langevin formula for the susceptibility of a paramagnetic gas. A derivation along that line was very apologetically offered by Debye[16] in 1925. According to this interpretation, η should be equal to $\mu H/kT$, where μ is the magnetic moment of an elementary magnet, in Debye's picture a crystal. Today we must interpret the elementary magnet as a domain. Its magnetic moment is J_sv_0, where $v_0 \leqq 10^{-9}$. The initial susceptibility thus calculated is 10^8 times too large, as was to be expected from our earlier discussion.

[16] P. Debye, *Handbuch der Radiologie*, Vol. 6 (1925), p. 721.

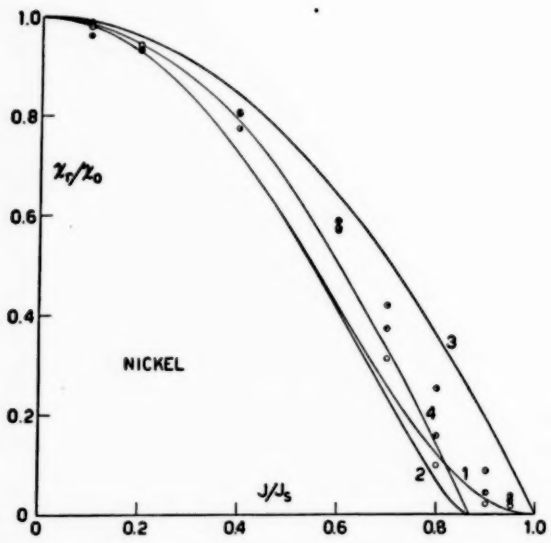

FIG. 1. Reversible susceptibility of polycrystalline nickel. Experimental points (D. Kirkham): open circles, 21.6°C; circles black at left, 99.0°C; black at right, 171.5°C. Theoretical curves: 1, J_s in any direction; 2, J_s along any [111] direction; 3, J_s along $\pm H$; 4, J_s along [111] directions nearest $\pm H$.

If the domains are crystalline, in iron or nickel, the functions are more complicated in form, but the curves differ very little from this one; in fact the series expansions for J are identical to the sixth order in H (see Eqs. (15), (23), and (36) of II). This explains Gans's success in fitting his curve to data on various specimens of iron, steel, and nickel.

Figure 1 shows several attempts to fit Kirkham's[17] results on annealed nickel. These measurements were not taken on the same ellipsoid as the magnetostriction data analyzed in II, but on a thinner ellipsoid, $7\frac{1}{2}''$ long and $\frac{1}{8}''$ in diameter. For this specimen the domains are probably crystalline at room temperature; but according to the value of χ_0 the anisotropy forces are not enormously larger than the random forces, so that the neglected rotation effect may not be entirely negligible, and the specimen may be expected to be intermediate in its properties between one with crystalline domains of high anisotropy and one with isotropic domains.

Curve 1 is calculated for isotropic domains, curve 2 for crystalline domains with [111] as the direction of easy magnetization. There is a difference only at high J, and here 2 is unreliable because of rotation. The data do not fit at all well.

In the discussion of the magnetostriction of an iron ellipsoid (II, p. 488), it was suggested that when an elongated ellipsoid is demagnetized by a longitudinal field, more domains are left oriented along directions nearly parallel to the ellipsoid axis than along directions nearly perpendicular to it. This applies to the present case. Curve 3 is calculated for the extreme case in which all the domain magnetizations are either parallel or antiparallel to the field (as might be the case if the specimen were long and thin and the domains magnetically isotropic). Curve 4 is calculated for domain moments oriented along only the [111] directions nearest the field.[18] Most of the data fall between these curves. As the temperature rises, the anisotropy constant decreases, the effect of rotation (or the tendency toward isotropy) increases, and in the range where rotation is important the points should fall nearer to the isotropic curve—as in fact they do.

In Fig. 2, the points are experimental data of Samuel[19] on soft cobalt. Curve 1 is the Gans formula, which does not fit at all. Cobalt crystals have two opposite directions of easy magnetization; the anisotropy constant is large, so that rotation should be negligible except at high fields, and the calculation for crystalline domains should be a good approximation. This calculation gives

$$J/J_s = E(\eta), \quad \chi_r/\chi_0 = 3E'(\eta), \tag{8}$$

where

$$E(\eta) = (1/\eta^2)\int_0^\eta u \tanh u\, du. \tag{9}$$

Series expansions for the function $E(\eta)$ may be obtained from the expansions in II, Eqs. (22)–(27). The function (8) is plotted as curve 2 in Fig. 2.

The deviation at high J is expected. The deviation at low J may be partly due to a poor value of χ_0. The experimental results deviate considerably among themselves; the agreement

[17] D. Kirkham, Phys. Rev. **52**, 1162 (1937).

[18] The formulas are: curve 3, $J/J_s = \tanh \eta$, $\chi_r/\chi_0 = \operatorname{sech}^2\eta = 1-(J/J_s)^2$; curve 4, $J/J_s = (12/\pi)\int_0^{\pi/3} d\psi \int_{\alpha'}^1 \alpha \tanh \alpha\eta\, d\alpha$, $\frac{1}{3}(1+4/\pi)\chi_r/\chi_0 = (12/\pi)\int_0^{\pi/3} d\psi \int_{\alpha'}^1 \alpha^2 \operatorname{sech}^2 \alpha\eta\, d\alpha$, $\alpha' = \cos\theta'$, $\cot\theta' = \sqrt{2}\cos\psi$; the result of the integration with respect to α can be expressed in terms of the functions E and E' defined by Eq. (9).

[19] M. Samuel, Ann. d. Physik **86**, 798 (1928): specimen *H*.

with theory is probably as good as can be expected. Gans[2] found a considerably worse deviation between the experimental results at higher fields and the theoretical curve calculated by the rotation theory.

Cobalt is interesting because, with only two directions of easy magnetization, it is easy to work out a more specialized theory, with more definite assumptions about the internal forces. Internal stresses, being impartial with respect to opposite directions, should have no effect on the reversible magnetization, and only internal fields need be considered. Curve 3 is calculated on the assumption that the magnetic moment of each crystalline domain is along that one of the two possible directions favored by the resultant H, external plus internal; it is assumed that the values of the relevant component of internal field are constant and are distributed according to a Gaussian error curve. This gives

$$J/J_s=\left[(2u^2-1)\int_0^u e^{-x^2}dx+ue^{-u^2}\right]/2(\pi)^{\frac{1}{2}}u^2, \quad (10)$$

$$\chi_r/\chi_0=3\left[\int_0^u e^{-x^2}dx-ue^{-u^2}\right]/2u^3. \quad (11)$$

The difference between curves 2 and 3 is unimportant at the present stage of development of the theory, and the wider applicability of the general method is strongly in its favor.

Modification of Earlier Formulas

The theorem that $L_0(=-L$ of I) is a constant enables us to replace Eq. (16) of I by the simpler relation, which now follows immediately from (14),

$$\partial Y_r/\partial y_s=LP_{rs}. \quad (12)$$

Hence only the first terms remain in the right members of Eqs. (34) when the differentiation is at constant H. From the second of Eqs. (44), $\chi_1=0$. This explains why good agreement with experiment was obtained by neglecting χ_1 in Eq. (54).[20] It is now clear, also, that the coefficients χ_1 and χ_2 in Eq. (40) have no relation to the actual magnetization curve of a crystal, but are determined by the curve of the equivalent reversible specimen, which may be obtained from the χ_r *vs.* J curve by the formula

$$H_r=\int_0^J (1/\chi_r)dJ. \quad (13)$$

Here H_r is the field strength corresponding to the magnetization J for an ideal reversible specimen whose reversible properties coincide with those of the actual specimen.

Criticism of the Theory

The fact that the theory gives only reversible properties is a serious limitation, but less serious than might have been feared, provided the concept of the "equivalent reversible specimen" is used as a guide in interpreting the theoretical results. The assumption of complete randomness of the internal forces is an oversimplification; whether it is too drastic an oversimplification can only be decided by comparison of the predictions of the theory with experiment, and it would not be at all surprising if the theory proved useless for pure, well-annealed crystals. The replacement

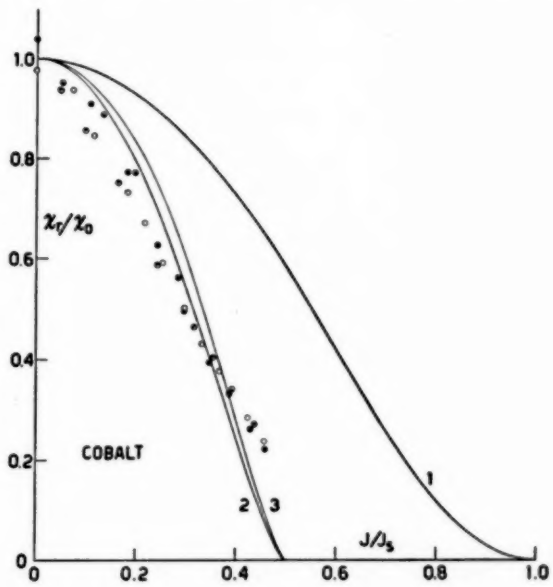

FIG. 2. Reversible susceptibility of polycrystalline cobalt. Experimental points (M. Samuel): open circles, virgin curve; solid circles, ideal curve; circles black at bottom, descending magnetization curve; black at top, ascending. Theoretical curves: 1, general theory, isotropic domains; 2, general theory, crystalline domains; 3, special theory of internal fields.

[20] It is possible to compute the variation of the elastic constants with magnetization without introducing the approximations of I, but this work is too far from completion to discuss at present.

of variable volumes with fixed magnetization directions by fixed volumes with variable magnetization directions is the step that is most difficult to justify. If this step is defensible, then the final results should be capable of derivation without it. Some efforts in that direction are presented in the appendix.

Despite these limitations, the theory seems successful enough to justify its further study; it may help to give a partial understanding of the complex processes that occur at low fields, until a more detailed theory becomes possible.

The writer wishes to express his appreciation to Professor Francis Bitter, of the Massachusetts Institute of Technology, for helpful comments and criticisms.

Appendix

(a) Alternative derivations of the distribution formulas.

These parallel familiar arguments of statistical mechanics.

Method 1.—Assume, as before, that in a large number of copies of our simplified model, all subject to the same fields and stresses, microstates of equal ordered energy occur equally often; and that this remains true even if the fields and stresses have different values in two adjacent parts v_1, v_2 into which the model may be divided. Then the relative frequency of occurrence of any microstate, for either part separately or for the model as a whole, is a function only of the corresponding ordered energy $E_1'=v_1V_1'$, $E_2'=v_2V_2'$, or $E'=v_1V_1'+v_2V_2'$; let this function be $f(E_1')$, $g(E_2')$, or $h(E')$. The probability that a copy selected at random is in a specified microstate, with ordered energies E_1' and E_2', is

$$h(E_1'+E_2')=f(E_1')g(E_2').$$

For two microstates with the same total energy $E_1'+E_2'$, the values of $f(E_1')g(E_2')$ are therefore equal; or, $f(x)g(y)=f(z)g(x+y-z)$, for arbitrary x, y, and z. Differentiation with respect to x and y gives $f'(x)g(y)=f(z)g'(x+y-z)=f(x)g'(y)$, or $f'(x)/f(x)=g'(y)/g(y)=\text{constant}=A$. Hence $f(E_1')=Be^{-AE_1'}$, $g(E_2')=Ce^{-AE_2'}$. By varying the fields or stresses in v_2 without varying them in v_1, and assuming action at a distance negligible, we infer as before that A is a constant of the material. Thus for unit volume, the probability of a microstate of ordered energy $V'=\sum_\sigma n_\sigma V_\sigma$ is $Be^{-AV'}$; B is determined by $\sum_\mu Be^{-AV'}=1$, where $\sum_\mu$ denotes a summation over all microstates. The mean n_σ's for the whole collection of copies are now given by $(n_\sigma)_{Av}=B\sum_\mu n_\sigma e^{-AV'}$. When the summation is carried out,[21] Eq. (3) is obtained, with $L_0=A/N$.

Method 2.—For given fields and stresses, the actual microstate of any copy of a volume v, containing N domains, is that for which $E'+E''=v(V'+V'')$ is a minimum. If we knew E'' for each microstate of each copy, we could solve the problem by first finding the normal minimum E'', say E_0'', attainable by varying the microstate, for given N_σ's; and then minimizing $E'+E_0''$ by variation of the N_σ's. The E_0'' obtained in the first step is a function of the N_σ's, but if the internal forces are random it depends on the N_σ's only because the normal minimum V'' to be found in W microstates is lower, the greater the number W of microstates there are to choose from. Thus E_0'' is a function of $W=N!/N_1!N_2!\cdots$, and hence of $\log W$, or of $-N\sum_\sigma n_\sigma \log n_\sigma$. With negligible action at a distance, E_0'' must be proportional to N for large N and for given n_σ's, hence $E_0''=AN\sum_\sigma n_\sigma \log n_\sigma$, or $V_0''=\epsilon\sum_\sigma n_\sigma \log n_\sigma$. Upon minimizing $V'+V_0''$ with respect to the n_σ's we obtain the same formulas as before, with L_0 replaced by $1/\epsilon$. In the demagnetized state each $n_\sigma=1/k$, where k is the number of directions of easy magnetization, and $V_0''=-\epsilon \log k$; when the field is large one $n_\sigma=1$ and the others vanish, and $V_0''=0$. Hence the work done against internal forces in magnetizing unit volume of the specimen, or $\int HdJ$, is $\epsilon \log k$.

(b) Boundary displacement against random forces.

In the following discussion we abandon the somewhat arbitrary replacement of variable

[21] Cf. J. Frenkel, *Wave Mechanics: Elementary Theory* (1932), p. 199.

volumes by fixed volumes. We assume that a fraction v_σ of the total volume has J_s in direction σ, and that each of the quantities $v_1, v_2, \cdots$ is a function of the quantities $V_1, V_2, \cdots$.

Consider the ratio v_i/v_j. When $V_i = V_j$, this is 1, whatever the values of the other V_σ's. When V_i is much larger algebraically than V_j, v_i/v_j is practically zero; and when V_i is much smaller algebraically than V_j, v_i/v_j is very large, whatever the values of the other V_σ's. Thus when $V_i - V_j = -\infty$, 0, or $+\infty$, v_i/v_j has a definite value, independent of the other V_σ's and also of the absolute value of V_i or V_j (with respect to any zero). Let us *assume* that in general v_i/v_j is a function only of $V_i - V_j$, say $v_i/v_j = f(V_i - V_j)$. Then for any three directions i, j, k we have

$$1 = (v_i/v_j)(v_j/v_k)(v_k/v_i) = f(V_i - V_j)f(V_j - V_k)f(V_k - V_i),$$

or if $\phi = \log f$,

$$\phi(x-y) + \phi(y-z) + \phi(z-x) = 0.$$

Differentiating with respect to z and then setting $z=0$ gives $\phi'(y) = -\phi'(-x) = \text{constant} = -A$, or $f(y) = Be^{-Ay}$. When $y=0$, $f=1$, therefore $B=1$. Thus $v_2 = v_1 e^{-A(V_2 - V_1)}$, $v_3 = v_1 e^{-A(V_3 - V_1)}$, $\cdots$, or $v_1 e^{AV_1} = v_2 e^{AV_2} = v_3 e^{AV_3} = \cdots = C$, or finally $v_1 = Ce^{-AV_1}$ etc., where C is determined by $v_1 + v_2 + \cdots = 1$.

This derivation fails when there are only two directions of easy magnetization, but this case may be regarded as a limiting case attained by letting the value of V_σ for the other directions become very large.

It is not obvious that the assumption made in this argument is equivalent to the assumption that the internal forces are random. The derivation is therefore incomplete; but it does suggest that the introduction of fixed instead of variable volumes, and the resulting superficial analogy to statistical mechanics, are probably not essential to the theory.

Note added in proof: The following additional results of the theory are interesting because of their relation to some recently published work of Kondorsky.[22] In an iron crystal, when the field is along a specimen axis for which the demagnetizing factor is negligible, it may be assumed that only the [100] directions nearest this axis are occupied. Let the cosine of the acute angle between such a direction and the specimen axis be l, and let $j = J_p/J_s$, $\eta = L_0 J_s H_r$: then the magnetization curve of the equivalent reversible specimen is given by $j = l \tanh \eta l$, so that $\chi_r = L_0 J_s^2 dj/d\eta = L_0 J_s^2 l^2 \operatorname{sech}^2 \eta l = L_0 J_s^2 l^2 (1 - j^2/l^2)$. It follows that for three crystals of the same material with their specimen axes along [100], [110], and [111] ($l^2 = 1$, $\frac{1}{2}$, and $\frac{1}{3}$, respectively), and with the field in each case along the specimen axis, the initial susceptibilities should be in the ratios 6 : 3 : 2, and χ_r/χ_0 should be given by $1 - j^2$, $1 - 2j^2$, and $1 - 3j^2$, respectively. The ratios 6 : 3 : 2 were observed in Williams'[23] measurements and are predicted by Kondorsky's theory when $\kappa_1 \gg \kappa_2$, and also by earlier theories of Akulov and of Bozorth.[22] The expressions for χ_r/χ_0 are identical with those of Kondorsky's theory.

[22] E. Kondorsky, Phys. Rev. **53**, 319 and 1022 (1938).
[23] H. J. Williams, Phys. Rev. **52**, 1004 (1937).

Measurements of Magnetic Viscosity in Iron

C. W. HEAPS
The Rice Institute, Houston, Texas

(Received June 20, 1938)

Magnetic viscosity—the change of induction occurring after the magnetizing field has ceased to vary—has been measured in a bar of commercial iron, with a measuring circuit designed to eliminate spurious effects arising from sparking at switches. Magnetic viscosity is found to depend on previous magnetic states, in agreement with observations of Mitkevitch and contrary to Preisach's results. It appears, therefore, as if reversible domains could retain their lagging propensity while the magnetic force is varying over a considerable range. The viscous effect is found to depend on the magnitude of the previous change of induction if the latter is small, but is independent of this change if it is greater than 60 gauss. In small, subsidiary hysteresis loops, such as are used in determining reversible permeability, it is found that the Barkhausen effect is not present although there is hysteresis and magnetic viscosity. It is therefore concluded that the movement of the boundaries of saturated domains in the material is subject to time-lag.

WHEN a ferromagnetic material is subjected to a magnetizing field and this field is suddenly changed, the magnetic induction in the material will, in general, continue to change for an appreciable time after the magnetizing field has ceased to vary. Eddy currents in the specimen are responsible for part of this time-lag in magnetization. By a method given by Rayleigh[1] it is possible to calculate the magnitude of this part of the phenomenon. In addition to the effect arising from eddy currents there is another time-lag which may persist long after the eddy currents have died away. The cause of this additional time-lag of induction, usually called magnetic viscosity, is not clearly understood at present. In the experiments described below measurements of magnetic viscosity in commercial iron wire have been made, and certain factors which modify this viscosity have been investigated.

EXPERIMENTAL TECHNIQUE

Figure 1 gives a diagram of the apparatus used. A pendulum closes switch K_1, and shortly afterwards, K_2. When K_1 is closed the current through the solenoid C is short circuited and the field in C falls practically to zero. The induction in the iron specimen S continues to change after K_1 closes, and with the closing of K_2 the galvanometer G begins to deflect as a result of the induced e.m.f. in the pick-up coil P. This deflection is quickly brought back to zero by closing the switch K_3, thus adding through the mutual inductance M enough flux in the galvanometer circuit to balance the flux removed from P. As the magnetic induction of S continues to decrease the rheostat R_3 is varied by hand so as to keep the galvanometer deflection zero. From the final reading of the ammeter A_2 (after no more induction decrease can be observed), the number of turns in P, the mutual inductance M, and the cross-sectional area of S, it is possible to calculate the change of induction which occurred in S after the closing of the switch K_2.

This method is superior to the ballistic method because the inductive changes may be followed over a long period of time. Another advantage of the circuit shown in Fig. 1 is that it eliminates uncertainties connected with the spark produced when a switch is opened in an inductive circuit. An extended series of measurements was made with a circuit in which the solenoid current was reduced to zero by opening a switch in series with the battery. It was found that when proper values of resistance and capacity were used as shunt across the solenoid so as to produce

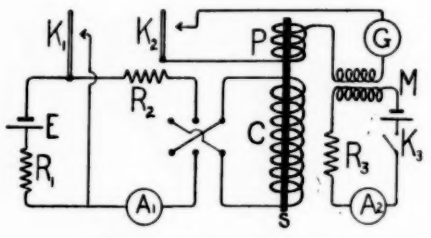

FIG. 1. Circuit diagram.

[1] Lord Rayleigh, Rep. Brit. Assoc. **52**, 446 (1882).

theoretically a nonoscillatory decay of current in the solenoid, nevertheless a high frequency oscillation of short duration occurred at the instant of break. This oscillation was detected with a cathode-ray oscillograph connected across a noninductive resistance in series with the solenoid. Under certain conditions no magnetic viscosity whatever could be observed, probably because of the spark oscillations superposed on the unidirectional decay current. Under other conditions of resistance and capacity these superposed spark oscillations did not appear to affect the viscosity. Pending a more complete investigation of this phenomenon it was decided to eliminate uncertainties by the use of the short-circuiting device of Fig. 1. There is a very definite probability that some of the conflicting results of previous experimenters may be due to the unsuspected presence of spark oscillations in their circuits.

Further details of the circuit are as follows: The galvanometer was of the high sensitivity type, of period 19 seconds, used with a scale distance of 470 cm. It was necessary to insulate the circuits with considerable care in order to avoid spurious effects. The battery E was a 6 volt storage battery. The solenoid C, wound on a micarta tube, was 30.6 cm long, contained 7000 turns, and had a resistance of 42.5 ohms. Its mean diameter was 9.26 cm. The coil P had 10,000 turns and was supported in the center of the solenoid. The specimen S was centered with respect to C and P. It was a wire of commercial iron, 0.30 cm in diameter and 15.1 cm long. It was annealed by slow cooling from a bright red heat. Figure 2 gives the descending branch of the hysteresis loop of this specimen, without correction for the factor of demagnetization.

In order for the eddy currents to have time to die away in a specimen of this diameter it is necessary to have a fairly large time interval between the closing of switches K_1 and K_2. In most of the work the switches were set so that this time interval, by calculation, was 0.61 seconds. During this time the current in the solenoid must fall to a negligible value and the eddy currents in the specimen must die away. If R_2 in Fig. 1 is taken to be 100 ohms, the value usually used, a simple calculation shows that 0.13 second after the closing of K_1 the current in C is reduced by the factor 1.1×10^{-6}. The maximum current used in the experiments was 0.125 ampere. Thus after 0.13 second the current has fallen to a value 1.4×10^{-7} ampere. Tests showed that with the specimen in the solenoid the induction changes caused by a current of 6×10^{-7} ampere produced no detectable effect on the galvanometer. We may therefore assume the solenoid current to be zero 0.13 second after the closing of K_1. The eddy currents—and therefore

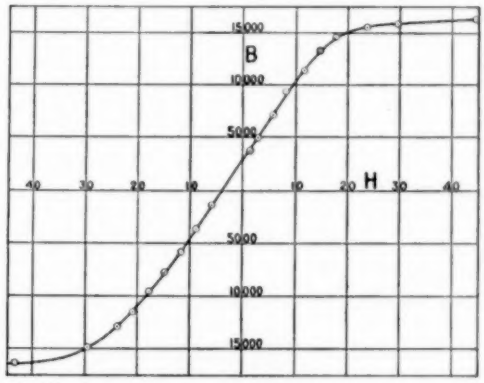

FIG. 2. Descending branch of the hysteresis loop of a commercial iron wire which had been annealed by slow cooling from red heat. No correction has been made for demagnetization.

the magnetic induction—in the specimen will require some time to die away after the solenoid current has become zero. Rayleigh's formula for the decay of eddy currents may be put in the form $\log b = -1.44t/(A\sigma\mu)$, where b is the fraction of the total induction change which occurs after a time t, and t is the time after the magnetic field is removed; σ and A are the conductivity and cross-sectional area, respectively, of the specimen. The value of the permeability μ is set equal to dB/dH and can be obtained from the B–H curve of Fig. 2 after the appropriate factor of demagnetization has been applied. By using the least favorable value of dB/dH and taking $t=0.48$ second, which is the time remaining after the solenoid current becomes effectively zero before K_2 is closed, b is calculated to be 2.6×10^{-6}. The maximum value of the total induction change in the experiments where viscosity was measured was 6400. Thus we obtain for the induction change ($\delta B=6400b$) which occurs after K_2 is closed, and which is caused by eddy currents, the value 0.017. The smallest induction

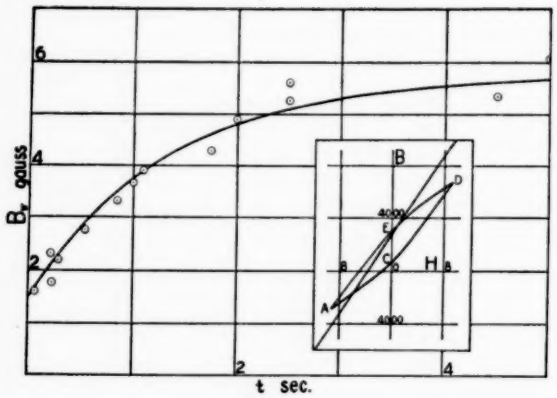

FIG. 3. The magnetic viscosity of iron as a function of the time it was kept at the point D of the hysteresis loop.

change which could be detected with certainty by the apparatus was about 0.2 gauss. Thus any effect arising from eddy currents is too small to be detected in any of the present experiments.

INFLUENCE OF PREVIOUS MAGNETIC STATES

The small hysteresis loop shown in Fig. 3 was traversed several times so as to stabilize the loop. The viscosity at E following the drop from D was then measured and found to depend on the length of time the iron was kept at point D. The experimental points on the large curve of Fig. 3 were obtained as follows. The iron was left at state A of the small loop for about one minute—a sufficient time for all appreciable viscous effects to disappear—then by a reversing switch carried to state D. After a time t the pendulum was allowed to close key K_1, and 0.61 second later, K_2. Thus the iron was carried to state E and the viscous effect, B_v, measured. In order to measure t a noninductive resistance of 40 ohms was connected in series with the solenoid and potential leads from the ends of this resistance were led to the filament and grid, respectively, of a triode amplifying tube. When the reversing switch was thrown the potential change across the 40 ohms caused a change of plate current and thus actuated, through a sensitive relay, the stylus of a revolving drum chronograph. When the key K_1 closed the stylus was again actuated. In this way a sufficiently accurate determination of t could be made.

Figure 3 shows that the magnetic viscosity, B_v, at E is diminished when t is reduced below about 3.5 seconds. For larger values of t it appears that B_v is constant as t changes. In interpreting the curve it is to be noted that when t is less than about 0.3 second the iron at D may still be the seat of eddy currents of appreciable magnitude at the instant the key K_1 is closed. However, it is quite evident that after all eddy currents have died away there is still a magnetic readjustment going on at D which must be completed if the full value of the viscosity at E is to be obtained. When the iron is carried to D we may say that the magnetic viscosity at that point consists in the reversal of lagging magnetic domains, so that the induction at D continues to increase for some time after point D is reached by the magnetic field. If all of these lagging domains are not allowed to reverse before the field is reduced to the value at E we do not find so big a viscous effect at E. The decrease of viscosity at E is due to the fact that certain members of a group of viscous domains have not had time to reverse at D, hence these members are oriented in the right direction at E and do not need to reverse under the influence of the demagnetizing field.

Let N_D and N_E be the numbers of domains which show magnetic viscosity in reversing at the respective points D and E. Assume (1) that members of the group N_D which do not have time to reverse their magnetism at D are detracted from the viscous group N_E at E; (2) that the number of unreversed viscous domains at D varies exponentially with the time t after the field becomes constant. That is, let $N=N_De^{-mt}$, where N is the number of domains still unreversed t seconds after the field has ceased to vary, and m is a constant.

The measured magnetic viscosity at E is then given by $B_v=k(N_E-N)=k(N_E-N_De^{-mt})=k_1-k_2e^{-mt}$, where k, k_1, and k_2 are constants. The curve of Fig. 3 is drawn with $k_1=5.75$, $k_2=4.25$, and $m=0.75$ in the above equation. The experimental points fit the curve as well as could be expected.

A consequence of the above equation for B_v is that when point D is chosen far out on the saturated part of the magnetization curve the value of B_v should be independent of t; for in this case the viscosity at D is found experimentally to be very small, so that N_D may be set equal to zero and thus $B_v=k_1$. The constant k_1 in this

case, however, may be different from the k_1 for other positions of D, because, in general, N_E depends on the previous magnetic history of the specimen. Experimental tests showed that when point D is taken to a field of 34 gauss the value of B_v at C is about the same, whether t is 0.3 second or one minute.

In case N_D is larger than N_E the value of B_v would be negative for small values of t. The specimen of iron used in this experiment did not give negative values of B_v for the part of the hysteresis loop examined. Previous experiments disagree to some extent in this matter. Mitkevitch[2] and Richter[3] were able to observe the negative effect predicted by the above equation. Preisach[4] not only failed to report the negative effect but also he states that the time during which a specimen is subjected to a field has no effect on the viscosity appearing when the field is cut off. Preisach states that the "superposition principle" is not applicable to magnetic viscosity. The conflict between the results of Preisach and those of Mitkevitch, Richter, and the writer could very well be due to the presence of spark oscillations in the solenoid of Preisach. He does not give a diagram of his circuit nor does he mention any precautions taken to stop oscillations.

Relation Between the Magnitude of an Induction Change and the Ensuing Magnetic Viscosity

The procedure in this experiment was as follows. From a saturating field of 35 gauss the field was decreased to a definite small value, H', and kept constant at that value for one minute. Then the pendulum was allowed to operate the switches K_1 and K_2, thus removing the field H', producing the induction decrease ΔB, and allowing the resulting magnetic viscosity B_v to be measured. Curve I of Fig. 4, obtained in this way, shows that B_v is constant for large values of ΔB but diminishes rapidly when ΔB is decreased below about 60 gauss.

If the time of holding H' constant is diminished from one minute to 5 seconds curve II is obtained. Curves I and II coincide for large values of ΔB but below 50 gauss curve II is the higher.

These curves show that the number of viscous domains which reverse after the induction jump ΔB has occurred is practically independent of the magnitude of ΔB when the latter is large, but as ΔB becomes small this number decreases. Curve II is higher than I because for the former curve some of the viscous domains which had no time to reverse during the pause at H' remain unreversed during the change ΔB and thus contribute to the viscosity after ΔB has occurred. The curve II does not pass through the origin because when the saturating field of 35 gauss is brought to zero for 5 seconds and no further change made, i.e., $\Delta B=0$, then even after 5 seconds there are still numerous domains which have not yet had time to reverse. These domains give the viscosity measured when K_2 is closed at the end of the 5 seconds.

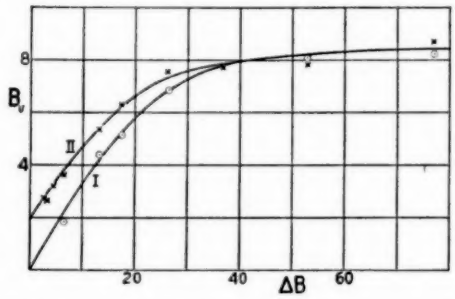

Fig. 4. Magnetic viscosity of iron as a function of the induction decrease ΔB.

Relation Between Magnetic Viscosity and Barkhausen Discontinuities of Magnetization

In the previous experiments if the galvanometer is replaced by an amplifier and telephone receivers it is possible to detect Barkhausen discontinuities which persist and can be heard in decreasing numbers for some time after the magnetic field has ceased to vary. In line with this observation, therefore, it is usually considered that the entire phenomenon of magnetic viscosity is due to the existence of delayed Barkhausen reversals of magnetization. The cause of this delay in the reversal of Barkhausen domains has been attributed[5] to persisting eddy currents and to the resulting microscopic strains

[2] A. Mitkevitch, J. de phys. **7**, 133 (1936).
[3] G. Richter, Ann. d. Physik **29**, 605 (1937).
[4] F. Preisach, Zeits. f. Physik **94**, 277 (1935).
[5] H. Kuhlewein, Physik. Zeits. **32**, 860 (1931); C. W. Heaps, Phys. Rev. **49**, 409 (1936).

set up by the local inequalities of temperature. The experiments described below indicate that magnetic viscosity is not to be explained entirely in terms of these delayed Barkhausen reversals.

A small subsidiary hysteresis loop similar to that shown in the inset of Fig. 3 was examined, with an amplifier and telephone receivers, for a lagging Barkhausen effect at the points A, C, D, and E. At these same points the magnetic viscosity was also measured with the galvanometer as described above. It was found for a loop of large area that Barkhausen jumps and magnetic viscosity were both present at all the specified points. When the loop was made smaller and stabilized by repeated traversing of the cycle the Barkhausen jumps disappeared at certain of the points.

For example, when the limits of variation of B and H were, respectively, 390 and 1.6 gauss no Barkhausen effect could be detected at any of the points. The magnetic viscosity, however, amounted to 1.0 gauss at each point. This figure represents, as before, the total induction change occurring 0.61 second after the solenoid current is switched on or off. For points A and D this time is only approximate, as here the key K_1 could not be used and it was necessary to close the reversing switch, and subsequently K_2, by hand. In observing the Barkhausen effect the amplifier system which had been substituted for G was kept connected at all times, i.e., K_2 was kept closed. Thus when the reversing switch was operated there was always a loud, sharp noise caused by the big inductive jump. This noise was followed, in case of lagging Barkhausen jumps, by a crackling, or popping noise which gradually died away as the individual impulses became less frequent.

For the loop of limits specified above this lagging Barkhausen effect was at first large at point A. After about five circuits of the loop it vanished at this point. The other points of the loop showed no lag at any time. The magnetic viscosity as measured with the galvanometer showed a similar initial large effect at A—approximately 9 gauss—which diminished to the constant value 1.0 gauss after about eight circuits of the loop.

It seems improbable that this viscous effect of 1.0 gauss is due to Barkhausen jumps too small to be heard in the telephone receivers. As the Barkhausen effect diminishes with successive trips around the loop it is not the intensity of the individual impulses which seems to weaken, it is their number. It appears, therefore, as if the members of a definite group of lagging, reversible domains were gradually removed from this lagging group by repeated trips around the loop. If the magnetic viscosity which remains after several cycles is due to discontinuities of magnetization these discontinuities must be of a different order of magnitude from those ordinarily observed because none whatever could be detected even when four stages of amplification were used.

Small loops of the kind here described are used in determining reversible susceptibility. The area of these loops may be made very small by decreasing the amplitude of the field variation but the statement which is sometimes made[6] that these small cyclic processes involve no dissipation of energy appears to be incorrect according to the best experimental evidence.[7] It is only in the limit, as the amplitude of the field variation approaches zero, that the area becomes zero. For the loop as used above the width along the B axis was about 45 gauss. Accordingly the disappearance of lagging Barkhausen jumps is not to be attributed to the disappearance of hysteresis.

The question arises as to whether the Barkhausen discontinuities merely fail to lag behind the field or disappear for all points around the loop. An experimental test of this question was made as follows. The field was caused to vary slowly and continuously around the loop and simultaneously a check was made, with the use of the telephone receivers, to see whether Barkhausen discontinuities occurred. The slow continuous field variation was obtained by passing the plate current of a radio tube, type 89, through the solenoid. When the heater current of the tube was switched on or off the plate current rose or fell smoothly and slowly. After several cycles had stabilized the loop no Barkhausen jumps could be detected at any point. Accordingly we conclude that in these small

[6] F. Bitter, *Introduction to Ferromagnetism* (McGraw-Hill Book Co., 1937), p. 182.

[7] E. Spuhrmann, Zeits. f. Physik **39**, 332 (1926); K. Uller, Zeits. f. Physik **38**, 72 (1926); G. J. Sizoo, Ann. d. Physik **3**, 270 (1929).

subsidiary loops there is hysteresis and magnetic viscosity without any Barkhausen effect.

According to the domain theory of ferromagnetism a material may change its intensity of magnetization by three different processes: (1) reversal of the saturated magnetization of small domains, (2) reorientation of the magnetization of the domains, (3) increase of size of one domain at the expense of another. The first process is supposed to produce the sudden inductive jumps associated with the Barkhausen effect. The last two processes may take place slowly and continuously, so would not be detected by the use of telephone receivers. It appears, therefore, in view of the experiments just described, that the phenomenon of magnetic viscosity is involved in one or both of the two last named processes, as well as in the first.

It is usually considered that process (2) occurs in strong fields, process (3) in weak fields.[8] For the loop used in the present experiment there is always a demagnetizing field present; however, it seems reasonable to suppose that process (3) is largely responsible for the induction changes of these small loops.

In this case the conclusion to be drawn is that when the boundaries of domains move under the influence of applied fields a certain time is required for equilibrium to be attained after the magnetic field ceases to change. These moving boundaries would be the seat of eddy currents and magnetostrictive strains, so that magnetic viscosity would make its appearance in process (3) as a result of the time required for the disappearance of microscopic temperature gradients and the readjustment of the local strains.

[8] F. Bloch, Zeits. f. Physik **74**, 333 (1932); R. Becker, Physik. Zeits. **33**, 905 (1932).

AUGUST 15, 1938 PHYSICAL REVIEW VOLUME 54

The Variation of the Elastic Constants of Crystalline Sodium with Temperature Between 80°K and 210°K*

S. L. QUIMBY AND SIDNEY SIEGEL
Columbia University, New York, N. Y.

(Received June 20, 1938)

Methods are described for growing single crystals of sodium in the form of rods 4.7 mm in diameter and 10 cm long, for handling the crystals in an atmosphere of helium, and for measuring the principal elastic moduli at low temperatures. Values of the adiabatic and isothermal moduli and constants are tabulated at ten degree intervals between 80°K and 210°K. The value of the Debye characteristic temperature, calculated from the values of the elastic constants at 80°K, is 164°K.

EXPERIMENTAL METHOD FOR MEASURING THE ELASTIC CONSTANTS

A COMPLETE description of the dynamical method employed in this research has appeared in previous issues of this journal.[1] Accordingly, it will suffice here briefly to review its essential features, and their adaptation to the present experimental problem. The specimen is in the form of a right circular cylinder 4.7 mm in diameter and a few centimeters long. The required data are deduced from the observed behavior of a separately excited composite piezoelectric oscillator constructed by cementing to one end of the specimen a suitably cut cylinder of crystalline quartz of identical cross-section. Silver electrodes are chemically deposited in proper position on the quartz, and the oscillator is suspended vertically by delicate supports attached at the middle of the quartz cylinder. One or more harmonic frequencies of free longitudinal or torsional vibration of this system are measured by observing the variation of the electrical impedance of the composite oscillator with the frequency of the applied voltage, and

* Publication assisted by the Ernest Kempton Adams Fund for Physical Research of Columbia University.

[1] Balamuth, Phys. Rev. **45**, 715 (1934); Rose, Phys. Rev. **49**, 50 (1936); Durand, Phys. Rev. **50**, 449 (1936).

from these the fundamental frequencies, f, of free longitudinal and torsional vibration of the specimen cylinder *alone* are calculated. The latter quantities are related, respectively, to the Young's modulus, E, and the torsion modulus, G, of the specimen material for the direction of the cylinder axis by the formula

$$2fL=(M/\rho)^{\frac{1}{2}}, \tag{1}$$

where L is the length of the specimen cylinder, ρ is the density, and M the elastic modulus. It remains only to relate E and G to the principal elastic moduli and elastic constants of the crystal.

Young's modulus for an arbitrary direction in a cubic crystal is related to the principal elastic moduli by the formula[2]

$$1/E=s_{11}-2s\Gamma, \tag{2}$$

where $$s=s_{11}-s_{12}-\tfrac{1}{2}s_{44},$$

$$\Gamma=\alpha^2\beta^2+\alpha^2\gamma^2+\beta^2\gamma^2,$$

and α, β, γ are the direction cosines with respect to the principal crystal axes.

When torsional surface tractions are applied across the end faces of a crystalline cylinder, the resultant twist is, in general, accompanied by a bend. This additional strain can be, and in static measurements usually is, prevented by additional contraints, but the relation between the torsion modulus and the principal elastic moduli is quite different according as this is or is not done. If bending is not prevented

$$1/G=s_{44}+4s\Gamma, \tag{3}$$

while if bending is prevented[3]

$$1/G=s_{44}+4s\Gamma-2s^2(\Gamma-4\Gamma^2+3\chi)/(s_{11}-2s\Gamma), \tag{4}$$

where $$\chi=\alpha^2\beta^2\gamma^2.$$

At first it was thought that the torsional vibration of the specimen cylinder would be governed by the formula (3), and the experimental results on the first three crystals grown were not inconsistent with this view. The results of subsequent experiments, however, showed conclusively that the high frequency[4] torsional vibration of the specimen constituent of the composite oscillator is governed instead by the formula (4). The earlier error arose from the fortuitous circumstance that the cylinder axes of the three crystals lay very nearly in the (100), (110) and (111) directions, for which directions the two formulae are identical.

The elastic moduli and elastic constants are related by the formulae,

$$\begin{aligned} c_{11}&=(s_{11}+s_{12})/(s_{11}-s_{12})(s_{11}+2s_{12}),\\ c_{12}&=-s_{12}/(s_{11}-s_{12})(s_{11}+2s_{12}),\\ c_{44}&=1/s_{44}. \end{aligned} \tag{5}$$

Lastly, the compressibility, κ, is given by the formula,

$$\begin{aligned} \kappa&=3(s_{11}+2s_{12}),\\ &=3/(c_{11}+2c_{12}). \end{aligned} \tag{6}$$

The method yields immediately the adiabatic moduli and constants. These are related to the isothermal quantities by the formulae[5]

$$\begin{aligned} (s_{11})_{\text{ad.}}-(s_{11})_{\text{is.}}&=(s_{12})_{\text{ad.}}-(s_{12})_{\text{is.}}=-T\alpha^2/\rho c_p,\\ (c_{11})_{\text{ad.}}-(c_{11})_{\text{is.}}&=(c_{12})_{\text{ad.}}-(c_{12})_{\text{is.}},\\ &=T\alpha^2/(\rho c_p)(s_{11}+2s_{12})^2, \end{aligned} \tag{7}$$

where T is the absolute temperature, α is the coefficient of linear expansion, c_p is the specific heat at constant pressure, and ρ is the density. The adiabatic and isothermal s_{44} and c_{44} are the same.

To recapitulate: The essential measurements of the method are the fundamental frequencies of the specimen, its length and density, and the orientation of the cylinder axis in the crystal lattice. In addition, the specimen cylinder must be homogeneous and of uniform cross section.

Preparation of the Crystals

The crystals are grown of Mallinckrodt analytic reagent grade sodium triply distilled in vacuum, with the rejection of the first and last quarters of the distillate in the first distillation. The still is constructed of Pyrex glass. Spectroscopic analysis shows the final product to contain traces of copper, vanadium, and aluminum, together with an amount of potassium which defies quantitative chemical analysis. The second distillation leaves the sodium in an ampule, which is sealed off and placed in a Pyrex glass

[2] Voigt, *Lehrbuch der Kristalphysik*, p. 739.
[3] Goens and Schmidt, Naturwiss. **19**, 520 (1931).
[4] The frequencies employed lie between 28 and 55 kilocycles.
[5] Voigt, reference 2, p. 789.

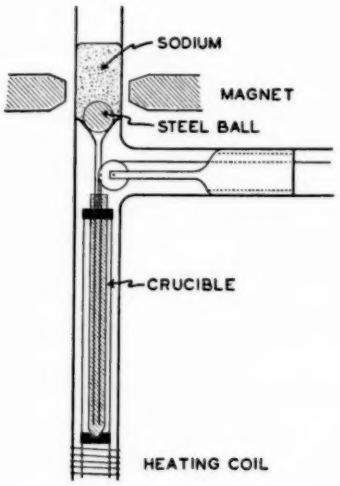

FIG. 1. Cross section of apparatus for growing the sodium crystals.

tube connected with the upper chamber of the apparatus diagrammed in Fig. 1. This apparatus is evacuated and kept at about 125°C with an enveloping furnace which has a glass front.

The ampule is broken in vacuum and the sodium distilled into the upper chamber. The bottom of this chamber is drawn out into a long tube of about 1 mm bore, which projects downward into a crucible and is closed at the top by a nickel plated steel ball. The crucible is made from a very thin walled glass tube, of the sort used for the stems of hydrometer bulbs, carefully selected for uniformity of bore.[6] The interior of the crucible is thinly coated with Socony Super Hecla mineral oil, previously boiled in vacuum in the presence of sodium. The crucible hangs in a nickel frame, suspended by a nickel chain which passes over pulleys to an iron counterweight. The position of the counterweight is controlled by a solenoid, which can be raised or lowered either manually or by a geared down electric motor.

When the distillation into the upper chamber is complete, helium at about 2 mm pressure is admitted above the molten sodium and the steel ball is raised by an electromagnet. The crucible is lowered steadily, by hand, as it fills, so that the bottom of the filling tube remains only a few millimeters below the surface of the sodium. After the crucible is filled it is lowered electrically out of the furnace, past the auxiliary heating coil shown at the bottom of the figure, at the rate of 5 cm per hour. Helium is then admitted to the lower chamber, the apparatus is opened at a ground joint level with the top of the lowered crucible, and the crucible is quickly capped with soft wax in the emerging stream of helium. The yield of good crystals, single over the entire 10 cm of length, is about one in three. The crystals appear to have no tendency to grow in any preferred orientation.[7]

[6] The writers are indebted to the firm of Kessler and Mumberg, of New York, for permission to make this selection directly from their stock.

LOCATION OF THE CYLINDER AXIS IN THE CRYSTAL LATTICE

The orientation of the cylinder axis with respect to the principal crystal axes is obtained by the measurement of four Laue x-ray transmission photographs. The diffraction camera has a G. E. Co. model CA 2 molybdenum x-ray tube operated at 35 kv and 20 ma. The specimen-to-film distance is 4.86 cm. Dupont film backed by a Patterson fluorazure screen is used, and the exposure time is 10 minutes.

The crystal, in the crucible, is set with its cylinder axis normal to the x-ray beam, and the pictures are taken after successive 90-degree rotations of the cylinder about its own axis. The spots are identified by comparison with the admirable set of Laue transmission photographs of a body-centered cubic lattice published by Majima.[8] The three direction cosines of each beam with respect to the crystal axes are calculated by the method of least squares from measurements of the radial distances of 8 to 12 spots from the center spot. The specimen-to-film distance used in these calculations is obtained by analysis of a picture taken through a cylinder of crystalline NaCl, in which the cylinder axis coincides accurately with a principal axis.

The four x-ray beams lie on the surface of a cone whose axis is the cylinder axis and the supplement of whose vertex angle is twice the error in setting the cylinder axis normal to the x-ray beam. If the latter were zero, the direction cosines of the cylinder axis would be those of the

[7] This method may be compared with that devised independently by Andrade and Tsien, "The Glide of Single Crystals of Sodium and Potassium," Proc. Roy. Soc. **163**, 1 (1937).

[8] Majima, *Scientific Papers of the Institute of Physical and Chemical Research*, Vol. 7, p. 249.

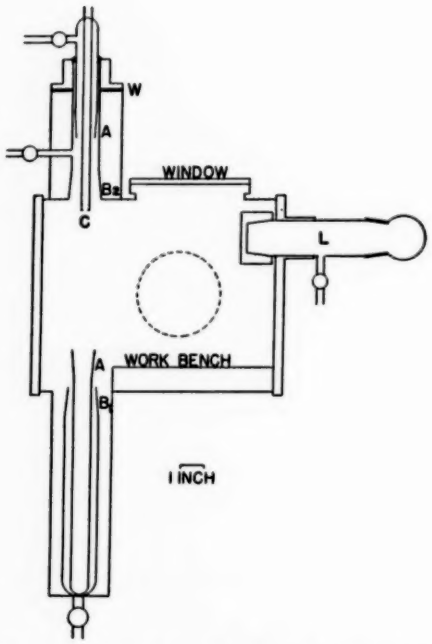

FIG. 2. Cross section of the chamber in which the crystals are handled.

vector cross product of any two mutually perpendicular x-ray beams. The values which are adopted are the arithmetic means of the four corresponding direction cosines obtained from the four possible vector cross products among the four x-ray beams.

The writers were rather surprised to discover that the orientation of the cylinder axis can be obtained in this manner with an accuracy of about five minutes of arc.

HANDLING THE CRYSTALS

After the x-ray analysis the crystal is placed in the handling chamber diagrammed in Fig. 2. The chamber, which is cylindrical in form and built of brass, is evacuated and filled with dry helium at atmospheric pressure. The crystals are handled through opposite holes in the chamber (shown by the dotted lines of Fig. 2), with the hands and arms encased in long obstetrical rubber gloves whose openings are securely clamped about the peripheries of the holes. The auxiliary chamber, L, is a lock which permits the introduction of crystals and tools to the chamber with a minimum expenditure of helium.

The crystal is removed from the crucible and cleaned with anhydrous ether kept standing in the presence of sodium. It is then laid in a V block and cut to the desired length with a thin strip of nickel under tension. The strip moves in a transverse slot in the V block. The quartz cylinder is prepared by coating one end with a very thin film of Empire stopcock lubricant,[9] which has been boiled in vacuum immediately before use. The quartz and specimen cylinders are laid end to end in the V block, and the join is made with the specimen held gently in place, by imparting a forward rotatory motion to the quartz.

The quartz cylinder has minute diametrically opposed transverse nicks at its center, and the composite oscillator is mounted by engaging these nicks with the jaws of a clip, shown at C, Fig. 2. The jaws are constructed by stretching fine wires horizontally across the forked lower termini of adjacent light vertical strips of spring metal. Two such strips are necessary for a longitudinal and four for a torsional oscillator.

The oscillator is enclosed by joining the glass tubes AA (Fig. 2), and the mount lock is closed by joining the glass tube B_1 to the brass tube B_2. Lastly the envelope containing the mounted oscillator is disengaged from the handling chamber at the point W, where it rests on a rubber washer, is removed and inserted in a dewar of boiling liquid nitrogen or liquid oxygen, or in the cryostat described in a previous paper.[10]

CALCULATION OF THE ELASTIC MODULI AND CONSTANTS

The quantities which follow immediately from the measurements made in the cryostat are the

TABLE I. *Typical data on a single sodium crystal.*

Quartz No.		n	f	Velocity $\times 10^{-5}$ cm/sec.
L	I	5	11004	1.443
	II	3	13107	1.468
	I	3	18187	1.472
	II	2	18263	1.478
T	III	2	20237	2.267
	IV	1	27837	2.253

[9] Empire Laboratory Supply Co., New York.

[10] Siegel and Quimby, Phys. Rev. **54**, 76 (1938). The temperature of this cryostat is measured with a copper-constantan thermocouple, calibrated by comparison with a platinum resistance thermometer certificated by the National Bureau of Standards.

frequencies of longitudinal and torsional vibration of the specimen crystal cylinder. The length of the cylinder at room temperature is measured on a comparator. The value adopted for the density of sodium at 20°C is 0.9712.[11] The lengths and densities at other temperatures are calculated from these numbers and the data on the thermal expansion of crystalline sodium previously published in this journal.[10] Corresponding values of E and G are computed with Eq. (1).

Twelve crystals in all were examined in the course of the present research. Of these, six were investigated very thoroughly at the temperature 79°K, and contributed twenty-four values of E and G at this temperature. Where possible measurements were made with two different longitudinal and two different torsional quartz cylinders, and at two or more different harmonic frequencies. A typical set of data is given in Table I. The first column designates the quartz cylinder by number, the second contains the harmonic numbers, i.e., the approximate number of half-waves of vibration in the specimen cylinder, the third the measured fundamental vibration frequency, and the last the calculated velocity of propagation, $V(=2fL)$.

TABLE II. *Observed and computed values of the longitudinal and torsional velocities in cylinders of crystal sodium at 79°K.*

	Longitudinal Velocity $\times 10^{-5}$ cm/sec.		Torsional Velocity $\times 10^{-5}$ cm/sec.	
Γ	Observed	Computed	Observed	Computed
0.0004	1.399	1.440	2.364	2.423
0.0130	1.465*	1.457	2.260*	2.342
0.1175			1.793	1.833
0.1476	1.795*	1.807	1.656*	1.680
0.1488	1.766	1.812	1.678	1.708
0.2128	2.104*	2.102	1.406*	1.389
0.2286	2.146	2.198	1.259	1.257
0.2491			1.148	1.149
0.2661	2.472	2.492	1.132	1.131
0.2907	2.780*	2.765	1.187*	1.181
0.3044	2.962	2.962	1.073	1.089
0.3145	3.206	3.137		

* Indicates the mean of several observations.

The remaining six crystals contributed ten values of E and G at 79°K,[12] and all of the data which show the variation of the elastic moduli with temperature. The number is adequate, for it is characteristic of the present experimental method that the temperature variation of the several elastic moduli can be measured with considerably greater accuracy than their absolute values. Imperfections in the specimen and other sources of error affect the former measurements less than the latter.

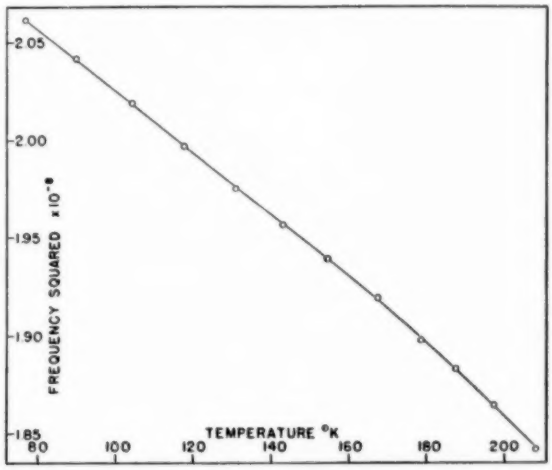

FIG. 3. The variation of f^2 with temperature for the torsional vibration of one of the crystals.

The adiabatic elastic moduli at 79°K were evaluated by solving thirty-four equations of the forms (2) and (4) simultaneously, by the method of least squares, for the three unknown quantities s_{11}, s_{12} and s_{44}. The concordance of the data on all twelve crystals is exhibited in Table II, in which the observed propagation velocities may be compared with those computed from the values of the elastic moduli obtained in this manner. The maximum deviation is 3.6 percent and the average deviation is 1.3 percent. It will be noted that, since the value of the orientation factor, Γ, must lie between 0 and $\frac{1}{3}$, the range of possible values is well covered by the twelve crystals.

The variation of the elastic constants with temperature is obtained as follows: The squares of the observed frequencies, f, of longitudinal and torsional vibration are plotted as functions of the temperature. The observations on the six crystals are thus represented by ten curves, of which that shown in Fig. 3 is typical. Values of f^2 at ten different temperatures between 80°K and 210°K

[11] Richards and Brink, J. Am. Chem. Soc. **29**, 117 (1907).

[12] Instead of twelve. The occurrence of a parasitic mode of vibration, feebly excited, vitiated the torsional measurements on one of these crystals, and another was, after the removal of a flaw, too short to permit reliable measurement of E. One of the first six crystals was dropped before E was measured.

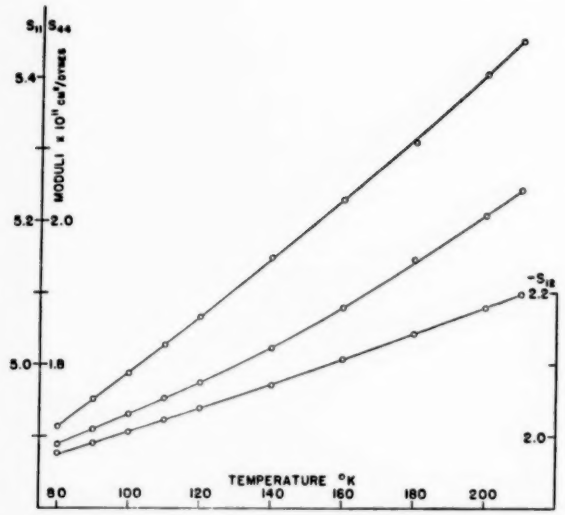

FIG. 4. The variation of the adiabatic elastic moduli of sodium with temperature.

are read from each curve, and corresponding values of E and G are calculated with Eq. (1). These data yield ten sets of ten equations of the forms (2) and (4), each set corresponding to a single temperature. Each set of equations is solved simultaneously, by the method of least squares, for s_{11}, s_{12} and s_{44}. The result of this computation is shown by the curves of Fig. 4.

The absolute values of the elastic moduli at 79°K read from the curves of Fig. 4 differ slightly from those previously computed, since the former are based on ten observations and the latter on thirty-four. Thus the values of s_{11}, $-s_{12}$ and s_{44} at 80°K deduced from all observations are, in units of 10^{-11} cm²/dyne, 4.83, 2.09 and 1.69, respectively, while those deduced from the ten observations alone are 4.91, 1.98 and 1.69. However, these curves are used simply to determine the *ratios* of the values of the moduli at T°K to the values at 79°K. The values hereinafter recorded for the elastic moduli at T°K are obtained by applying the ratios obtained from the curves of Fig. 4 to the values at 79°K deduced from the thirty-four observations at 79°K in the manner previously described. The concordance of the data from which the ratios are evaluated is exhibited in Table III, in which the observed ratios of the velocities at 80°K to those at 210°K for the six crystals may be compared with the ratios computed with the values of the elastic moduli at 80°K and 210°K, thus obtained. The results confirm the remark made above, that the present method yields a more accurate determination of the temperature variation of the elastic moduli than of their absolute values. The maximum deviation in Table III is 1.5 percent and the average deviation is 0.4 percent.

The isothermal moduli and constants are computed from the adiabatic quantities with Eqs. (7), in which, since the difference is small,

TABLE III. *The observed and computed ratios of the longitudinal and torsional velocities at 80°K to those at 210°K for six crystals.*

LONGITUDINAL		TORSIONAL	
OBSERVED	COMPUTED	OBSERVED	COMPUTED
1.073	1.065	1.060	1.060
1.052	1.053	1.086	1.101
1.072	1.075		
1.061	1.061	1.060	1.064
		1.061	1.059
1.070	1.071	1.086	1.078

the values $\rho=1.0$, $c_p=1.1\times10^7$ and $\alpha=6.0\times10^{-5}$ are substituted.

RESULTS

The elastic moduli and constants

The adiabatic and isothermal elastic moduli and constants, and the isothermal compressibility, are given as functions of the temperature in Tables IV and V. The estimated uncertainty in the absolute values of s_{11} and s_{44} is about 2 percent and of s_{12} about 3 percent. The precision with which the tabulated values are given is significant only for the calculation of the temperature variation.

Fuchs[13] has given a quantum-theoretical calculation of the quantities $(c_{11}-c_{12})$ and c_{44} for sodium at 0°K, which yields the values 0.141 and 0.58, respectively, in units of 10^{11} dynes/cm². The corresponding experimental values at 80°K are 0.145 and 0.59.

The compressibility

The accuracy of the present measurement of the compressibility is very poor. A significant figure is lost in the evaluation of the difference

[13] Fuchs, Proc. Roy. Soc. **157**, 444 (1937).

quantity $(s_{11}+2s_{12})$, and the uncertainty in s_{12} is doubled. Thus a change of one percent in the assumed values of s_{11} and s_{12} will, if the errors are additive, change the calculated value of κ from 1.98×10^{-11} to 1.70×10^{-11}. The writers have little doubt that the values given in Table V are high.

Bridgman[14] has measured the variation of the compressibility of polycrystalline sodium with pressure between 2000 and 20,000 kg/cm². As the pressure is lowered the compressibility increases toward the (extrapolated) value 1.7×10^{-11} cm²/dyne at zero pressure and room temperature. If the linear variation of compressibility with temperature here found to hold between 80°K and 210°K be assumed to hold over the entire range from 0°K to 293°K, then Bridgman's value reduces at absolute zero to 1.2×10^{-11}, and the value here found to 1.8×10^{-11}. A quantum-theoretical calculation of the compressibility at 0°K[15] gives $\kappa=1.6\times10^{-11}$.

TABLE IV. *The adiabatic elastic moduli and elastic constants of sodium. The number of significant figures does not indicate the accuracy of the absolute value.*

	Adiabatic Moduli $\times10^{11}$ cm²/dyne			Adiabatic Constants $\times10^{-11}$ dyne/cm²		
T°K	s_{11}	$-s_{12}$	s_{44}	c_{11}	c_{12}	c_{44}
80	4.826	2.087	1.685	0.608	0.463	0.593
90	4.861	2.102	1.705	0.603	0.459	0.586
100	4.898	2.118	1.726	0.598	0.456	0.579
110	4.937	2.134	1.747	0.593	0.451	0.572
120	4.975	2.151	1.770	0.589	0.448	0.565
130	5.014	2.168	1.793	0.585	0.445	0.558
140	5.054	2.186	1.818	0.581	0.443	0.550
150	5.094	2.205	1.846	0.579	0.442	0.542
160	5.135	2.224	1.874	0.576	0.440	0.534
170	5.177	2.243	1.904	0.572	0.437	0.525
180	5.220	2.262	1.936	0.568	0.434	0.516
190	5.263	2.281	1.968	0.564	0.431	0.508
200	5.308	2.301	2.002	0.560	0.428	0.499
210	5.354	2.321	2.037	0.555	0.425	0.491

[14] Bridgman, Proc. Am. Acad. Arts and Sci. **70**, 94 (1935).
[15] Mott and Jones, *The Theory of the Properties of Metals and Alloys*, p. 143.

The Debye characteristic temperature

A calculation of the Debye characteristic temperature from the elastic constants requires the evaluation of the reciprocal cubes of each of three propagation velocities, averaged over a unit sphere in the crystal.[16] The latter problem can only be solved by approximate methods, whose difficulty increases enormously when the anisotropy of the crystal is large.[13] In the present instance the averages are calculated by simply evaluating the velocities at 386 points on the sphere and taking the arithmetic means. The result at 0.80°K is, $\Theta_{80}=164$°K. The value obtained from specific heat data is $\Theta=159$°K.[17]

TABLE V. *The isothermal elastic moduli, constants, and compressibility of sodium.*

	Isothermal Moduli $\times10^{11}$ cm²/dyne		Isothermal Constants $\times10^{-11}$ dyne/cm²		Isothermal Compressibility
T°K	s_{11}	$-s_{12}$	c_{11}	c_{12}	κ $\times10^{11}$
80	4.829	2.084	0.601	0.456	1.98
90	4.864	2.099	0.597	0.453	2.00
100	4.901	2.115	0.592	0.449	2.01
110	4.939	2.131	0.586	0.445	2.03
120	4.977	2.147	0.581	0.441	2.05
130	5.018	2.164	0.575	0.436	2.07
140	5.058	2.181	0.571	0.432	2.09
150	5.099	2.199	0.567	0.430	2.10
160	5.140	2.218	0.564	0.428	2.11
170	5.183	2.237	0.560	0.425	2.13
180	5.226	2.256	0.556	0.422	2.14
190	5.269	2.275	0.552	0.419	2.16
200	5.315	2.294	0.546	0.415	2.18
210	5.361	2.313	0.541	0.410	2.20

In conclusion, the writers gratefully acknowledge their indebtedness to Dr. Don Kirkham and Dr. Seymour Rosin for their help in the design and construction of the diffraction camera and handling chamber, and to the Ernest Kempton Adams Fellowship Committee of Columbia University for the financial assistance which made this research possible.

[16] Reference 15, p. 3.
[17] Simon and Zeidler, Zeits. f. physik. Chemie **123**, 403 (1926).

Direct Determination of Crystal Structure from X-Ray Data

MELVIN AVRAMI
University of Chicago, Chicago, Illinois

(Received May 23, 1938)

The empirical similarity in the behavior of scattering-factor curves for different atoms is used to replace the structure-factor formulae by an *approximating system*. This system is shown to lead to m'th degree algebraic equations, designated *fundamental equations*, whose coefficients are calculable in terms of crystal structure and atomic scattering factors. The roots of these equations give the coordinates of the unknown atomic positions. Thus if the values of a sufficient number ($2m$ in general; $m+1$ where there is a center of symmetry) of sequential structure-factors are known, the problem of direct structure determination is solved. If only the absolute magnitudes are known, one may derive reciprocal equations of the $m(m-1)$th degree whose coefficients are calculable in terms of the squared moduli of the structure factors. We can then write *fundamental equations* of degree $m(m-1)/2$ whose roots give the coordinates of the *interatomic* distances from which the unknown parameters themselves may readily be determined. If the number of unknown parameters in any projection is m, the minimum number of structure factor moduli required in this case is $m(m-1)+1$. The method developed in the paper is applied to the KH_2PO_4 crystal, and the results are found to compare very well with the values found by West on the basis of a trial-error and Fourier synthesis investigation.

IN the problem of determining crystal structure from x-ray data, only the absolute values of the "crystal structure factors" F_{hkl}, associated with Laue indices hkl, are known.[1, 2] The F_{hkl} are related by theory to the distribution of scattering centers (atoms or ions) in the unit cell as follows:

$$F_{hkl}=\sum_{j=1}^{m} f_j(hkl)e^{-2\pi i(hx_j+ky_j+lz_j)}. \qquad (1)$$

Here $f_j(hkl)$ is the scattering factor in the hkl direction of the j'th center, xyz are its coordinates in fractional parts of the unit axial ratios, and m is the number of scattering centers in the unit cell. The $f_j(hkl)$ may be taken as known from independent experimentation. From these and the absolute values of the F_{hkl} we seek to determine the x_jy_j and z_j. In the past crystallographers have resorted to methods of trial and error for solving (1). We shall here show how these repeated trials may be avoided and the structure obtained directly from the experimentally given quantities. This method can be seen to be connected with a quasi-direct method of Patterson,[3] but has, however, many advantages over the latter. A more detailed treatment will be given in a forthcoming paper in the *Zeitschrift für Kristallographie*.

[1] W. L. Bragg and J. West, Zeits. f. Krist. **69**, 118 (1928).
[2] A. H. Compton and S. Allison, *X-Rays in Theory and Experiment*.
[3] W. L. Patterson, Zeits. f. Krist. **90**, 517 (1935).

I. THE APPROXIMATING SYSTEM

To carry through our treatment we make use of a simplification permitted by the experimental data. Examination of any table of atomic scattering factors[4] will show that the general variation at low temperatures of the $f_j(hkl)$ with hkl is similar for different atoms.[3] Thus to an approximation (which is better the lower the temperature and the larger the values of hkl) we may put $f_j(hkl)=f_jf(hkl)$ where f_j is a positive constant characteristic of atom j, and $f(hkl)$, the same for all atoms, may be taken as

$$\sum_{j=1}^{m} f_j(hkl) \Big/ \sum_{j=1}^{m} f_j.$$

Thus (1) may be written

$$\frac{F_{hkl}}{f(hkl)}=\sum_{j=1}^{m} f_j e^{-2\pi i(hx_j+ky_j+lz_j)} \qquad (2)$$

and it is this *approximating system* which we shall solve for the $x_jy_jz_j$; these and the phases of the F's are the only unknowns. It can be shown that the quantities in (2) may be regarded as the formal Fourier coefficients of a step function whose highest order singularities (poles) coincide in position with the centers of scattering in the crystal.

It is possible to set up equations depending only on the (F/f)'s whose roots are the x_jy_j and

[4] James and Brindley, Phil. Mag. **12**, 81 (1931).

z_j, respectively. These cannot be used in their simple forms to determine the $x_j y_j$ and z_j in the general case because the phases of the (F/f)'s are unknown. Nevertheless, as we shall show later, it is possible to eliminate the unknown phases and get equations entirely similar in form, so that it is advantageous to work out these equations and their solutions.

Suppose that it is the x_j which we wish to determine. Then keeping k and l fixed and setting

$$F_{kkl}/f(hkl)=A_h, \quad e^{-2\pi i x_j}=\alpha_j, \quad f_j e^{-2\pi i(ky_j+lz_j)}=d_j$$

we may write from (2)

$$A_h=\sum_{j=1}^{m} d_j \alpha_j{}^h. \tag{2'}$$

An m'th degree equation of which the α's are the roots may be determined as follows. Into

$$a_0+a_1\alpha+a_2\alpha^2+\cdots+a_m\alpha^m=0 \tag{3}$$

we successively substitute the various α's and multiply by the associated d's. Adding and using (2') we find

$$a_0 A_p+a_1 A_{p+1}+\cdots+a_m A_{p+m}=0, \tag{4}$$

which may be regarded as a recursion formula for the A's applicable for all p. Choosing a set of m+1 successive equations of the form (4) we find

$$a_r=(-1)^r\begin{vmatrix} A_p & \cdots & A_{p+r-1} & A_{p+r+1} & \cdots & A_{p+m} \\ A_{p+1} & \cdots & A_{p+r} & A_{p+r+2} & \cdots & A_{p+m+1} \\ \cdot & \cdots & \cdot & \cdot & \cdots & \cdot \\ A_{p+m-1} & \cdots & A_{p+m+r-2} & A_{p+m+r} & \cdots & A_{p+2m-1} \end{vmatrix} \tag{5}$$

or (3) may also be written

$$\begin{vmatrix} 1 & \alpha & \cdots & \alpha^m \\ A_p & A_{p+1} & \cdots & A_{p+m} \\ \cdot & \cdot & \cdots & \cdot \\ A_{p+m-1} & A_{p+m} & \cdots & A_{p+2m-1} \end{vmatrix}=0. \tag{3'}$$

While (3') may be evaluated for different commencing indices p and different fixed values of k and l, it is actually independent of these except perhaps for a common proportionality factor. (3) or (3'), and its analogs for the determination of y_j and z_j, may be designated *fundamental equations*. Once these are solved, the identification of the roots, i.e. the correct association of each α_j with its d_j, may be carried out by solving the linear system obtained upon selecting any m equations from the system (2').

In cases where the *fundamental equations* are too high in degree to be solved by elementary methods, general procedures for the approximation of roots must be resorted to. With the aid of the recursion formula (4) a valuable method of this kind may be established. This simple method, which is applicable to any system of the form (2'), with α's general, and therefore to the solution of any algebraic equation (since such may always be associated with a system (2')), will be described elsewhere.

II. Application to the Case of Unknown Phase Factors

(3') cannot be used in its simple form to determine the $x_j y_j$ and z_j because the phase of the (F/f)'s, and hence of the A's, are unknown. In certain cases, i.e., where the distribution has a center of symmetry, the (F/f)'s are all real and the ambiguity is merely one of sign[1] which can often be determined by other methods. In such cases the distribution of scattering centers may be obtained independently of our method by a Fourier synthesis. There are also important cases where (as in KH_2PO_4; see below) the phases are known of a sequence of F's sufficient in number to determine the unknown parameters. In the most general case, however, we are faced with an ignorance of the phases and the necessity of eliminating them. To do this we multiply (2) by its conjugate complex. We then get

$$|F_{kkl}|^2/f^2(hkl)=\sum_{j=1}^{m} f_j{}^2+\sum_{\substack{j,s=1 \\ j\neq s}}^{m} f_j f_s \times e^{-2\pi i[h(x_j-x_s)+k(y_j-y_s)+l(z_j-z_s)]}.$$

Introducing the abbreviations

$$G_{hkl}=|F_{hkl}|^2/f^2(hkl)-\sum_{j=1}^{m}f_j^2,$$

$$f_jf_s=g_{js}=g_w, \qquad \begin{matrix} e^{-2\pi i(x_j-x_s)}=\xi_{js}=\xi_w, \\ e^{-2\pi i(y_j-y_s)}=\eta_w, \\ e^{-2\pi i(z_j-z_s)}=\zeta_w, \end{matrix} \tag{6}$$

$$m(m-1)=n,$$

where $w=1, 2, \cdots n$ runs over the entire range for j, s $j\neq s$, we get

$$G_{hkl}=\sum_{w=1}^{n}g_w\xi_w{}^h\eta_w{}^k\zeta_w{}^l, \tag{7}$$

which is exactly the same as (2) in form, and may be treated in the same way to get *fundamental equations* whose roots are the ξ's, η's and ζ's. These roots occur in conjugate complexes, i.e. the *fundamental equations* are reciprocal and may be replaced by equations of half their degree. The roots give the coordinates of the *interatomic* distances rather than those of the atomic positions. The latter may easily be deduced from the former when the associated pair of atoms is identified by the procedure outlined above for (2).

Upon examination it may be seen that these roots correspond very closely to the positions of the peaks in Patterson's "sharpened up" series.[3] These positions, which Patterson's method can rarely locate because of the slow convergence of his series, are here determined in a simple algebraic way.

In case some of the positions of the scattering centers are known, their contributions may also be subtracted from $|F_{hkl}|^2/f^2(hkl)$ and an expression of the form (7) with n smaller than $m(m-1)$ will result.

When the experimental data are inaccurate, it will be advisable to get the coefficients of the *fundamental equations* by averaging the results from a number of the available sequences of F's (G's). Since both our assumptions and the experimental data are generally more valid for F's with higher indices, it will be wise to restrict ourselves to the use of these wherever possible. In the case of symmetry, $F_p=F_{-p}$, and the minimum number of sequential F's (including F_0) which must be known to determine an n'th degree *fundamental equation* is $n+1$.

TABLE I.

hkl	SIN θ	F (CORR.)	f_K+f_P	f_0	$\bar{G}$
060	0.248	40	10.8	2.3	−1.4
260	0.262	49	10.3	2.1	3.7
460	0.298	39	9.1	1.7	1.5
660	0.351	18	7.5	1.4	−8.6
860	0.413	20	6	1.05	−3.8
1060	0.482	24	4.4	0.75	8.5
1260	0.554	14	2.35	0.6	7.7

III. APPLICATION TO KH_2PO_4

We shall now apply our method to the simple case of the KH_2PO_4 crystal which has been investigated very carefully by J. West.[5] The space group is V_d^{12}. The unit cell contains four molecules,

4 P atoms at $000; \frac{1}{2}0\frac{1}{4}; \frac{1}{2}\frac{1}{2}\frac{1}{2}; 0\frac{1}{2}\frac{3}{4}$
4 K atoms at $00\frac{1}{2}; \frac{1}{2}0\frac{3}{4}; \frac{1}{2}\frac{1}{2}0; 0\frac{1}{2}\frac{1}{4}$

and 16 O atoms in the general positions xyz; $y\bar{x}\bar{z}$; $\bar{x}\bar{y}z$; $\bar{y}x\bar{z}$; $(\frac{1}{2}-x)$, y, $(\frac{1}{4}-z)$; $(\frac{1}{2}-y)$, $\bar{x}$, $(z+\frac{1}{4})$; $(x+\frac{1}{2})$, $\bar{y}$, $(\frac{1}{4}-z)$; $(y+\frac{1}{2})$, x, $(z+\frac{1}{4})$ and these $+\frac{1}{2}\frac{1}{2}\frac{1}{2}$. It is the parameters xyz which we wish to determine.

With West we may neglect the effect of the eight H atoms. Then, considering first the hk_0 reflections, it is found that "Owing to the special positions occupied by the potassium and phosphorus atoms, the (hk_0) spectra reduce to two types . . . *viz.*

Type I. (h even) Contribution of atoms is potassium +phosphorus+oxygens.
[Type II.] (h odd) Contribution from oxygen atoms only.

The spectra of type II are all weak compared with those of type I which receive a full contribution from potassium and phosphorus. We conclude that the signs of the phase factors (and therefore of the structure amplitudes $F(hk_0)$) for type I spectra are governed by the potassium and phosphorus atoms. It follows that . . . we shall know the signs of . . . $F(hk_0)$, for all planes with h even though not with h odd."

The knowledge of the signs of a sufficient sequence of F's permits us, in this case, to determine a *fundamental equation* for the atomic coordinates themselves. The contribution to $F(hk_0)$, with h even, from **K** and **P** is $4[f_k(hk_0)+f_P(hk_0)]$. Subtracting this and dividing by

[5] J. West, Zeits. f. Krist. **74**, 306 (1930).

$f_0(hk_0)$ we get a set of numbers, $\bar{G}_{hk_0}$, which, from (8), can be seen to be equal to

$$\bar{G}_{hk_0}=16[\cos 2\pi ky(e^{2\pi ihx}+e^{-2\pi ihx}) + \cos 2\pi kx(e^{2\pi ihy}+e^{-2\pi ihy})]. \quad (9)$$

Thus, keeping k constant, and varying h over even values, we see that we have a system, with a center of symmetry, in which the roots are $e^{4\pi ix}$, $e^{4\pi iy}$ and their conjugate complexes. The *fundamental equation* for the determination of these roots is then a reciprocal equation of the fourth degree. To determine its coefficients we here use only one of the available sequences of F's since this yields adequate accuracy. The values, as calculated from F_{h60} and f curves given by West, are given in Table I. These values yield

$$\begin{vmatrix} 1 & \alpha & \alpha^2 & \alpha^3 & \alpha^4 \\ 3.7 & -1.4 & 3.7 & 1.5 & -8.6 \\ -1.4 & 3.7 & 1.5 & -8.6 & -3.8 \\ 3.7 & 1.5 & -8.6 & -3.8 & 8.5 \\ 1.5 & -8.6 & -3.8 & 8.5 & 7.7 \end{vmatrix} =$$

$$2130\alpha^4-608\alpha^3+3178\alpha^2+211\alpha+2020=0. \quad (10)$$

Since this *fundamental equation* should be reciprocal and the symmetric coefficients equal, i.e., $a_0=a_4$, $a_1=a_3$, we may average these. Doing this, and dividing through by the first (last) coefficient, we have

$$\alpha^4-0.42\alpha^3+1.5\alpha^2-0.42\alpha+1=0. \quad (10')$$

This reciprocal equation may be solved by elementary methods and the roots are found to be

$$e^{\pm 4\pi ix}=0.475\pm 0.88i, \quad e^{\pm 4\pi iy}=-0.265\pm 0.965i,$$

or in degrees $x\approx 31°$, $y\approx 53°$,

which agrees well with West's values of 29° and 52°. Once x and y are known, the third parameter is readily found in the manner given by West.

The remarks of West concerning the trial-error and double Fourier series methods apply with equal force to our procedure. "The extent to which these methods are applicable without modification to complex structures must depend on the structures e.g. whether some of the parameters of the heavier atoms are fixed by symmetry considerations. In any case, however, it should not often be necessary to use a laborious trial and error method throughout to determine completely the structure. By the aid of certain reasonable assumptions and a qualitative examination of the experimental data a complex structure may often be partially solved. This partial solution may well be sufficient to determine the signs of a considerable portion of the F values for the reflections from planes in some important zone."

In conclusion we may make one general remark. Our method bears the same relation to the ordinary trial and error method as the systematic solution of a polynomial equation (e.g. the *fundamental equation*) bears to a cut and try attempt to determine its roots from linear combinations of homogeneous powers of these roots (e.g. 2′).

The author wishes to acknowledge his indebtedness for helpful advice and suggestion to Dr. W. H. Zachariasen and Dr. W. Bartky of the University of Chicago.

LETTERS TO THE EDITOR

Prompt publication of brief reports of important discoveries in physics may be secured by addressing them to this department. Closing dates for this department are, for the first issue of the month, the eighteenth of the preceding month, for the second issue, the third of the month. Because of the late closing dates for the section no proof can be shown to authors. The Board of Editors does not hold itself responsible for the opinions expressed by the correspondents.

Communications should not in general exceed 600 words in length.

Evidence for the Production of Penetrating Secondary Cosmic-Ray Particles in the Atmosphere

At the suggestion of Professor A. H. Compton, the following experiment of the Hsiung[1] type was performed to obtain some evidence concerning the production of penetrating cosmic-ray secondaries in the atmosphere. This subject was formerly discussed by A. H. Compton,[2] and now the problem has renewed interest because of the discovery of the heavy electron and a recent paper by Bowen, Millikan and Neher[3] in which they suggested that all radiations observed at sea level are secondaries produced in the upper atmosphere.

For the present experiment, four Geiger-Müller tubes (2.5 cm diam. and 30 cm long) were arranged for fourfold vertical coincidence according to Fig. 1. The writers are

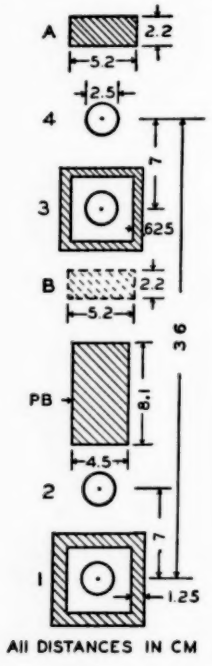

FIG. 1.

indebted to Mr. Francis Shonka for these tubes. 8.1 cm of lead were placed between tubes 2 and 3 to absorb the soft radiation, thus enabling one to record only the penetrating rays. The bottom tube was shielded from soft shower particles by 1.25 cm of lead, and a 0.625 cm lead shield was placed about tube number 3 to absorb Compton recoil electrons produced in the lead plate below. Any penetrating ionizing rays produced in the lead between the counters by a nonionizing incident ray will not be recorded since the upper two tubes will not be activated. However, if part of the lead (in this case 2.2 cm) is moved to a position above all four tubes, penetrating ionizing rays produced in the upper piece of lead will be recorded if they traverse the four tubes. Therefore, by alternately recording fourfold coincidences with the same piece of lead first between tubes two and three (position B) and then above all four tubes (position A), one may determine the relative number of penetrating rays produced in that piece of lead.

The experiment was performed in an aeroplane up to an altitude of 25,000 feet. The results are shown in Table I.

TABLE I. *Results of measurements.*

ALTITUDE	13,000 ft. to 20,000 ft.		20,000 ft. to 25,000 ft.		25,000 ft.	
Position of Lead See (Fig. 1)	A	B	A	B	A	B
Number of Fourfold Coincidences in 3 min. intervals.	7 4 6 6 1	5 5 4 7	8 9 9 11	4 7 5 5 9	11 10 10 10 10 15	2 4 11 2 6 6
Average	4.8±0.7	5.2±0.7	9.2±1.0	6.0±0.7	11.0±0.9	5.2±0.6
	Ratio $A/B=0.9$		Ratio $A/B=1.5$		Ratio $A/B=2.1$	

Three-minute readings were made with the lead alternately in positions A and B. Up to 20,000 feet no appreciable differences between A and B were observed. From 20,000 feet to 25,000 feet, the excess with the lead above is quite apparent, and at 25,000 feet the ratio $A/B=2.1$. This is well outside of the rather large statistical errors.

This experiment indicates that above 20,000 feet penetrating ionizing rays (heavy electrons) are produced by nonionizing agents (photons). It is of interest to note that the "hump" in the cosmic-ray absorption curve at about 25,000 feet is made more prominent when the apparatus is shielded with 6 cm of lead.[4] This indicates that this hump is possibly related to the production of penetrating secondaries.

The results of the present experiment are in good agreement with Heitler's[5] assumptions that the heavy electrons are formed by secondary photons which are abundant at high altitudes and are strongly absorbed by 2 cm of lead.

With the lead in position B the fourfold vertical coincidences at 25,000 feet were three times as numerous as at sea level. This represents the ratio of the intensities of the vertical penetrating component, which agrees well with Heitler's[6] calculations. Braddick and Gilbert[7] found a ratio of 9 to 1 at 35,000 feet. This high ratio is explained by Heitler as due to insufficient shielding of the soft rays (3 cm of lead).

Twofold coincidences for the upper two tubes at 25,000 feet and at sea level give a ratio of 12 to 1 for the total vertical radiation. This is in good agreement with Pfotzer's[8] data obtained by balloon flights with threefold coincidences. Special care was taken to have the efficiency of the apparatus a maximum. By activating the tubes with a radium source, conditions similar to those at 25,000 feet were reproduced in the laboratory, without any apparent change in the efficiency. The above agreements seem to indicate this also.

The writers wish to express their appreciation to Professor A. H. Compton not only for suggesting the experiment, but also for his continued support.

MARCEL SCHEIN
VOLNEY C. WILSON

Ryerson Physical Laboratory,
University of Chicago,
Chicago, Illinois,
August 2, 1938.

[1] D. S. Hsiung, Phys. Rev. **46**, 653 (1934). B. Rossi, Proc. Lond. Conf. on Nuclear Phys. (1934).
[2] A. H. Compton, Proc. Phys. Soc. London **47**, 747 (1935).
[3] T. S. Bowen, R. A. Millikan, and H. V. Neher, Phys. Rev. **53**, 217 (1938).
[4] A. H. Compton and R. J. Stephenson, Phys. Rev. **45**, 442 (1934).
[5] W. Heitler, Proc. Roy. Soc. **A166**, 529 (1938).
[6] W. Heitler, Proc. Roy. Soc. **A161**, 261 (1937).
[7] T. Braddick and C. W. Gilbert, Proc. Roy. Soc. **A156**, 570 (1936).
[8] G. Pfotzer, Zeits. f. Physik **102**, 23 (1936).

A New Rydberg Series in N_2

The absorption spectrum of nitrogen below 1000A shows some interesting features that appear to have been overlooked by previous investigators because of insufficient dispersion. The lower spectrum of Fig. 1 (negative; absorption appears white) shows the general aspect between 785 and 850A at a pressure of 0.1–0.2 mm and path length 130 cm. The complex of overlapping band systems at longer wave-lengths definitely terminates at about 800A with a converging series of band heads. These are shown with greater enlargement in the upper spectrogram. They obviously constitute the higher and intermediate members of an electronic series, the lower members of which ($n<6$) are presumably confused with the complex of bands at longer wave-lengths. Diffuse absorption (O_2?) overlaps the bands $n=6$, 8, 10, 11, 12, 13, blotting out the first three and also the fourth except on two plates taken at lower pressures.

The frequencies of the heads follow a Rydberg law closely. With $n=7$ to 25 and $\alpha=0.34$ ($n+\alpha=$Rydberg denominator) only the lowest measured member deviates appreciably, being shifted about -10 cm^{-1}. The limit of the series lies at $125{,}670\pm2$ cm^{-1}, or 15.503 volts. This is just the first ionization potential of N_2 computed indirectly by Mulliken[1] from the data on Hopfield's Rydberg series. The latter converge to the $^2\Sigma_u^+$ excited state of N_2^+, while the limit of our series is the $^2\Sigma_g^+$ normal state. The latter has an internuclear distance of 1.11A as compared to 1.09 for the normal state of neutral N_2, a circumstance which is favorable to the observation of such series. Further evidence that this is actually an electronic series comes from the fact that no discrete bands are observed beyond the limit, but a region of continuous absorption extends from here with gradually diminishing intensity to at least 600A. The Hopfield series just referred to does not appear on these plates, while at higher pressures the continuum below 800A is almost completely absorbed.

That the high dispersion and resolution of a 3-meter grazing-incidence spectrograph were required to show the existence of this series will be apparent from the spectrograms. We are using the Lyman continuum, which covers the longer wave-length region not accessible with the helium continuum. A thorough analysis of the whole absorption spectrum below 1000A is in progress.

R. E. WORLEY
F. A. JENKINS

Department of Physics,
University of California,
July 19, 1938.

[1] R. S. Mulliken, Phys. Rev. **46**, 144 (1934).

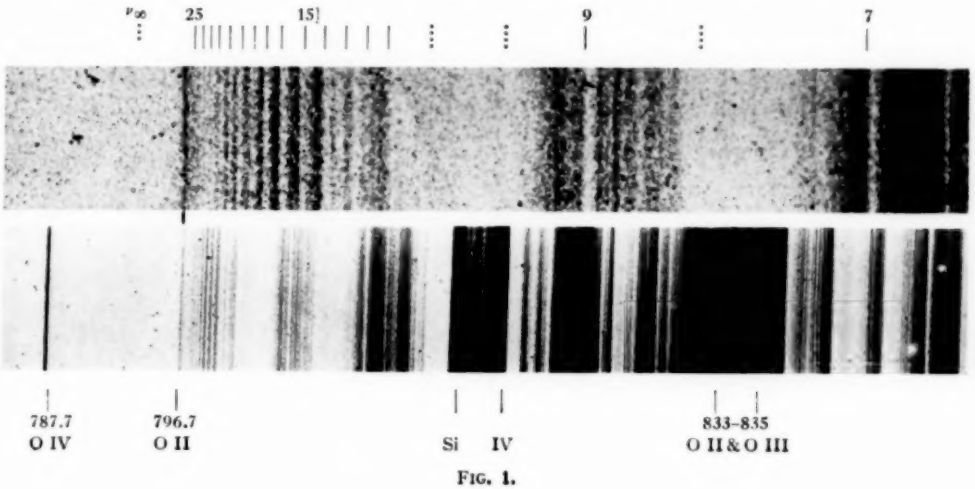

FIG. 1.

Remarks on the Article by H. R. Crane and J. Halpern—"New Experimental Evidence for the Neutrino"

The beautiful β-ray tracks of Cl^{38}, obtained by H. R. Crane and J. Halpern, show at their initial points clusters of droplets which the authors attribute to the ionization produced by the recoiling atom of A^{38}. From the statistical relation between the number of ions and the energy of the β-ray they calculate the value of the kinetic energy of the atom which they find to be in general agreement with the hypothesis of the simultaneous emission of an electron and a neutrino.

I should like to point out that the relation between the energy of an atom and the ionization produced by this atom is much too complicated to allow any direct test of this kind. The average energy expenditure per ion pair increases rapidly when the energy of the ionizing charged or uncharged atom tends towards zero. Even in the case of the α-recoil, when the energy of the atom is more than 1000 times larger than the energy of the recoiling A^{38} atom, the average energy spent for a pair of ions is of the order of 300 ev. Another example is the ionization produced in argon by moving argon ions, which starts at 240 ev and even at 400 ev is many times smaller than the maximum specific ionization, corresponding to about 30 ev per ion pair.[1]

It seems very probable that the A atoms, having an energy of about 400 ev, are either uncharged or undergo frequent losses of charge. The β-recoiling atoms of naturally radioactive elements are, as is well known, uncharged.

On the other hand, even if the energy of the A atoms were converted into ionization with the maximum efficiency, one must not consider the absolute value of the kinetic energy, but the energy of the movement relative to the center of gravity of the system formed by the argon and, say, a nitrogen atom. This last energy is, however, equal only to $14/(14+38)=0.27$ of the total kinetic energy.

All these considerations show that the number of ion pairs produced by a 400 ev A atom must be very small, probably of the order of unity. I think that the clusters observed by Crane and Halpern cannot be considered as giving support to the hypothesis of the neutrino, unless the energy of the neutrino, and, consequently, the total energy evolved in the β-transformation is much larger than the energy deduced from the upper limit of the β-ray spectrum.

L. WERTENSTEIN

Laboratory of Atomic Physics,
Free University of Poland, Warsaw,
July 10, 1938.

[1] Geiger and Scheele, *Handbuch der Physik*, second edition, Vol. 22, p. 127.

A Reply to the Above Note by L. Wertenstein

Professor Wertenstein has very kindly given us the opportunity of commenting upon his remarks published above. Professor Wertenstein is entirely justified in calling attention to the danger in our assumption[1] that one ion pair is formed for every 30 ev lost by the slowly moving argon atom in air. This value was adopted by us only as a working hypothesis, because of the lack of experimental data on the *total ionization* produced by argon atoms (or ions) of 400 ev and less, in air. We are now undertaking a measurement of this quantity, and prefer to postpone an opinion until the results have been obtained. In the meantime, we wish to point out (1) that our conclusion that a neutrino participates in the beta-ray disintegration can be arrived at without detailed consideration of the complicated mechanism by which droplets are produced in the cloud chamber by the recoiling atom, and (2) that a small efficiency of ionization by the recoiling atom does not necessarily imply a small efficiency in production of droplets.

(1) Let us consider the comparison between the results obtained with radiophosphorus (upper limit $\sim$1.7 Mev) and radiochlorine (upper limit $\sim$5 Mev). More specifically, let us compare the recoils resulting from the emission of beta-rays of the same energy in the two cases, namely between 1 and 1.5 Mev. The energy of recoil given to the atom by the beta-ray alone, is in the two cases essentially the same, about 25 ev, which is too little to produce a cluster of droplets on any reasonable assumption about ionization efficiency. The quantity which we may expect to differ radically in the two cases is the energy of the neutrino, which is 3.5 to 4 Mev in the chlorine case and 0.2 to 0.7 Mev in the phosphorus case. The experiment shows that the chlorine disintegrations of this group produce clusters of from 15 to 34 droplets, while the corresponding phosphorus disintegrations produce no visible clusters at all. Entirely similar results have been obtained by comparing radiochlorine with radionitrogen (upper limit 1.25 Mev). The most reasonable explanation of this effect seems at present to be that the much greater energy of recoil in the chlorine case is due to the escape of a neutrino of high energy (3.5 to 4 Mev).

(2) We have recently become aware of a mechanism other than ionization, by which a moving atom may bring about the formation of droplets in the cloud chamber, namely dissociation. Whether or not this is an important effect in our experiment we are not yet prepared to say. It is well known that a moving atom of several hundred ev energy strongly dissociates the molecules of the gas through which it passes, for example, in air, $O_2 \rightarrow 2O(\sim 6$ ev) and $N_2 \rightarrow 2N(\sim 9$ ev). The most probable fate of the free atoms is combination (in triple collisions) with molecules to form NO_2, N_2O, and other combinations, including those due to reactions with the alcohol vapor, which is present in the cloud chamber. We have attempted a preliminary test of the ability of such molecules to act as centers of condensation under normal operating conditions in a cloud chamber. The injection of minute amounts of NO_2 gas was found to produce an extremely dense cloud. Injection of air by the same method produced no cloud. It is therefore possible (but must be proved) that *every molecule* of NO_2 and of some other compounds resulting from dissociation by the recoil atom is effective in bringing about the condensation of a droplet.[2] If this effect should prove to be at all large, it would mean that the interpretation of droplet counts in terms of energy of recoil would have to be made on the basis of a direct experiment, and not on the basis of the efficiency of ionization alone. It will be fortunate if such an

effect is large, because it will increase the sensitivity for detection of slow heavy particles in a cloud chamber.

To sum up, (1) the conclusions of the experiment are arrived at by a comparison of Cl^{38}, P^{32} and N^{13}, rather than by an absolute estimate of the energy of recoil, and (2) at least one possible mechanism in addition to ionization exists for the production of droplets by slowly moving atoms, but its importance relative to ionization remains to be determined.

H. R. CRANE
J. HALPERN

University of Michigan,
Ann Arbor, Michigan,
July 30, 1938.

[1] Crane and Halpern, Phys. Rev. **53**, 789 (1938).
[2] The gases in the chamber were air, alcohol and ethylene dichloride in the experiment with Cl^{38}; nitrogen, alcohol and PH_3 in the P^{32} experiment; air and alcohol in the N^{13} experiment.

The Hard and Soft Component of Cosmic Radiation in Terms of a Common Primary Background [1]

The fundamental assumptions which control the view here discussed are the following:

1. There is a single primary background of charged, but nonelectronic type, with energy distribution function $F(E)$ of the form A/E^p.

2. Each primary ray experiences, per unit of path, a number of "events" or collisions, the average number of these per unit of path being β. This number we assume independent of the energy, and we assume the events to be distributed individually and collectively at random in any interval concerned. It results from the latter part of the assumption that the probability of occurrence of n events within the interval βx is $(\beta x)^n e^{-\beta x}/n!$

3. In each of these events the ray loses an amount of energy ϵ, which is the same for all energies. No ray of energy E can, of course, experience more than m losses ϵ, where $m\epsilon = E$.

4. If a ray has energy less than ϵ, it has, nevertheless, the same chance of experiencing an event; but in such an event it loses all of its energy.

5. When a primary ray loses energy, the energy loss goes into secondaries (possibly in part heavy electrons) and some of it gets converted directly or indirectly into ordinary electrons, which then proceed according to the Bethe-Heitler theory, the energy being lost, finally, in ionization and in radiative losses in all cases.

6. The story of the relationship between the number of secondaries per primary and the loss of energy of the primaries is controlled by

$$\eta dn/dx + \alpha n = dW/dx, \qquad (1)$$

where η is the average energy of all the particles other than primaries, α is the loss per particle per unit of path in ionization and in radiative losses, n is the number of secondaries and higher order particles per primary, and W is the average energy lost by a primary between the top of the homogeneous atmosphere and the depth x.

On the basis of the foregoing assumptions, expressions have been developed for the intensities of the primaries and secondaries—using the latter term to include all the higher order particles. The particular case considered is one where β is less than the energy for entry through the earth's magnetic field at the magnetic equator, but is equal to the energy for entry at some higher magnetic latitude φ, taken as 42° in the example.

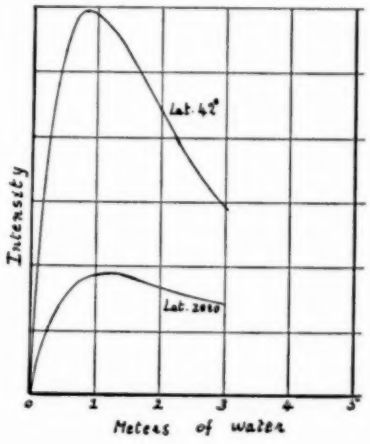

FIG. 1.

For both the primaries and the secondaries, the intensity comes out in the form of a series whose terms correspond to the probabilities of successively larger and larger numbers of events. The earlier terms dominate the story at small values of x, and these terms show a latitude variation. At greater depths, the later terms of the series dominate the situation. These terms show no latitude effect. Moreover, they correspond to an ever increasing "hardening" of the radiation until finally an absorption coefficient is attained which depends *entirely* upon the distribution function $F(E)$, and is independent of all other elements of the theory. This absorption coefficient varies with x and is given by $\mu = (p-1)/x$.

We thus realize a condition in which the *latitude effect increases with altitude*, and in which the *measured radiation at any latitude "hardens" with increase of depth.*

The growth of secondaries as determined by (1) results in *a maximum for the intensity* of the secondaries. Moreover, this *maximum occurs at depths which are greater the smaller the latitude.*

Figure 1 shows, for magnetic latitude 42° and for the equator, the intensity of the secondaries plotted against depth for $\beta = 4$ per meter of water, $\epsilon = 6\times10^9$ ev, and $p = 3$. These curves are only drawn for illustration and not necessarily with the best choice of constants to fit all the experimental data.

The large value of $\beta\epsilon$ determines a large number of secondaries per primary, which results in the phenomena measured being mainly secondary.

W. F. G. SWANN

Bartol Research Foundation of the Franklin Institute,
Swarthmore, Pennsylvania,
July 25, 1938.

[1] Part of a paper presented at the Cosmic-Ray Symposium held at the University of Chicago, June 27–30, 1938, which paper is in process of publication in full in the *Journal of the Franklin Institute.*

Search for Gamma-Rays from the Deuteron-Deuteron Reaction

The discovery by Bonner[1] of a second group of neutrons from the reaction

$$H^2+H^2\rightarrow He^3+n^1 \qquad (1)$$

has suggested the possibility that He^3 may be formed in an excited state about 2 Mev above the ground state. The difficulty of reconciling such a state with present nuclear theory has been emphasized by Share[2] and Schiff.[3] If such a state exists we should expect to observe gamma-rays due to the transition of He^3 to its normal state. Evidence for a gamma-ray has been given by Kallmann and Kuhn,[4] who used coincidence counters to investigate the reaction. We have made a search for this gamma-ray by means of a cloud chamber.

The cloud chamber was placed about 25 cm from a heavy phosphoric acid target bombarded by 0.5 Mev deuterons. A lead collimator was placed between the target and the cloud chamber and both were provided with thin aluminum windows. A sheet of carbon 0.15 cm thick extended across the center of the chamber as a source of Compton electrons. A magnetic field of 715 gauss was used to determine the electron energies. Many recoil electrons were observed, but most of these appeared to be due to the gamma-rays from slow neutron capture and from the inelastic scattering of fast neutrons in the material around the chamber. In order to determine whether any gamma-rays came directly from the target, the following experiment was performed. On alternate expansions the hole in the lead collimator was filled with a lead block 4 cm thick. This would have decreased the intensity of a gamma-ray from the target by a factor ten. Actually no difference in the numbers of electrons between 1 and 2 Mev energy was observed in the two cases.

In order to determine the ratio of the number of gamma-rays to the number of neutrons from the reaction, the target holder was placed directly within the cloud chamber and surrounded by a foil of Cellophane 0.1 mm thick. From the number of proton tracks coming from this foil the neutron intensity could be estimated using the known cross section for neutron-proton scattering. The gamma-ray intensity was determined simultaneously by counting the Compton electrons produced in a sheet of carbon in the center of the chamber. Since the time of sensitivity of the cloud chamber for electron tracks is smaller than the time of sensitivity for proton tracks, a correction factor was necessary. An estimate of this ratio was found by placing in the chamber a natural radioactive source which emitted a known ratio of beta-rays and alpha-particles. From the ratio of Compton electrons to protons obtained in this way it was calculated that there is not more than one gamma-ray for every 200 neutrons. This figure agrees with the estimate of Kallmann and Kuhn;[4] the intensity of Bonner's second neutron group[1] is, however, one-tenth of the 2.6 Mev group.

During the course of this investigation many protons were observed which penetrated a carbon sheet 0.15 cm thick, and consequently had an energy greater than 15 Mev. Since these were present when the chamber was separated from the target by 4 cm of lead, they must be due to neutrons, possibly from the secondary reaction

$$H^3+H^2\rightarrow He^4+n^1+17.6 \text{ Mev} \qquad (2)$$

due to recoiling H^3 nuclei from the reaction

$$H^2+H^2\rightarrow H^3+H^1. \qquad (3)$$

We understand that energetic protons from the analogous reaction of He^3 with H^2 have been reported by Oliphant.[5] The ratio of the number of these very energetic recoil protons to those of the 2.6 Mev group was of the order of one to one thousand; consequently reaction (2) must be an exceedingly probable one.

I wish to express my thanks to Dr. H. R. Crane for his helpful advice and encouragement.

ARTHUR J. RUHLIG

Department of Physics,
University of Michigan,
Ann Arbor, Michigan,
August 1, 1938.

[1] Bonner, Phys. Rev. **53**, 711 (1938); also Baldinger, Huber and Staub, Helv. Phys. Acta **11**, 245 (1938).
[2] Share, Phys. Rev. **53**, 875 (1938).
[3] Schiff, Phys. Rev. **54**, 92 (1938).
[4] Kallmann and Kuhn, Naturwiss. **26**, 106 (1938).
[5] Unpublished; private communication from Professor H. A. Bethe.

Observation of H^1 and H^3 Ranges from the Disintegration of Deuterium by Deuterons

Recent cloud chamber experiments[1] on the energy spectrum of recoil protons produced by neutrons from the reaction

$$H^2+H^2\rightarrow He^3+n^1$$

have shown the presence of a low energy group of neutrons, and indicate the existence of an excitation level in He^3 at 1.89 Mev. Ionization chamber studies[2] have led to this same conclusion. In view of this excitation level in He^3 it seems reasonable to expect a similar level in H^3. Consequently we have looked for a short range group of protons from the reaction

$$H^2+H^2\rightarrow H^3+H^1.$$

We used apparatus previously described.[3] The protons were observed in a cloud chamber filled with air and alcohol vapor. They were allowed to pass into the chamber through an aluminum foil which had a stopping power of approximately 0.5 cm. A slit system defined the direction

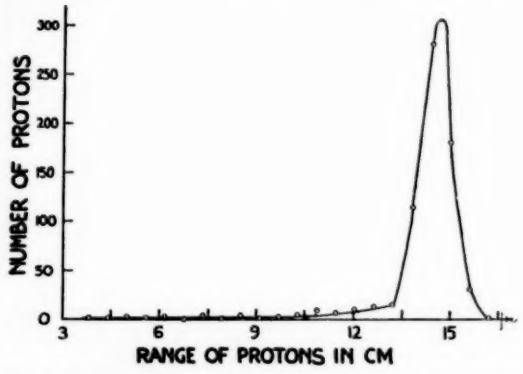

FIG. 1. Range distribution of protons from the disintegration of deuterium by deuterons.

of the disintegration particles to an angle of 99.5°±2° to the direction of the incident 100 kev deuterons, which bombarded a D_3PO_4 target. The stopping power of the gas in the chamber (1.18) was determined from the mean range (14.7 cm) of the proton group of maximum energy.

Figure 1 gives the range distribution of the protons observed, and, contrary to what one might expect, there is no indication of more than a single group. Preliminary experiments with a D_2O target frozen by liquid air gave similar results, though a higher background was present. From this experiment and that described below we conclude that H^3 is excited to a level between 0.4 and 2.9 Mev in less than 2 percent of the disintegrations, if at all.

While looking for low energy protons from the deuterium reaction we observed the range of the H^3 particles produced in the same reaction. An accurate determination of the range of these particles is useful in checking the range-energy relation for H^3 particles, and hence the range-energy curve for short range protons.

The H^3 particles were observed in a cloud chamber filled with helium and water vapor. They were allowed to pass into the cloud chamber through the slit system and an aluminum foil with a stopping power of 0.50 cm.[4] Fig. 2 gives the range distribution of the particles. The stopping power of the gas was found to be 0.30±0.01 cm for particles with a range of 3.80 cm (polonium alpha-particles).

The most probable range is 1.28±0.10 cm, which corresponds to a mean range of 1.31±0.10 cm at 99.5°. Since the

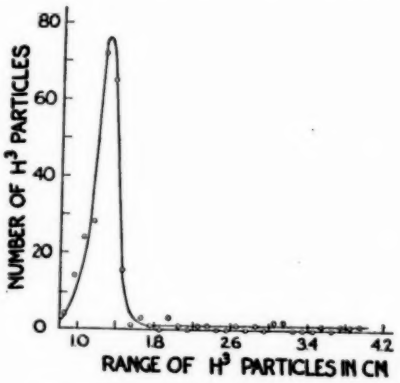

FIG. 2. Range distribution of the charged particles as observed in the helium filled chamber.

stopping power of the helium would probably be slightly higher for 1.3 cm particles than for polonium alpha-particles, this is actually a lower limit to the H^3 particle range.

The energy of the H^3 particles emitted at 99.5° was calculated from the Q value of 3.98 Mev.[5] The energy of the H^3 particles is 0.89 Mev at this angle. The range of a H^3 particle of this energy theoretically is three times the range of a proton with an energy of 0.89/3 Mev. If we use the new range-energy curve of Livingston and Bethe for protons, the mean range of the H^3 particles should be 0.95 cm. This is beyond the limits of experimental error and we conclude that their range-energy curve for protons in this region is in error. The experimental range of 1.31 cm is in much better agreement with the old curve of Livingston and Bethe[6] which predicts an H^3 range of 1.38 cm.

This suggested change in the range-energy relation for protons is important since it would necessitate raising the mass of the neutron, and lowering the mass of He^3 and C^{14}.

EMMETT HUDSPETH
T. W. BONNER

The Rice Institute,
Houston, Texas,
June 21, 1938.

[1] T. W. Bonner, Phys. Rev. **52**, 685 (1937); **53**, 711 (1938).
[2] Baldinger, Huber, and Staub, Helv. Phys. Acta **11**, 245 (1938).
[3] T. W. Bonner, Phys. Rev. **52**, 685 (1937).
[4] The stopping power of the foil was calculated by assuming 1.41 mg/cm² = 1 cm air.
[5] Oliphant, Kempton, and Rutherford, Proc. Roy. Soc. **A149**, 406 (1935).
[6] Livingston and Bethe, Rev. Mod. Phys. **9**, 245 (1937).

Ferromagnetic Colloid for Studying Magnetic Structures

The magnetic structure of a ferromagnetic material can be revealed by depositing a fine ferromagnetic powder from suspension onto the smooth surface of a specimen which is suitably magnetized. F. Bitter,[1] who first studied magnetic structures by this method, used finely ground gamma-ferric oxide suspended in ethyl acetate. Stray fields near the surface of the specimen guide such a ferromagnetic powder as it settles; the powder thereby forms a pattern recording regions where H^2 is greater than in near-by regions. A similar technique for obtaining patterns has been used by most of the other investigators[2] who have extended the work of Bitter. McKeehan and Elmore,[3] however, used a true colloid (rather than a temporary suspension) of gamma-ferric oxide. They discovered that the colloid formed patterns consisting of swarms of sol particles which under favorable conditions did not settle out or coagulate but which retained their mobility within the solution. Although this latter technique possesses many advantages over the former, no great use seems to have been made of it, a fact undoubtedly due to the difficulty of securing or of preparing a suitable colloidal suspension. This situation has prompted the writer to look for a simple means of making a ferromagnetic colloid for magnetic powder investigations.

A series of experiments have led to the preparation of a very satisfactory colloidal magnetite. The new colloid forms patterns rapidly, does not coagulate once the pattern is formed, and is superior for subjective observation and for photography since its color is a very dark reddish-black (gamma-ferric oxide is a light brick-red). Several colloidal magnetites which were prepared proved unsatisfactory. One of these, protected by dextrin, had such a fine particle size that it formed patterns only in regions possessing very intense stray fields. Another one, unprotected, produced instead of the expected pattern tree-like structures which did not disperse when the applied magnetic field was removed from the specimen. To be useful for forming patterns evidently the colloid particles must not be too small, i.e., they must lie in the upper range of colloidal size. They must also be protected by another colloid to

prevent their coagulation when they congregate near the surface of the specimen. The surface itself should be protected by a thin layer of lacquer made, for instance, by dissolving a little celluloid in amylacetate.

To make the new colloid, first prepare a coarse, flaky precipitate of magnetite by Lefort's method:[4] dissolve 2 grams of $FeCl_2 \cdot 4H_2O$ and 5.4 grams of $FeCl_3 \cdot 6H_2O$ (or equivalent amounts of the sulphates) in 300 cc of hot water and add with constant stirring 5 grams of NaOH dissolved in 50 cc of water. Filter to remove salt and excess sodium hydroxide. Rinse precipitate in filter several times with water and finally once with 0.01 *N* HCl. Then transfer precipitate to one liter of one-half percent soap solution and boil for a short time. The former precipitate will now have become entirely colloidal with the exception of a very small quantity of undispersed oxide which should be removed by filtering hot. It is interesting that the success of the method depends entirely on the peptization of the precipitate with HCl before it is added to the water containing soap which serves as a protective colloid. A drop or two of the colloidal magnetite placed on the magnetized specimen will give an ample supply of sol particles for forming a pattern.

W. C. ELMORE

Massachusetts Institute of Technology,
Cambridge, Massachusetts,
July 19, 1938.

[1] F. Bitter, Phys. Rev. **38**, 1903 (1931); **41**, 507 (1932).
[2] F. Bitter, *Introduction to Ferromagnetism* (McGraw-Hill Book Co., 1937), p. 59.
[3] L. W. McKeehan and W. C. Elmore, Phys. Rev. **46**, 226 (1934).
[4] See, for instance, L. A. Welo and O. Baudisch, Phil. Mag. **3**, 396 (1927).

Proceedings of the American Physical Society

Minutes of the Toronto, Canada, Meeting, June 24–25, 1938

THE 222nd regular meeting of the American Physical Society was held at Toronto, Canada on Friday and Saturday, June 24 and 25, 1938 at the University of Toronto as a joint meeting with the American Association of Physics Teachers. All scientific sessions were held in the McLennan Laboratory. The presiding officers were Dr. Lyman J. Briggs, President of the Society and Professor John T. Tate, Vice President. The visiting members of the Society were housed in the Student Residences. The attendance at the meeting was about two hundred and fifty.

A joint meeting with the American Association of Physics Teachers was held on Friday morning at 9:30 o'clock in the McLennan Laboratory with Professor F. K. Richtmyer, President of the American Association of Physics Teachers, presiding. A short address of welcome from the President of the University of Toronto, the Hon. Dr. H. J. Cody, opened the meeting. The invited speakers were as follows: Professor John Satterly, University of Toronto on *A Comparison of the Teaching of Physics in England and America;* Professor E. F. Burton and Members of the Staff in Physics, University of Toronto, and Teachers of Physics in Secondary Schools of the Toronto Area, prepared a *Demonstration of Experiments;* and liquid helium was produced and exhibited at the Cryogenic Laboratory of the University of Toronto.

A symposium of invited papers was arranged for Saturday morning at 9:30 o'clock in the McLennan Laboratory with President Lyman J. Briggs presiding. The speakers were: Professor H. A. McTaggart, University of Toronto on *Monomolecular Films;* Professor J. W. Beams, University of Virginia on *High Speed Centrifuges and Some of Their Applications;* and Professor H. Grayson Smith, University of Toronto, on *Superconductivity.* Professor H. A. Kramers of Leiden, Holland, who was scheduled to speak on *Magnetic Phenomena at Low Temperatures* did not arrive from Europe in time to make his address.

The local committee arranged for various excursions as well as for golf and swimming. The President of the University of Toronto invited all members of the two societies and their wives and friends to a garden party on the lawn of the Royal Ontario Museum at 4:30 o'clock on Friday afternoon, June 24.

The dinner was held on Friday evening at 7:00 o'clock for the members of the two societies and their friends at Hart House on the university campus. President Briggs presided and called upon President Cody, Vice President Tate and Dean F. K. Richtmyer. There were about one hundred and fifty guests at the dinner.

Meeting of the Council: At its meeting held on Friday, June 24, 1938 the death of one member (Elon H. Hooker) was reported. One candidate was elected to membership, thirteen candidates were transferred from membership to fellowship and eighteen candidates were elected to membership. *Elected to fellowship:* Eugene Guth. *Transferred from membership to fellowship:* Daniel S. Elliott, Walter B. Ellwood, Walter Gordy, Clarence W. Hickman, Victor E. Legg, Frederick B. Llewellyn, Carol G. Montgomery, Rose C. L. Mooney, Foster C. Nix, Rogers D. Rusk, John C. Schelleng, Ralph D. Wyckoff, and Jerrold R. Zacharias. *Elected to membership:* William J. Bailey, Jr., B. Vivian Bowden, E. Bretscher, George P. Brousseau, Eugene Brunner, Herman Feshbach, Robert C. Herman, Otto G. Koppius, J. K. Kostko, Karl D. Larsen, H. R. Letner, William W. McCormick, Edson R. Peck, Roy W. Prince, Jr., Solomon Schwebel, Arthur K. Solomon, Paul F. Spremulli and Turrell Uleman.

The regular scientific program of the Physical Society consisted of twenty-two contributed papers of which numbers 1, 7, 9, 16 and 17 were read by title. The abstracts of these papers are given in the following pages. An Author Index will be found at the end.

W. L. Severinghaus, *Secretary*

Abstracts to Contributed Papers

1. Spectrochemical Analysis of Fertilizers, Particularly for the Micrometabolic Elements. Stanley S. Ballard, *University of Hawaii.**—Samples of twelve basic commercial fertilizers have been analyzed by the spectrochemical methods developed in the spectroscopic laboratory of the Experiment Station of the Hawaiian Sugar Planters' Association.[1] Analyses were performed semi-quantitatively, the amount of each element present in a sample being indicated by one of the following designations: *Lots, Some, Less, Trace, Not Detected.* Such an analysis reveals the presence or absence in a sample of the fifty-odd arc sensitive elements, of which twenty-one were encountered in the present investigation. The various fertilizers were found to differ greatly in the number of mineral elements present. Particular attention was given to the minor plant nutrients, the micrometabolic or so-called "less essential" elements iron, manganese, boron, copper, zinc and aluminum, as well as to the major elements phosphorus, potassium, calcium and magnesium which often occurred as impurities when they were not present as major constituents. The fertilizers tested included two sulfates of ammonia, two nitrates of soda, two nitrates of potash, muriate of potash, two raw rock phosphates, two superphosphates, and phosphate of ammonia. The last five named proved to be the best sources of the minor elements. This paper will appear in full in *The Hawaiian Planters' Record.*

* To be read by title.
[1] S. S. Ballard, Phys. Rev. **52**, 253A (1937).

2. The Effects of Pressure and Temperature on the Viscosity of Monosubstituted Toluenes. H. E. Morgan and R. B. Dow, *Pennsylvania State College.*—The viscosity of *ortho-*, *meta-*, and *para-* forms of chloro-, bromo-, nitro- and iodotoluene was determined at 30°, 75°, and 99°C at pressures ranging from atmospheric to 4000 kg/cm² by means of the rolling-ball type of high pressure viscometer. Calibration of the viscometer enabled the absolute viscosity to be computed at the three temperatures of the experimental range of pressure. The applicability and validity of the log coeff. of viscosity-pressure relation to represent the data are discussed. The tendency of the pressure coefficient both to increase and decrease as the substituted group is moved in the series, leads to the conclusion that no general rule can be stated for the effect of change of position of the substituted group. A plot of the pressure coefficient against atomic weight (M.W. for NO_2) shows that while the former tends to increase with the latter for the *ortho-* and *meta-* bindings, it clearly decreases for the *para-* binding. Increase of temperature reduces these differences. It is suggested that this anomaly may be due to a fundamental difference in the vibration of the toluene ring when the substituted group is attached in the para position, a result which would be expected to influence the type of "interlocking" at high pressures as pictured by Bridgman.

3. Viscosity Characteristics of Lubricating Oils at High Pressure at Various Temperatures. R. B. Dow, *The Pennsylvania State College.*—The study of the physical properties of oils at high pressures begun at Harvard University and being continued at the School of Chemistry and Physics, The Pennsylvania State College, is reviewed briefly. The pressure coefficient of viscosity at 100°, 130°, and 210°F and its relation to composition, molecular weight, and viscosity index is discussed for data obtained in this laboratory on Pennsylvania, Oklahoma, and California blends, and solvent extracted oils. Similar analysis is given for interpolated data from other laboratories for lard and castor oil. Comparison of a rolling ball viscometer with an absolute, concentric cylinder type shows that both instruments are capable of good accuracy and satisfactory precision at various pressures and temperatures. No evidence of a semi-colloidal or non-Newtonian behavior, as observed by the independence of the coefficient of viscosity and the rate of shear, has been observed for these oils at the pressures and temperatures investigated.

4. New Survey of the Spectrum of the International Iron Arc in the Range 10,000 to 2000A. Dorothy W. Weeks, *Wilson College,* and George R. Harrison, *Massachusetts Institute of Technology.*—Wave-length measurements have been made on some 10,000 lines obtained in the international iron arc. A 10-meter concave grating having 30,000 lines per inch was used in Paschen mounting at dispersion 0.4A/mm for the range 2000 to 6900A. For 6900 to 10,000A, a 10-meter grating having 15,000 lines per inch was used in a Wadsworth mounting at dispersion 3.3A/mm. Two hundred twenty inch plates were measured on a computing-recording comparator, the resulting wave-lengths being self-consistent to 0.003Å or better as determined by repeat runs and by the combination principle. After elimination of all impurity lines and possible ghosts the number of known iron lines is approximately trebled. The able assistance of W.P.A. clerical help is gratefully acknowledged.

5. Electric Arc Reignition at High Pressures. J. D. Cobine, R. B. Power* and L. P. Winsor, *Harvard Graduate School of Engineering.*—A study has been made of the reignition of short a.c. arcs in air at pressures from one to eight atmospheres, for currents under 3.5 amperes, in a resistance circuit. Pure graphite electrodes were used and were separated by distances from 1/8 mm to 3 mm. As previously indicated for nitrogen, the reignition voltage under these conditions increases with pressure when the r.m.s. arc current is kept constant. The reignition potential for constant gas pressure decreases as the current is increased. The characteristic of reignition potential vs. current has been found to exhibit a discontinuity at a critical current. For this current the reignition potential decreases by about 1000 volts to a new characteristic typical of the higher currents. This critical current depends upon the gas pressure and to a lesser degree upon the electrode separation. For pressures of atmospheric, or below, the transition is not abrupt but is completely defined. As the r.m.s. current is increased from low values to values near the critical value, the number of cycles for which the reignition

potential is on the higher characteristic decreases. For currents equal to, or greater than the critical value, only the low reignition potentials are obtained. This transition is accompanied by a change in the burning voltage of the arc. The factors influencing reignition are discussed and possible mechanisms are considered.

* Kennecott Wire and Cable Company.

6. Townsend Ionization Coefficients in Argon Phototubes. W. S. HUXFORD, *Northwestern University*.—Values of the ionization coefficient α have been obtained in Cs-Ag-O tubes with parallel plates in which the cathodes were activated by the usual commercial process. Six tubes having electrode separations of 2, 4, 6, 8, 12 and 16 mm were employed containing argon at a pressure of 0.175 mm of mercury. The P.D. values lie in the neighborhood of the minimum sparking potential and the measurements cover a range which includes the maximum value of α/E plotted as a function of E/p. The results are in substantial agreement with other recent measurements of the electron ionization coefficient in highly purified argon. Calculations of the coefficient γ, which represents the number of electrons leaving the cathode for each positive ion reaching it, yield values which are considerably greater than those obtained with cathodes having a higher electron work function. In this calculation account must be taken of an increased photo-sensitivity of the cathode which occurs at high gas amplification and is apparently induced by the action of positive ions. Sparking potential measurements for pure argon in tubes having nickel cathodes, nickel cathodes activated with barium, and Cs-Ag-O cathodes show a progressive lowering of the minimum sparking potential and a shift of this minimum to lower P.D. values as the work function of the cathode decreases.

7. Ultrasonic Reflection Losses in Air, Helium and CO_2.* R. S. ALLEMAN AND J. C. HUBBARD, *Johns Hopkins University*.—The new heat conduction theory of acoustic reflection developed by Herzfeld[1] requires a modification of the theory of the acoustic resonator interferometer.[2] As a result the values of γ^2, the intensity reflection coefficient, first obtained by Hubbard,[2] and those of Curtis,[3] showing a dependence upon frequency, have been recalculated, and together with new values by the authors are given below, showing excellent general agreement with Herzfeld's theory.

			$1-\gamma^2$	
Author	Gas	kc/sec.	Exp.	Theo.
1. H	Air	597	0.034	0.034
2. A	"	1237	.051	.049
3. C	CO_2	189	.015	.0122
4. H	"	597	.0148	.0216
5. C	He	252	.048	.046
6. A	"	792	.089	.081
7. C	"	1001	.085	.092
8. A	"	1192	.101	.097
9. A	"	1976	.118	.124

* To be read by title.
[1] K. F. Herzfeld, Phys. Rev. **53**, 899 (1938).
[2] J. C. Hubbard, Phys. Rev. **38**, 1011 (1931); **41**, 523 (1932); **46**, 525 1934).
[3] R. W. Curtis, Phys. Rev. **46**, 811 (1934).

8. An X-Ray Test of Superstructure in $FeNi_3$. F. E. HAWORTH, *Bell Telephone Laboratories, Inc.*—A search has been made for superstructure in permalloy of composition near $FeNi_3$. Curves of x-ray scattering power near the absorption edges of Ni and Fe show that Fe$K\beta$ radiation should give the strongest superstructure lines, and calculations indicate that reflection from (321) planes of a perfectly ordered structure should have about one-seventh the intensity of the ordinary (222) reflection. The specimen was a powdered alloy containing 70 percent nickel, annealed at 1000°C and baked at 425°C. It was placed in a focusing camera in a beam of Fe$K\beta$ rays which were selected and concentrated by a curved rocksalt crystal, and exposed for one hundred hours. No superstructure lines appeared, although superstructure in β-brass was easily detected with similar technique. The negative result indicates that no long range order exists in the region near $FeNi_3$.

9. The Spectrum of Doubly Ionized Lead, Pb III.* M. F. CRAWFORD, A. B. MCLAY AND A. M. CROOKER, *University of Toronto*.—The spectrum of lead has been measured in the region 800A to 10,000A. The lines were excited by an electrodeless discharge in lead vapor. A series of spectrograms of the entire region were taken for different excitation conditions in the source, and the variation of intensity of a line with excitation showed, in general, to which spectrum it belonged. About four hundred lines have been classified as transitions between ninety levels of the following configurations: $6sns$, $n=6$ to 10; $6snp$, $n=6$ to 8; $6snd$, $n=6$ to 9; $6snf$, $n=5$ and 6; $6sng$, $n=5$ to 8; $6snh$, $n=6$ to 9; $6p^2$; $6p\ 7s$; $6p\ 6d$; $5d^9\ 6s^2\ 6p$. The hyperfine structures of sixty-four of the classified lines have been measured with a twenty-one foot grating by Crooker.[1] The observed structures of these are consistent with this multiplet analysis. The $6sng$ configurations show interesting anomalous multiplet and hyperfine structures. A theoretical interpretation of these will be published soon by one of the authors (M. F. C.).

* To be read by title.
[1] Can. J. Research **14**, 115 (1936).

10. The Number of Lines in a Series as a Function of Electron Concentration. FRED L. MOHLER, *National Bureau of Standards*.—In the spectrum of an intense discharge the successive lines of a series are increasingly broadened until they merge into a continuous spectrum at an effective quantum number which can be quite definitely evaluated. Spectra of capillary discharges under conditions of nearly complete ionization have been obtained with electron concentrations, N_e, ranging from 5×10^{13} to 1.3×10^{16}. In this range the maximum effective quantum number n for the violet component of the diffuse series decreases from 17.0 to 8.0. Values are about 0.3 greater for the red component and 0.5 greater for the F series. A plot of log n *versus* log N_e gives a straight line with a slope indicating that $n^{-7.3}$ is proportional to N_e. Spectra of low current discharges give n about 25 for $N_e=10^{12}$ but values seem to depend on vapor pressure and resolving power for N_e less than 10^{13}. Sugita has shown that if the number of states is limited by electron collisions then n^{-7} is proportional to N_e. On the view that n determines the number of discrete states it follows that the ionization potential is reduced by about 0.2 volt when $N_e=10^{16}$.

11. The Effect of Magnetic Fields on Persistent Currents in a Closed Superconducting Circuit. K. C. MANN, H. GRAYSON SMITH AND J. O. WILHELM, *University of Toronto.*—A study has been made of the effect of external magnetic fields in preventing persistent currents from flowing in a closed superconducting circuit, in order to determine as closely as possible the field strength at which the first traces of electrical resistance appear. In agreement with earlier work by a less accurate method,[1] and with the resistance measurements of de Haas,[2] but in contradiction to the idealized theory of the transition state,[3] it is clearly shown that no resistance appears until the mean magnetic induction within the specimen becomes considerable. It has been found further that the amount of resistanceless current which the specimen can carry under these conditions is limited. The results are greatly affected by the addition of small amounts of impurity. When the current strength was slightly greater than its equilibrium value, it required a measurable time to decay, the behavior being similar to the relaxation effects observed in the magnetic and thermal properties of superconductors. Several authors have suggested that the relaxation in magnetic properties is due to the decay of eddy currents. A thermodynamic argument now shows that relaxation in the thermal properties will be caused in the same way.

[1] K. C. Mann and J. O. Wilhelm, Trans. Roy. Soc. Canada **31**, 19 (1937).
[2] W. J. de Haas, J. Voogt and J. M. Jonker, Physica **1**, 281 (1934).
[3] F. London, Physica **3**, 450 (1936); Nature **137**, 991 (1936).

12. A Theoretical Lower Bound for the Energy of the Normal State of Helium. A. F. STEVENSON AND M. F. CRAWFORD, *University of Toronto.*—A method of using Weinstein's expression[1] for a lower bound for the energy, as given recently by one of us,[2] has been applied to the normal state of heljum, using the same sequence of functions as was used by Hylleraas in his calculation of an upper bound. The successive approximations obtained by the lower bound method show a satisfactory convergence towards the upper bound finally obtained by Hylleraas.

[1] D. H. Weinstein, Proc. Nat. Acad. Sci. **20**, 529 (1934).
[2] A. F. Stevenson, Phys. Rev. **53**, 199 (1938).

13. Experiments and Theory on the Performance of the Geiger Point Counter. J. LLOYD BOHN AND JOSEPH MORGAN, *Temple University.*—Preparation of sensitive and insensitive points, why rough points or very sharp ones will not work properly, and why a point and plane combination may cease to function as the point approaches the plane will be discussed. Curves showing operating characteristics of various combinations of points, planes and tubes at atmospheric pressure and for point and tube combination at various pressures will be shown—also curves showing the variation in time for the reappearance of counts, after a Bakelite cap on the front of the tube had been touched, with voltage. That a modified form of Zeleny's[1] theory suffices to explain the action of the Geiger point counter is concluded.

[1] Phys. Rev. **15**, 566 (1922).

14. A Vacuum Tube High Voltage Stabilizing Circuit for d.c. Sources. H. L. SCHULTZ,* *Yale University.*—When the stabilizing circuit to be described is applied to a conventional rectified-filtered source, initial voltage variations are reduced to less than 0.03 percent and the apparent internal resistance viewed from the output is of the order of a few thousandths of an ohm. Continuous control of output voltage from several hundred to several thousand volts at currents as high as several hundred milliamperes is possible using tubes of the receiving type. The circuit is similar to one developed by C. D. Bock, formerly of this laboratory, and has the following principle of operation. A triode or group of triodes connected in parallel is employed as a variable impedance in the positive line from the source to be stabilized. Residual voltage variations across part of a bleeder resistance in the output are amplified and actuate the grid of the control tube or tubes in proper phase with respect to the incoming variations. Simplicity and an actual improvement in operation is attained when plate and screen voltages for this amplifier are derived from taps on the common bleeder resistance. Instability occurs only if the load has appreciable reactance.

* Sterling Fellow.

15. Threshold Energies for Some (p,n) Reactions. M. G. WHITE, L. A. DELSASSO, RUBBY SHERR AND L. N. RIDENOUR, *Princeton University.*—Measurements of yield as a function of energy have been made by the method of stacked foils for several nuclear reactions of the (p,n) type. The maximum incident proton energy is 4.2 Mev; the ion currents employed are about 1 microampere. The results to date indicate that the energy thresholds of three reactions studied are as follows:

Reaction	Half-life of Radioelement	Threshold energy, Mev
$Ni^{60}(p,\gamma)Cu^{61}$ or $Ni^{61}(p,n)Cu^{61}$	3.4 hours	<1.9
$Ni^{64}(p,n)Cu^{64}$	12.8 hours	2.1
$Ag^{?}(p,n)Cd^{?}$	6.7 hours	2.4

16. The Dirac Equation with Spin Greater Than 1/2.* ARTHUR BRAMLEY, *Washington, D. C.*—The interesting feature of the equations for electron with spin greater than 1/2 and rest mass different from zero is that besides the Hamiltonian there exist linear equations of constraint acting on the wave functions.[1] Their invariance under reflection demands that the two numbers l and k characterizing the spin be identical. From these two sets of four linear equations second order differential equations can be constructed. In order to make the spin components definite we shall take the electron as propagated in the direction of a constant magnetic field. The second order equation corresponding to the relativistic Pauli equation[2] shows that the magnetic interaction is proportional to the velocity vector, not, as we might expect, the spin vector. Another consequence of the equations is that the matrices α must be expressed in terms of hypercomplex numbers such that $\alpha_x^2=\alpha_y^2=\alpha_z^2=k(k+1)/3$. In that case it follows from the equations of constraint that

$$\left(\frac{p\bar{z}}{pl}\right)^2=\frac{(3+R)k+R}{(3R+1)k+1} \quad \text{where} \quad R=-\left|\frac{u'v'^*+u^2v^{2*}}{u'v'^*-u^2v^{2*}}\right|^2$$

in Dirac's notation. This extra condition among the components of the momentum requires that for every velocity there shall be a characteristic rest mass.[3]

* To be read by title.
[1] Dirac, Proc. Roy. Soc. **155**, 447 (1936).
[2] Sakata and Yukawa, Japan Proc. Phys. Math. Soc. **19**, 91 (1937).
[3] Bramley, Science **87**, 281 (1938).

17. Virtual Levels of Be^8 and the Alpha-Particle Model. JENNY E. ROSENTHAL, *Brooklyn College.*—It is known experimentally that the normal state of Be^8 is barely stable and that there is a broad virtual level at about 3 Mev. A theoretical calculation has been made assuming a "molecular" model with a Morse potential between the α-particles adjusted to a 10 Mev depth of the potential well. The wave functions ψ were evaluated for the continuum region; only the order of magnitude of the moment of inertia and not its exact value is important in this calculation. Theoretically we can speak of a virtual state if, for a given value of the angular momentum, the ratio of the amplitude of ψ inside the potential well to that outside reaches an appreciable maximum for some energy range. The calculations show that no maximum exists for any value of the energy; a consideration of the Coulomb barrier should not modify the results appreciably. We conclude that the molecular model does not account for the existence of virtual levels.

18. The β-Ray Spectrum of I^{128}. R. H. BACON, E. N. GRISEWOOD AND C. W. VAN DER MERWE, *New York University, Washington Square College.*—The β-ray spectrum of I^{128} has been measured in a Wilson cloud chamber. A K.U. plot shows an abrupt change of slope indicating two intersecting straight lines. If the assumption is made that a single straight line means the existence of a single group our results would indicate two groups with end points at 2.1 Mev and 1.05 Mev, respectively. The end point of the high energy group agrees with that found by Alichanian, Alichanow and Dzelepow,* but the literature, to our knowledge, makes no mention of the other group. Details of the method used will be given at the meeting.

* Physik. Zeits. Sowjetunion **10**, 78–102 (1936).

19. The Radioactive Isotope of Samarium. T. R. WILKINS, *University of Rochester* AND A. J. DEMPSTER, *University of Chicago.*—G. Hevesy (1934) reported that samarium was a natural α-emitter with an *apparent* half-life of 1.2 $\times 10^{12}$ years. The *real* half-life can be calculated only if the active isotope can be identified and its percentage abundance known. Various suggestions have been made as to this isotope, some based on hyperfine structure abnormalities and some on relations between decay constant, nuclear radius and abundance ratios. We have devised a new tool for such studies by combining the mass spectrograph and the photographic emulsion track technique. A direct deposit of the isotopes of samarium was made on an Ilford R type emulsion in the mass spectrograph. The plate was set aside for several months and then developed and examined by the microscope. These tracks lie in the emulsion, and are seen by focusing on the emulsion through the half-transparent samarium deposited on the gelatin supercoating of this type of plate. The typical α-ray track (1.13 cm air range and α-ray spacing) was found under the isotope of Sm^{148}. Schumann plates have been used for calibration but these are actually unnecessary since the numbers of "spots" comprising the visible deposits correspond to the abundance ratios of the isotopes. Taking the abundance of Sm^{148} as 14 percent, the *real* half-life will be 14 percent of the *apparent* half-life.

20. Altitude Variation of the Relative Frequency of Occurrence of Pairs and Larger Cosmic-Ray Showers. DAROL K. FROMAN, *Macdonald College, McGill University* AND J. C. STEARNS, *University of Denver.*—The ratio of triple to quadruple frequency of coincidence of Geiger-Müller counters, arranged to detect showers containing two or more and three or more ionizing shower rays, respectively, has been measured for various thicknesses of scatterer at two altitudes, *viz.* 36 meters and 4300 meters above sea level. In accordance with the predictions of the multiplicative theory of shower production, this ratio decreases rapidly with increase in the thickness of the scatterer. For very thin scatterers, the ratio is much greater at the higher altitude. For very thin scatterers it is expected, on the theory, that this ratio would be greater for showers produced by photons than it would for electron-induced showers. Experimental data on this point are being taken, and the preliminary results tend to confirm this view. The marked variation of the ratio with altitude suggests the possibility that the relative number of photons and electrons in the cosmic-ray complex is a function of altitude. Experiments, designed to test this point, are being initiated this summer.

21. The Michelson-Morley-Miller Experiment. W. B. CARTMEL, *Université de Montréal.*—According to Lorentz $t=lv^2/c^3\cdot(1+\cos^2-\theta)$. In an oblique interferometer we have $\cos^2\theta$ in one arm and $\sin^2(\theta-\Omega)$ in the other and for their difference,

$$t=lv^2/c^3[\cos 2\theta-\sin\Omega\sin 2(\theta+\tfrac{1}{2}\Omega)]. \quad (1)$$

But to find the velocity along the sides of the triangle we must consider the three rays which meet at the plate. From Huygens' principle $V_a/\sin i_a=V_{a'}/\sin i_{a'}=V_\theta/\sin r$ from which we derive $V_{a'}=V_a\sin i_{a'}/\sin i_a$. As shown by Lodge,[1] $i_{a'}=i_a+v^2/c^2\cos^2 i\sin 2\phi$, from which we derive for the reflected ray $V_{a'}=V_a[1+\frac{1}{2}v^2/c^2(1-\sin\Omega)\cot i\times\cos 2(\theta+\frac{1}{2}\Omega)]$, and finally

$$t=lv^2/c^3[(1-\sin\Omega)\cot i\cos 2(\theta+\tfrac{1}{2}\Omega)-\cos 2\theta+\sin\Omega\sin 2(\theta+\tfrac{1}{2}\Omega)]. \quad (2)$$

Since the obliquity is slight in the Michelson-Morley-Miller interferometer, being only $6\frac{1}{2}°$,

$$t=lv^2/c^3\cdot\sin\Omega\{[\sin 2\theta]_0^{\pi/4}+\sin 2(\theta+\tfrac{1}{2}\Omega)]_{(\pi/2)-\Omega}^{(3\pi/4)-\Omega}\}.$$

Disregarding the limits we have a perfect sine curve, but taking them into account the fringe shift curve has maxima and minima alternately $6\frac{1}{2}°$ and $83\frac{1}{2}°$ apart, which would lead to hit or miss results taking measurements every $22\frac{1}{2}°$, and this was found experimentally by Professor Miller.[2]

With a 45° interferometer the maxima and minima would be 45° apart. It is evident that with the very oblique interferometer of Kennedy, only a very small part of the actual fringe shift would be found taking measurements every 90°, which accounts for the smallness of the results found by Illingworth.[3] Eq. (2), however, is believed to be only approximate, the exact solution being

$$\delta F = 2l/\lambda \sin \Omega v^2/c^2 \sin 2(\theta \pm \tfrac{1}{2}\Omega),$$

an equation which may be derived from the integrals of Lorentz, also by the method given in New York two years ago.[4]

[1] Sir Oliver Lodge, Phil. Trans. **184A**, 727 (1894).
[2] Dayton C. Miller, Rev. Mod. Phys. **5**, 203 (1933).
[3] K. K. Illingworth, Phys. Rev. **30**, 692 (1927).
[4] W. B. Cartmel, Phys. Rev. **49**, 647, 649 (1936).

22. A Cloud-Chamber Study of the Alpha-Rays of Actino-Uranium. T. R. WILKINS AND D. P. CRAWFORD, *University of Rochester.*—W. M. Rayton and T. R. Wilkins[1] (1935) reported an analysis of the alpha-rays from a thinly evaporated film of metallic uranium in which complete resolution of the U I and U II isotopes was secured. In addition, there seemed to be evidence of a small group of alpha-rays, presumably due to actino-uranium, between the main peaks due to U I and U II. In the present work minor improvements have been made in the apparatus and a much larger number of tracks studied. The mean ranges check those reported (by R and W) for U I and U II (2.625±0.0020 and 3.179±0.0024). The main peaks are so well fitted by Gaussian curves that the residuum is unquestionably present. The mean range of actino-uranium appears to be nearer that of U II. The relative fewness of these tracks prevents high accuracy of range determination but it is felt that a mean air-range (15°C) of 2.99 cm will prove to be very close to the correct value. The determination of the relative activity is correspondingly uncertain. The number of tracks measured was 2140.

[1] Phys. Rev. **51**, 818–25 (1937).

AUTHOR INDEX TO ABSTRACTS OF TORONTO MEETING

Alleman, R. S. and J. C. Hubbard—No. 7

Bacon, R. H., E. N. Grisewood and C. W. van der Merwe—No. 18
Ballard, Stanley—No. 1
Bohn, J. Lloyd and Joseph Morgan—No. 13
Bramley, Arthur—No. 16

Cartmel, W. B.—No. 21
Cobine, J. D., R. B. Power and L. P. Winsor—No. 5
Crawford, D. P.—see Wilkins, T. R.
Crawford, M. F.—see Stevenson, A. F.
——, A. B. McLay and A. M. Crooker—No. 9
Crooker, A. M.—see Crawford, M. F.

Delsasso, L. A.—see White, M. G.
Dempster, A. J.—see Wilkins, T. R.
Dow, R. B.—see Morgan, H. E.
——No. 3

Froman, Darol K. and J. C. Stearns—No. 20

Grisewood, E. N.—see Bacon, R. H.

Harrison, George R.—see Weeks, Dorothy W.
Haworth, F. E.—No. 8
Hubbard, J. C.—see Alleman, R. S.
Huxford, W. S.—No. 6

Mann, K. C., H. Grayson Smith and J. O. Wilhelm—No. 11
McLay, A. B.—see Crawford, M. F.
Mohler, Fred L.—No. 10
Morgan, H. E. and R. B. Dow—No. 2
Morgan, Joseph—see Bohn, J. Lloyd

Power, R. B.—see Cobine, J. D.

Ridenour, L. N.—see White, M. G.
Rosenthal, Jenny E.—No. 17

Schultz, H. L.—No. 14
Sherr, Rubby—see White, M. G.
Smith, H. Grayson—see Mann, K. C.
Stearns, J. C.—see Froman, Darol K.
Stevenson, A. F. and M. F. Crawford—No. 12

van der Merwe, C. W.—see Bacon, R. H.

Weeks, Dorothy W. and George R. Harrison—No. 4
White, M. G., L. A. Delsasso, Rubby Sherr and L. N. Ridenour—No. 15
Wilhelm, J. O.—see Mann, K. C.
Wilkins, T. R. and D. P. Crawford—No. 22
—— **and A. J. Dempster**—No. 19
Winsor, L. P.—see Cobine, J. D.